G Protein Signaling at the Endosome

Erin Jayne Heenan

A dissertation submitted to the faculty of the University of North Carolina at Chapel Hill in partial fulfillment of the requirements for the degree of Doctor of Philosophy in the Department of Biochemistry and Biophysics

Chapel Hill
2010

Approved by:

(Advisor) Henrik G. Dohlman, Ph.D.

(Committee Chair) Beverly Errede, Ph.D.

(Reader) Jean Cook, Ph.D.

(Reader) John Sondek, Ph.D.

(Reader) Dale Ramsden, Ph.D.

Abstract

Erin Jayne Heenan: G Protein Signaling at the Endosome
(Under the direction of Henrik G. Dohlman, Ph.D.)

G protein coupled signal pathways are conserved from plants to fungi to humans, and mediate the responses to a diverse array of signals including pheromones, light, odorants and neurotransmitters. In the yeast *Saccharomyces cerevisiae*, activation of a G protein pathway by pheromone triggers a series of events leading to mating. Traditional paradigms have assumed that the pathway originates solely from the plasma membrane, and that the purpose of the $Gpa1^{G\alpha}$ protein is to sequester the $Ste4/Ste18^{G\beta\gamma}$ dimer in the absence of stimulus. However, evidence has come to light showing that the activated $Gpa1^{G\alpha}$ protein transduces a signal, and this signal originates from the endosome. Moreover, the catalytic and regulatory subunits of the only phosphatidylinositol-3-kinase in yeast, Vps34 and Vps15, are required to transmit this endosomal signal. The endosomal G protein signal activates many of the same events as the plasma membrane derived signal, and results in activation of the MAPK Fus3 in preference to Kss1.

Here, we show that the kinase domain with the intermediate domain of Vps15 is both necessary and sufficient for binding to Gpa1 and for transmitting the G protein coupled signal. The WD domain of Vps15 most likely serves as a scaffold to assemble binding partners, and folds into a 7-bladed propeller, as demonstrated by X-ray crystallography. Moreover, our investigation of the kinase domain of Vps15 shows that

fully activated Vps34 is also necessary for both the expression and phosphorylation of Vps15.

Finally, as Fus3 is preferentially activated at the endosome, we investigated the regulation of Fus3. Here, we show that Fus3 is positively and negatively regulated by PtdIns(3)P, a second messenger produced by Vps34 that localizes to the endosomes. Furthermore, we show that lysine and histidine point mutations of Fus3 in its basic patch result in a decrease of Fus3 ubiquitination at the lysine residue as well as a decrease in Fus3 phosphorylation of Far1. Together, these data further our knowledge of the differences between the endosomal and plasma membrane G protein pathways.

To my Mom, who has always believed I can do anything.

Acknowledgements

I would be remiss if I did not stop and thank the many, many people who have supported me, guided me, and made my time in graduate school a genuine pleasure. I would first like to thank my advisor, Dr. Henrik Dohlman, for his unwavering support and guidance. Dr. Dohlman's enthusiasm for every student's project is infectious, and his encouragment and guidance during experimental pitfalls is always patient. I count myself lucky to have been in his lab, and I could have asked for nothing more in a mentor.

I would also like to thank the members of the Dohlman lab, both past and present, for making coming to work every day that much more fun. Sarah, Jan, Jeff, Steve, Michal, Matt, Mike, Laura, Gauri, Rachael, Justin, Jill, Josh, Janna, Nan and Corinne, thank you so much for being great resources for scientific knowledge, as well as NCAA bracket challenges, pranks, and lab lunches. You are all awesome.

Further, I would like to thank the members of my committee, Dr. Beverly Errede, Dr. Jean Cook, Dr. John Sondek, and Dr. Dale Ramsden, for their guidance and advice both during committee meetings, and the times when I just stopped by their offices. They served as instrumental forces in guiding the direction of my project. I must also thank Dr. Janeen Vanhooke and Dr. Brenda Temple for their beautiful work on the Vps15 crystal structure and homology model, as well as for informative discussions.

I would also like to thank the many members of the administrative staff of the Department of Biochemistry and Biophysics who have helped me along the way- Amanda, Susan, Lynn, Brenda, Rhonda, Doris, John and Karen, thank you so much for answering all of my questions and always reminding me when those critical documents had to be turned in. I would also like to thank our chair, Dr. Leslie Parise, for all her help and support during many periods in my graduate career. Additionally, I would like to thank all of my fellow Biochemistry and Biophysics graduate students, who have provided me with both scientific help as well as much needed downtime, in particular the Class of 2005 (Jenn, Ron, Anh, Joe, Andy, Yuan, Su, Elizabeth, Brett, Kate, Randy, and Tracy), who I am proud to count among my friends.

Finally, I must thank my family, without their support, I never could have come this far. In particular, I would like to thank my mom, Sarah Heenan, my aunt, Carrie Clements, and my brothers, Pete and Patrick Heenan, for always being interested, always asking questions, always making me feel important. I love you all. I also need to thank my wonderful boyfriend, Charles Davis, who has picked me up after every late night experiment, has never wavered when I went into work on a Sunday for 10 minutes that turned into 2 hours, and who has even taken the time to listen and learn about the system I work on. He is always patient, and I could not have gotten through graduate school without him and the supportive person he has always been.

Table of Contents

List of Tables

Page

List of Figures

Page

Abbreviations

Å	Angstrom
AlF_4^-	aluminum tetra-fluoride
CPY	carboxypeptidase Y
ER	glutamic acid 200 to arginine in Vps15
G6PDH	glucose-6-phosphate dehydrogenase
GDP	guanosine diphosphate
GFP	green fluorescent protein
Gpa1	G protein alpha subunit
GPCR	G protein-coupled receptor
GST	glutathione-S-transferase
GTP	guanosine-5'-triphosphate
Gα	G protein α subunit
Gβ	G protein β subunit
Gγ	G protein γ subunit
ID	intermediate domain of Vps15 between the kinase and WD domains
IP	immunoprecipitation
KD	kinase domain of Vps15
kDa	kilodalton
KR	lysine 335 to arginine in Fus3
MAP	mitogen-activated protein
MAPK	mitogen-activated protein kinase

MF	mating factor
Mg	magnesium
NK	asparagine 736 to lysine in Vps34
NSB	nonspecific band
PD	pulldown
PI3K	phosphatidylinositol-3-kinase
PI3P	PtdIns(3)P
PtdIns	phosphatidylinositol
QL	glutamine 323 to lysine in Gpa1
RA	arginine 1261 to alanine in Vps15
RFP	red fluorescent protein
RGS	regulator of G protein signaling
RK	arginine 1261 to lysine in Vps15
S. cerevisiae	*Saccharomyces cerevisiae*
SDS-PAGE	sodium dodecyl sulfate polyacrylamide gel electrophoresis
Ubi	ubiquitin
VPS	vacuolar protein sorting
WD	WD domain of Vps15
WT	wildtype
α-MF	alpha mating factor

Chapter 1

Introduction

For organisms to survive and reproduce, they must respond quickly and efficiently to external stimuli. In organisms from plants to fungi to humans, it is G protein-coupled receptors that mediate the responses of the cells to a wide array of stimuli, including light, neurotransmitters, odorants and pheromones. In humans, G protein-coupled receptors respond to serotonin, epinephrine, and thrombin among others. It is estimated that 30-50% of all drugs on the market today target G protein receptors and constituents of their pathways. Many of the drugs targeting G protein receptors, such as antihistamines and antidepressants, are some of the most commonly used in medicine today. A greater understanding of how these receptors are activated, and the members of their pathways, is therefore a critical goal in the pursuit of new drug targets (*1-4*).

G Protein Signaling: A Historical Perspective

The study of G protein signaling has a long and storied history, dating back to the early twentieth century and reaping no fewer than eight Nobel Prizes in Physiology or Medicine. The earliest inklings of the existence of GPCR's came in the first years of the twentieth century from Paul Ehrlich (Nobel Prize in Physiology or Medicine, 1908), who speculated that there must be a "receptive substance" that recognized chemical structures. His observations were supported by John Langley, a co-discoverer of acetylcholine, who posited around 1910-1915 that neurotransmitters act by being released and interacting with a receptive substance. However, it was not until the 1970's that it was commonly accepted that the receptor was really a protein (*5*).

In the 1950's, Earl Sutherland (Nobel Prize in Physiology or Medicine, 1971), performed elegant experiments discovering the mechanisms of action of many hormones, including epinephrine, and the second messengers that regulate them, most particularly cyclic AMP. In the early 1970's, Martin Rodbell (Nobel Prize in Physiology or Medicine, 1994) showed that it is GTP, not ATP, that is necessary for hormone activation by the guanine nucleotide protein (now known as the G protein). It was Alfred Gilman (Nobel Prize in Physiology or Medicine, 1994) who actually discovered, and eventually purified, the protein we now know as the G protein in the late 1970's and early 1980's. In 1977, Robert Lefkowitz purified the first receptor, the β-adrenergic receptor, and showed that it is a separate entity from adenylate cyclase (*5*). In the three decades that have followed these discoveries, the field of GPCRs and G proteins has exploded, and G proteins have been shown to be essential to the most key aspects of life.

Heterotrimeric G Protein Signaling

G protein-coupled receptors are comprised of seven membrane-spanning regions and transmit signals via G proteins, which are composed of a heterotrimeric complex containing a Gα, a Gβ, and a Gγ subunit. Upon activation by ligand binding, the G protein-coupled receptor catalyzes the exchange of GTP for GDP on the Gα subunit. This exchange leads to the dissociation of Gα from the Gβγ complex, which allows the free Gα and Gβγ the opportunity to activate downstream effectors. The signal transmitted by the free Gα and Gβγ subunits continues until the GTP of Gα is hydrolyzed to GDP, resulting in re-association of Gα with the Gβγ heterodimer. Regulators of G-

protein signaling serve to speed up the rate of GTP hydrolysis by Gα, promoting re-association of the Gα and Gβγ subunits and inactivating the signaling cascade (*1, 6*).

Yeast as a Model System

Yeast are a powerful tool for eukaryote genetic analysis. Yeast can be grown as haploids, which facilitates the study of recessive mutations. The entire yeast genome has been sequenced and nearly every open reading frame has been deleted. Additionally, yeast easily undergo homologous recombination, allowing the investigation by gene disruption. Furthermore, there are a wide variety of tools readily available for the study of G protein signaling in yeast, including GFP-tagged libraries and the previously mentioned deletion library. The G protein-mediated pheromone-response pathway is one of the best understood signal transduction pathways in eukaryotes. The components and mechanism of signal transmission in the yeast pheromone response-pathway are highly conserved in many pathways in humans, including those responsible for hormone and sensory responses, which makes yeast an ideal model system for the study of G protein signaling (*7-10*).

G Protein Signaling in the Yeast Pheromone Pathway

In *Saccharomyces cerevisiae*, a G protein-mediated pathway is employed for communication between cells to sense pheromones, resulting in mating. In yeast, there are two different haploid cell types, *MAT***a** and *MAT*α. These two cell types secrete pheromones in the form of small peptides, called **a**-factor and α-factor, respectively. The **a**-factor binds to an **a**-factor specific G protein coupled receptor called Ste3 on *MAT*α

cells, and the α-factor binds to an α-factor specific receptor called Ste2 on *MAT***a** cells. In *MAT***a** cells, upon pheromone binding to Ste2, the receptor activates the G protein heterotrimer comprised of Gpa1 (Gα subunit) and a Ste4/Ste18 heterodimer (Gβ/γ subunits respectively). Upon activation, Gpa1 exchanges its bound GDP for GTP. GTP-bound, or activated, Gpa1 then dissociates from the Ste4/Ste18 heterodimer. Dissociation of Gpa1 and Ste4/Ste18 leads to signal transmission through activation of the components of the mitogen-activated protein kinase (MAPK) cascade: Ste20, Ste11, Ste7, and Fus3, as well as the MAPK scaffold protein, Ste5, and a transcription factor, Ste12. Fus3 is a MAPK activated by the MAPKK Ste7. The activation of Fus3 by Ste7 leads to the phosphorylation of various proteins in the cell that mediate the arrest of cell division, cell morphology changes and gene transcription (**Figure 1.1**). One of the proteins that Fus3 phosphorylates is Far1. Far1 carries Cdc24, another effector of G protein signaling, as its cargo. Upon activation of the cell by pheromone, Far1 is exported from the nucleus. A complex formed of Far1-Cdc24-Ste4-Ste18 localizes at the mating projection, known as the shmoo tip, following pheromone stimulation, and is believed to play a pivotal role in the formation of the mating projection. Additionally, Far1 is postulated to play a key part in the imposition of pheromone mediated cell cycle arrest in G1 by acting as an inhibitor of Cdc28, a cyclin dependent kinase that is required for the cell to progress through G1 (*1, 11-13*).

Posttranslational Modifications and G Protein Signaling

The effect of posttranslational modifications on the regulation and propagation of G protein signals has been an area of detailed study. The posttranslational modification

of greatest interest to the G protein community has long been phosphorylation, which has been shown to play a large role in the regulation of both G proteins and MAP kinases (*1*). Phosphorylation plays a key role in the activation of the MAPK cascade and Far1 (*1, 13, 14*). Recently, the posttranslational modification ubiquitination, in which a small protein precursor called ubiquitin is added to specific lysine residues within a protein, has come to light as an important regulator in the propagation of G protein signals in cells. Poly-ubiquitination generally leads to degradation of the modified protein and has been shown to be important in the regulation of many components of the G protein signaling pathway (*15-20*).

In yeast, many key proteins in the G protein signaling pathway have been shown to be ubiquitinated, including Ste2, Gpa1, Ste7, and Ste12 (*15-21*). Mono-ubiquitination of Ste2 results in an internalization of the receptor and serves as a signal to direct the protein into the vacuole for degradation (*21-23*). Ste7 is ubiquitinated following its phosphorylation and activation by Ste11. The ubiquitination of Ste7 results in its degradation (*24*). Ste12 is also ubiquitinated and degraded in a pheromone-dependent manner (*20*). Unusually, Gpa1 is both poly- and mono-ubiquitinated, and the two different mechanisms of ubiquitination result in two very different outcomes. Mono-ubiquitination of Gpa1 targets it to the vacuole, while polyubiquitination of Gpa1 targets it to the proteasome (*19*). A similar panel of proteins involved in G protein signaling in mammals have also been shown to be ubiquitinated. Therefore, an enrichment of our understanding of the role of ubiquitination in the modulation of G protein pathways is extremely important to our understanding of the pathway as a whole (*17*).

Signaling by Activated Gpa1

As might be expected, mutations in Gpa1 that prevent it from binding to Gβγ do not block G protein-coupled signaling but instead result in uncontrolled signaling by free Gβγ, while overexpression of Gpa1 leads to decreased signaling, presumably due to a titration of free Gβγ. This evidence led to the supposition that Gβγ alone was sufficient to propagate the mating response signal, and that the role of Gα was to sequester Gβγ when no pheromone was present. Information has come to light that shows Gα itself plays an important role in the propagation of the G-protein coupled signal apart from its long-understood role of sequestering Gβγ (*1, 25, 26*).

Previous studies revealed that some organisms appear to have cooperative and antagonistic signaling regulation by both the Gα and Gβγ subunits (*27*). These studies prompted the Dohlman lab to examine whether Gpa1 could activate any part of the signaling pathway leading to mating events in yeast. It was found that $Gpa1^{Q323L}$, a mutant form of Gpa1 that is permanently active as it contains a mutation that blocks GTP hydrolysis, was able to activate many of the same events usually induced by Gβγ, such as morphological changes and new gene transcription, but not growth arrest. Overexpression of $Gpa1^{Q323L}$ also led to increased activation of the MAP kinase pathway, as measured by Fus3 phosphorylation. This GTPase deficient mutant did not affect signaling by Gβγ, as Gβγ does not bind the GTP-bound form of Gpa1 (*26*). Additionally, it was found that, while Gpa1 localizes primarily at the plasma membrane, constitutively active $Gpa1^{Q323L}$ localizes at the endosome (*28*).

Identifying Effectors for Activated Gpa1

A screen was performed to identify potential effectors of $Gpa1^{Q323L}$. In this screen, transcriptional activation was monitored in 4847 yeast strains, each containing a different, known, gene deletion. The activity of the pathway was monitored using a reporter gene under the control of a pheromone-inducible promoter. This assay allows screening for those mutants that affect the mating pathway (*28*).

Seven mutants were identified that suppressed signaling by $Gpa1^{Q323L}$ in multiple assays. The two mutants that provoked the most interest were Vps15 and Vps34, as they are already well known to play a role in other forms of signaling through the production of PI3P. Vps15 and Vps34 act as the regulatory and catalytic subunits, respectively, of the only phosphatidylinositol 3-kinase (PI3K) that is present in yeast (*28, 29*). Transformation of the deletion strains with the missing Vps15 or Vps34 restored signaling, confirming that these proteins are required for $Gpa1^{Q323L}$ signaling (*28*).

Vps15 and Vps34

Vps15 and Vps34 are classified as a Class III PI3K (*30, 31*). While it is well established that Class I PI3Ks are regulated by G protein coupled receptors, it has not previously been shown that Class III PI3Ks are regulated by G proteins (*31*). Class III (Vps34) PI3Ks are unique among other PI3Ks in that they are capable of utilizing just one substrate, phosphatidylinositol. As a result of this substrate specificity, Vps34 makes just one phosphoinositide product- PI3P. That Vps15 and Vps34 comprise the only PI3K

present in yeast makes the study of PI3P in yeast much more straightforward than it is in organisms with other PI3Ks, as all PI3P present in yeast must be made by Vps34 (*29*).

In addition to their described role in G protein-coupled signaling in yeast, Vps15 and Vps34 play integral roles in many other functions of the cell, including vesicular trafficking, nutrient sensing, and autophagy (*29*). The structure of Vps15 consists of a predicted protein kinase domain, with a central region containing multiple heat repeats, and a C-terminal WD-40 repeat domain (*29, 32, 33*). Vps15 has been shown to be a Ser/Thr protein kinase, and is believed to autophosphorylate (*33, 34*). However, other substrates for the kinase activity have never been identified, and Vps34 has been shown to autophosphorylate (*33*). Mutation of the protein kinase activity of Vps15 has been shown to abrogate its association with binding partners, including Vps34, as well as many of its functions in the cell, including G protein signaling (*28, 33, 35, 36*).

vps15Δ and *vps34Δ* strains are most similar to Class D vps mutants, and like some Class D mutants they have a mostly normal vacuolar morphology, but have deficiencies in vesicular sorting and vacuolar segregation (*29, 37*). *vps15Δ* and *vps34Δ* strains also are sensitive to growth at 37°C and to osmotic stress (*33, 34*). Additionally, in kinase dead Vps15, or *vps15Δ* cells, PI3P production by Vps34 is abolished (*36, 38*). Emphasizing the importance of the kinase domain of Vps15 is the fact that, when Vps34 is expressed at endogenous levels, Vps15 with an intact kinase domain is required for the activity of Vps34. Interestingly, overexpressed Vps34 can compensate for defective growth at elevated temperatures when expressed with single point mutations of the kinase

domain of Vps15, but overexpression of Vps34 can not compensate for a lack of Vps15 or for a triple mutation in the kinase domain of Vps15 (*39*).

Vps15 and Vps34 are present in at least four distinct complexes in yeast (**Figure 1.2)**, and are known to bind to each other (*29*). Residues 837-864 of Vps34 are sufficient to bind to the kinase domain and heat repeats of Vps15, which are required to bind Vps34 (*35*). The first Vps15-Vps34 complex, which is required for autophagy, also contains Vps30, and Atg14. Interestingly, we observed that the middle third of Atg14 has some sequence homology to typical Gγ proteins. In the second complex, which is required for the proper vesicular sorting of many proteins including the lysosomal hydrolase carboxypeptidase Y, Vps15, Vps34, Vps30 and Vps38 are present. The third complex, required for the sorting of several vesicular proteins, including Protein A and B, contains Vps15, Vps34 and potentially other, as yet unidentified, proteins. The fourth complex is the one responsible for G protein signaling, and it contains Vps15, Vps34, Gpa1 and potentially other, unidentified, proteins (*28, 29, 40-44*).

The production of PI3P by Vps34 is critical for the function of many pathways. It is thought that Vps34 regulates signaling by the recruitment of proteins that possess PI3P binding domains (*29*). PI3P binding domains include FYVE domains, zinc-finger binding domains (*45*), and PX domains (*46*). Pathways mediated by PI3P include, but are not limited to, assembly of PI3P binding proteins to regulate early endosomal docking and fusion (*47, 48*), the ubiquitin dependent sorting of internalized membrane proteins (*49*), and assembly of the retromer complex required for endosome to Golgi transport

(*50*). Additionally, as described in greater detail below, activation of the G protein signaling pathway has been shown to require Vps34, which produces PI3P, as well as increased production of PI3P, indications that PI3P may also play some role in mediating or regulating the G protein-coupled signal (*28, 51*).

G Protein Signaling at the Endosome

Vps15 and Vps34 were found to be necessary for multiple aspects of the pheromone-mediated response. *vps15Δ*, and *vps34Δ* yeast strains have diminished growth arrest, MAPK activation, mating, and gene transcription (*28*). Mutational inactivation of PI3K activity (*28, 41*), inactivation of the protein kinase activity of Vps15 (*28, 39*), and pharmacological inhibition of Vps34 using wortmannin (*28, 38*) also diminished mating, growth arrest, MAPK activation and gene transcription, indicating that Vps15 and Vps34 are required for all aspects of the $Gpa1^{Q323L}$ pheromone-mediated signaling pathway (*28*). These data are an indication that it is Vps15 and Vps34, and their PI3-kinase and ser/thr kinase activities, that are required for the $Gpa1^{Q323L}$signaling pathway (*28*).

In addition, it was shown that Gpa1 binds directly to Vps15 preferentially in its unactivated (GDP-bound) state and to Vps34 preferentially in its activated (GTP-bound) state (*28*). Vps34 binding to GTP-bound Gpa1 is interesting since binding to the activated form of a protein is a hallmark of an effector. Vps15 binding to GDP-bound Gpa1 is interesting as this is a hallmark of a Gβ protein. We were also intrigued by the WD-40 repeat domains of Vps15, as possessing 7 WD repeats is another hallmark of Gβ proteins (*52, 53*). In addition to these structural hallmarks, overexpressed $Gpa1^{Q323L}$

stimulated the PI3-kinase activity of the Vps15/Vps34 complex as monitored by an increase in phosphatidylinositol-3-phosphate (PI3P). $Gpa1^{Q323L}$ activation also stimulated recruitment of the PI3P binding protein Bem1 to the endosomal membrane, and this recruitment was abolished in a *vps34Δ* yeast strain (*28*).

It is known that Vps15 and Vps34 colocalize at several cellular organelles, including the endosome, Golgi, and vacuolar membrane (*33, 54*). Using fluorescence microscopy, wildtype Gpa1 was found to localize primarily at the plasma membrane as would be expected (*28, 54*). Constitutively active $Gpa1^{Q323L}$ was found instead to co-localize with Snf7 (endosome epecific marker) and Vps34 at the endosome. Deletion of Vps15 or Vps34 resulted in a decrease in $Gpa1^{Q323L}$ at the endosome and an increase in $Gpa1^{Q323L}$ at the plasma membrane, indicating that Vps15 and Vps34 promote endosomal localization of Gpa1 (*28*).

In the work presented in this thesis, I sought to further elucidate the role of endosomal G protein signaling by clarifying the role of Vps15 in transmitting the signal, as well as further characterizing how Fus3 is regulated. In Chapter II, I further investigate the role of Vps15 in G protein signaling. Here, we show that, as predicted, Vps15 contains 7WD repeats in a manner that is remarkably similar to Gβ proteins. However, it is the kinase domain with the intermediate domain of Vps15 that is both necessary and sufficient to bind to both $Gpa1^{G\alpha}$ and to Atg14, a protein with sequence homology to Gγ proteins that is in complex with Vps15 during autophagy. Finally, I show that it is the kinase domain with the intermediate domain of Vps15 that is both

necessary and sufficient to transmit the G protein-coupled signal. We hypothesize that while the kinase domain with the intermediate domain is necessary to transmit the signal, it is the WD domain that acts as a scaffold to assemble various interacting partners of Vps15.

As previously described, activated Gpa1 preferentially activates Fus3 over Kss1 when transmitting the G protein signal at the endosome. We sought to further elucidate the role of Fus3 in conducting the G protein signal in Chapter III. Here, we show that PI3P both positively and negatively (at very high concentrations) affects the kinase activity of Fus3. We also found point mutations in the basic patch of Fus3 that do not affect its general kinase activity or its role in mediating reporter gene transcription following pheromone stimulation of the cells. However, these point mutations do result in reduced growth arrest, Far1 phosphorylation *in vivo* and ubiquitination. The identification of specific residues in Fus3 that can uncouple the two branches of the pheromone response pathway mediated by Fus3 will prove to be a valuable tool for further investigation of G protein signaling and the differential activation of Fus3 and Kss1 from both the plasma membrane and the endosome.

As the kinase domain of Vps15 is important in G protein signaling, in Chapter IV we undertook a further investigation of the kinase domain. Here, I confirm that Vps15 does indeed undergo a phosphorylation event, and that a point mutation in the kinase domain of Vps15 is capable of blocking this event. Furthermore, we show that the presence of Vps34 is necessary for phosphorylation of Vps15. However, additional

experimentation shows that fully active Vps34 is also necessary for expression of Vps15, leaving the exact role of Vps34 in Vps15 phosphorylation an open question. Current efforts are underway to attempt to separate Vps34's role in promoting stable expression of Vps15 and any role Vps34 might play in the phosphorylation of Vps15.

The mechanism and components of the pheromone response pathway in yeast are highly conserved among eukaryotes, including humans. Therefore, a greater understanding of this pathway is a key component in the understanding of how signaling in humans proceeds and why it goes amiss in many diseases. Characterizing the novel effectors in the endosomal G protein pathway may lead to the discovery of other unique effectors. Finally, gaining a better understanding of the G protein signaling pathway at the endosome could allow for the discovery of new potential drug targets as it gives us a better understanding of how G protein signals are transmitted in cells.

REFERENCES

(1) Dohlman, H. G., and Thorner, J. W. (2001) Regulation of G protein-initiated signal transduction in yeast: Paradigms and principles. *Annu. Rev. Biochem. 70*, 703-54.

(2) Bardwell, L. (2005) A walk-through of the yeast mating pheromone response pathway. *Peptides 26*, 339-250.

(3) Neves, S. R., Ram, P. T., and Iyengar, R. (2002) G protein pathways. *Science 296*, 1636-9.

(4) Wang, Y., and Dohlman, H. G. (2004) Pheromone signaling mechanisms in yeast: a prototypical sex machine. *Science 306*, 1508-9.

(5) Gilman, A. G. (1995) G Proteins and regulation of adenylate cyclase (Nobel Lecture). *Agnew. Chem. Int. Ed. Engl. 34*, 1406-1419.

(6) Sprang, S. R. (1997) G protein mechanisms: insights from structural analysis. *Annu Rev Biochem 66*, 639-78.

(7) Dohlman, H. G. (2002) G proteins and pheromone signaling. *Annu Rev Physiol 64*, 129-52.

(8) Dohlman, H. G. (2002) Diminishing returns. *Nature 418*, 591.

(9) Sherman, F. (1997) An Introduction to the Genetics and Molecular Biology of the Yeast *Saccharomyces cerevisiae*. *The Encyclopedia of Molecular Biology and Molecular Medicine,* (Meyers, R. A., Ed.) pp 302-325, VCH Pub., Weinheim, Germany.

(10) Sherman, F. (2002) Getting Started with Yeast. *Methods Enzymol 350*, 3-41.

(11) Chang, F., and Herskowitz, I. (1990) Identification of a gene necessary for cell cycle arrest by a negative growth factor of yeast: FAR1 is an inhibitor of a G1 cyclin, CLN2. *Cell 63*, 999-1011.

(12) Peter, M., and Herskowitz, I. (1994) Direct inhibition of the yeast cyclin-dependent kinase Cdc28-Cln by Far1. *Science 265*, 1228-31.

(13) Gartner, A., Jovanovic, A., Jeoung, D. I., Bourlat, S., Cross, F. R., and Ammerer, G. (1998) Pheromone-dependent G1 cell cycle arrest requires Far1 phosphorylation, but may not involve inhibition of Cdc28-Cln2 kinase, in vivo. *Mol Cell Biol 18*, 3681-91.

(14) Gartner, A., Nasmyth, K., and Ammerer, G. (1992) Signal transduction in Saccharomyces cerevisiae requires tyrosine and threonine phosphorylation of FUS3 and KSS1. *Genes Dev 6*, 1280-92.

(15) Wang, Y., Marotti, L. A., Jr., Lee, M. J., and Dohlman, H. G. (2005) Differential regulation of G protein alpha subunit trafficking by mono- and polyubiquitination. *J Biol Chem 280*, 284-91.

(16) Wang, Y., and Dohlman, H. G. (2002) Pheromone-dependent ubiquitination of the mitogen-activated protein kinase kinase Ste7. *J Biol Chem 277*, 15766-72.

(17) Wang, Y., and Dohlman, H. G. (2006) Regulation of G protein and mitogen-activated protein kinase signaling by ubiquitination: insights from model organisms. *Circ Res 99*, 1305-14.

(18) Marotti, L. A., Jr., Newitt, R., Wang, Y., Aebersold, R., and Dohlman, H. G. (2002) Direct identification of a G protein ubiquitination site by mass spectrometry. *Biochemistry 41*, 5067-74.

(19) Torres, M. P., Lee, M.J, Ding, F., Purbeck, C., Kuhlman, B., Dokholyan, N.V., Dohlman, H.G. (2009) G Protein Mono-ubiquitination by the Rsp5 Ubiquitin Ligase. *Journal of Biological Chemistry 284*, 8940-8950.

(20) Esch, R. K., Wang, Y., and Errede, B. (2006) Pheromone-induced degradation of Ste12 contributes to signal attentuation and the specificity of developmental fate. *Eukaryot. Cell 5*, 2147-2160.

(21) Hicke, L., and Riezman, H. (1996) Ubiquitination of a yeast plasma membrane receptor signals its ligand- stimulated endocytosis. *Cell 84*, 277-87.

(22) Roth, A. F., and Davis, N. G. (1996) Ubiquitination of the yeast a-factor receptor. *J Cell Biol 134*, 661-74.

(23) Hicke, L., Dunn, R. (2003) Regulation of membrane protein transport by ubiquitination and ubiquitin-binding proteins. *Annu Rev Cell Dev Biol 19*, 141-172.

(24) Wang, Y., Ge, Q., Houston, D., Thorner, J., Errede, B., and Dohlman, H. G. (2003) Regulation of Ste7 ubiquitination by Ste11 phosphorylation and the Skp1-Cullin-F-box complex. *J Biol Chem 278*, 22284-9.

(25) Metodiev, M., Matheos, D., Rose, M. D., and Stone, D. E. (2002) Regulation of MAPK Function by Direct Interaction with the Mating-Specific Galpha in Yeast. *Science 296*, 1483-1486.

(26) Guo, M., Aston, C., Burchett, S. A., Dyke, C., Fields, S., Rajarao, S. J., Uetz, P., Wang, Y., Young, K., and Dohlman, H. G. (2003) The yeast G protein α subunit Gpa1 transmits a signal through an RNA binding effector protein Scp160. *Mol Cell 12*, 517-24.

(27) Jordan, J. D., Landau, E. M., and Iyengar, R. (2000) Signaling networks: the origins of cellular multitasking. *Cell 103*, 193-200.

(28) Slessareva, J. E., Routt, S. M., Temple, B., Bankaitis, V. A., and Dohlman, H. G. (2006) Activation of the phosphatidylinositol 3-kinase Vps34 by a G protein alpha subunit at the endosome. *Cell 126*, 191-203.

(29) Backer, J. M. (2008) The regulation and function of Class II PI3Ks: novel roles for Vps34. *Biochemical Journal 410*, 1-17.

(30) Yan, Y., and Backer, J.M. (2007) Regulation of class III (Vps34) PI3Ks. *Biochemical Society Transactions 35*, 239-241.

(31) Vanhaesebroeck, B., Leevers, S. J., Ahmadi, K., Timms, J., Katso, R., Driscoll, P. C., Woscholski, R., Parker, P. J., and Waterfield, M. D. (2001) Synthesis and function of 3-phosphorylated inositol lipids. *Annu Rev Biochem 70*, 535-602.

(32) Murray, J. T., Panaretou, C., Stenmark, H., Miaczynska, M., and Backer, J.M. (2002) Role of Rab5 in the recruitment of hVps34/p150 to the early endosome. *Traffic 3*, 416-427.

(33) Herman, P. K., Stack, J. H., and Emr, S. D. (1991) A genetic and structural analysis of the yeast Vps15 protein kinase: evidence for a direct role of Vps15p in vacuolar protein delivery. *Embo J 10*, 4049-60.

(34) Herman, P. K., Stack, J. H., DeModena, J. A., and Emr, S. D. (1991) A novel protein kinase homolog essential for protein sorting to the yeast lysosome-like vacuole. *Cell 64*, 425-37.

(35) Budovskaya, Y. V., Hama, H., DeWald, D. B., and Herman, P. K. (2002) The C terminus of the Vps34p phosphoinositide 3-kinase is necessary and sufficient for the interaction with the Vps15p protein kinase. *J Biol Chem 277*, 287-94.

(36) Stack, J. H., DeWald, D. B., Takegawa, K., and Emr, S. D. (1995) Vesicle-mediated protein transport: regulatory interactions between the Vps15 protein kinase and the Vps34 PtdIns 3-kinase essential for protein sorting to the vacuole in yeast. *J Cell Biol 129*, 321-34.

(37) Raymond, C. K., Howald-Stevenson, I., Vater, C. A., and Stevens, T. H. (1992) Morphological classification of the yeast vacuolar protein sorting mutants:

evidence for a prevacuolar compartment in class E vps mutants. *Mol Biol Cell 3*, 1389-402.

(38) Stack, J. H., and Emr, S. D. (1994) Vps34p required for yeast vacuolar protein sorting is a multiple specificity kinase that exhibits both protein kinase and phosphatidylinositol-specific PI 3-kinase activities. *J Biol Chem 269*, 31552-62.

(39) Stack, J. H., Herman, P. K., Schu, P. V., and Emr, S. D. (1993) A membrane-associated complex containing the Vps15 protein kinase and the Vps34 PI 3-kinase is essential for protein sorting to the yeast lysosome-like vacuole. *Embo J 12*, 2195-204.

(40) Heenan, E. J., Vanhooke, J.L., Temple, B.R., Betts, L., Sondek, J.E., and Dohlman, H.G. (2009) Structure and function of Vps15 in the endosomal G protein signaling pathway. *Biochemistry 48*, 6390-6401.

(41) Kihara, A., Noda, T., Ishihara, N., and Ohsumi, Y. (2001) Two distinct Vps34 phosphatidylinositol 3-kinase complexes function in autophagy and carboxypeptidase Y sorting in Saccharomyces cerevisiae. *J Cell Biol 152*, 519-30.

(42) Obara, K., Sekito, T., and Ohsumi, Y. (2006) Assortment of phosphatidylinositol 3-kinase complexes- Atg14p directs association of complex 1 to the pre-autophagosomal structure in Saccharomyces cerevisiae. *Mol Biol Cell 17*, 1527-1539.

(43) Itakura, E., Kishi, C., Inoue, K., and Mizushima, N. (2008) Beclin 1 forms two distinct phosphatidylinositol 3-kinase complexes with mammalian Atg14 and UVRAG. *Mol Biol Cell 19*, 5360-5372.

(44) Zhong, Y., Wang, Q.J., Yan, Y., Backer, J.M., Chait, B.T., Heintz, N., and Tue, Z. (2009) Distinct regulation of autophagic activity by Atg14L and Rubicon associated with Beclin 1-phosphatidylinositol-3-kinase complex. *Nat Cell Biol 11*, 468-476.

(45) Stenmark, H., Aasland, R., Toh, B. H., and D'Arrigo, A. (1996) Endosomal localization of the autoantigen EEA1 is mediated by a zinc-binding FYVE finger. *J Biol Chem 271*, 24048-54.

(46) Ponting, C. P. (1996) Novel domains in NADPH oxidase subunits, sorting nexins, and PtdIns 3- kinases: binding partners of SH3 domains? *Protein Sci 5*, 2353-7.

(47) Simonsen, A., Lippe, R., Christoforidis, S., Gaullier, J. M., Brech, A., Callaghan, J., Toh, B. H., Murphy, C., Zerial, M., and Stenmark, H. (1998) EEA1 links PI(3)K function to Rab5 regulation of endosome fusion. *Nature 394*, 494-8.

(48) Simonsen, A., Gaullier, J.M., D'Arrigo, A., and Stenmark, H. (1999) The Rab5 effector EEA1 interacts directly with syntaxin-6. *J Biol Chem 274*, 28857-28860.

(49) Piper, R. C., and Katzmann, D.J. (2007) Biogenesis and function of multivesicular bodies. *Annu Rev Cell Dev Biol 23*, 519-547.

(50) Seaman, M. N. J., Caffrey, J.M., and Emr S.D. (1998) A membrane coat complex essential for endosome-to-Golgi retrograde transport in yeast. *J Cell Biol 142*, 665-681.

(51) Slessareva, J. E., and Dohlman, H. G. (2006) G protein signaling in yeast: new components, new connections, new compartments. *Science 314*, 1412-3.

(52) Sondek, J., Bohm, A., Lambright, D. G., Hamm, H. E., and Sigler, P. B. (1996) Crystal structure of a G-protein beta gamma dimer at 2.1A resolution. *Nature 379*, 369-74.

(53) Lambright, D. G., Sondek, J., Bohm, A., Skiba, N. P., Hamm, H. E., and Sigler, P. B. (1996) The 2.0 A crystal structure of a heterotrimeric G protein. *Nature 379*, 311-9.

(54) Huh, W. K., Falvo, J. V., Gerke, L. C., Carroll, A. S., Howson, R. W., Weissman, J. S., and O'Shea, E. K. (2003) Global analysis of protein localization in budding yeast. *Nature 425*, 686-91.

FIGURE LEGENDS

Figure 1.1. G protein signaling in *Saccharomyces cerevisiae.* Schematic overview of the pheromone-activated G protein signaling pathway in yeast. Key components of the pathway that originates at the plasma membrane and the pathway that originates at the endosome are shown.

Figure 1.2. Complexes of Vps15 and Vps34. The four primary different complexes that Vps15 and Vps34 are known to be present in are shown. The major functions of these complexes are indicated.

Figure 1.1

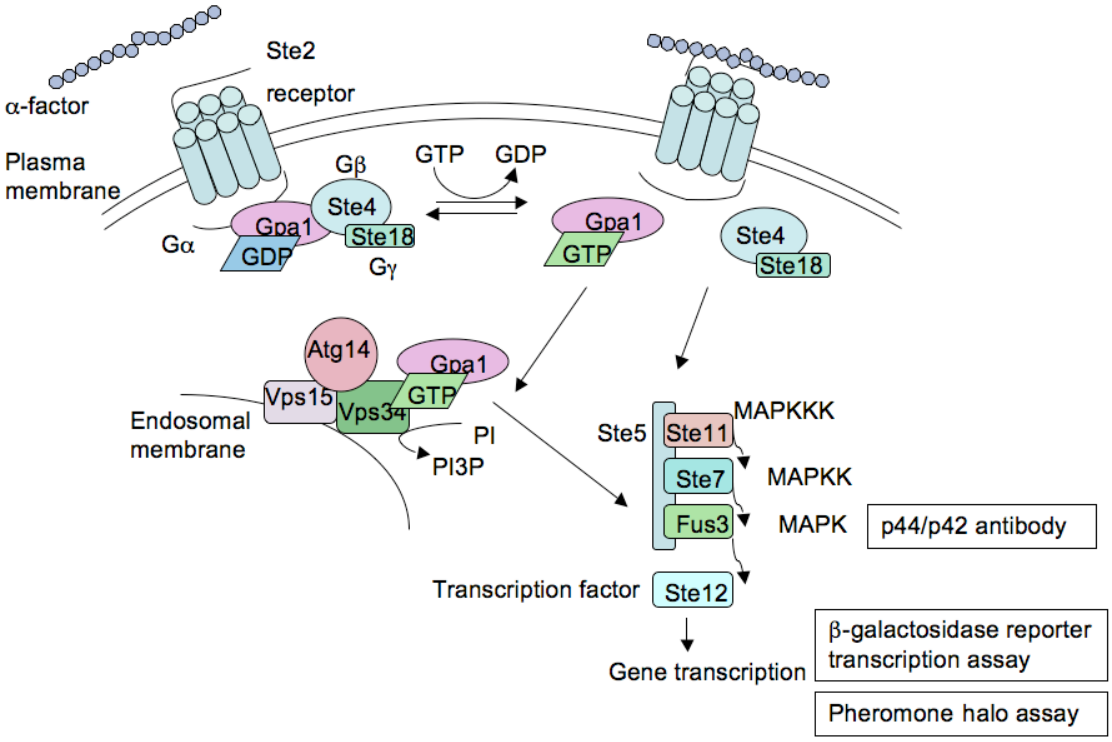
Ste2
receptor
α-factor
Plasma
membrane
Gβ
GTP
GDP
Ste4
Gpa1
Ste18
Gα
GDP
Gγ
Gpa1
GTP
Ste4
Ste18
Atg14
Gpa1
Vps15
GTP
Vps34
Endosomal
membrane
PI
PI3P
Ste5
Ste11
MAPKKK
Ste7
MAPKK
Fus3
MAPK
p44/p42 antibody
Transcription factor
Ste12
Gene transcription
β-galactosidase reporter
transcription assay
Pheromone halo assay

Figure 1.2

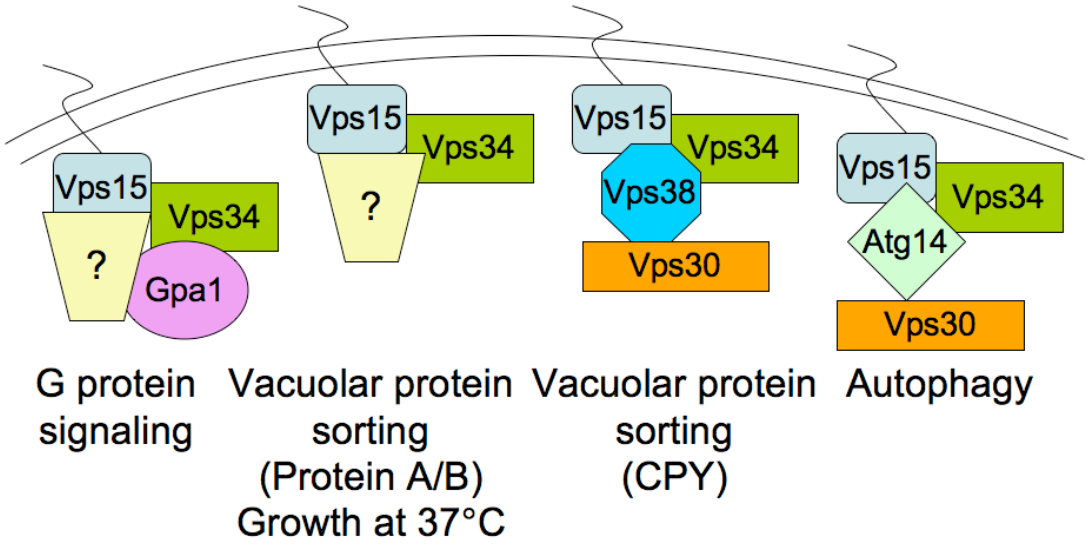
Vps15
Vps34
?
Gpa1
Vps15
Vps34
?
Vps15
Vps34
Vps38
Vps30
Vps15
Vps34
Atg14
Vps30
G protein signaling
Vacuolar protein sorting (Protein A/B) Growth at 37°C
Vacuolar protein sorting (CPY)
Autophagy

Chapter 2

Structure and Function of Vps15 in the Endosomal G Protein Signaling Pathway

Structure and Function of Vps15 in the Endosomal G Protein Signaling Pathway[†]

Erin J. Heenan[‡], Janeen L. Vanhooke[§], Brenda R. Temple[‡||], Laurie Betts[§⊥]

John E. Sondek[§‡], Henrik G. Dohlman[‡§*]

Department of Biochemistry and Biophysics and Department of Pharmacology,

University of North Carolina, Chapel Hill, NC 27599

[‡] Department of Biochemistry and Biophysics
[§] Department of Pharmacology
[||] R. L. Juliano Structural Bioinformatics Core

[⊥] Current Address:
Department of Structural Biology
University of Pittsburgh
1050 BST3
3501 Fifth Avenue
Pittsburgh, PA 15260

* Address correspondance to:
Henrik G. Dohlman, PhD
Department of Biochemistry and Biophysics
University of North Carolina
120 Mason Farm Road, CB 7260
Genetic Medicine, Suite 3010
Chapel Hill, NC 27599-7260
Tel.: (919) 843-6894, Fax: (919) 966-2852, E-mail: hdohlman@med.unc.edu

[†] Sources of Funding: This work was supported by National Institutes of Health Grants GM080739 (H.G.D.) and GM081881 (J.E.S.) and a T32 Cancer Cell Biology Training Grant (E.J.H.)

The coordinates and structure factors for the Vps15 WD repeat domain crystal structure have been deposited in the Protein Data Bank (accession code 3GRE) and will be released upon publication of this manuscript.

Running Title: Vps15 structure and function

ABBREVIATIONS

α-MF, alpha mating factor; CPY, carboxypeptidase Y; G6PDH, glucose-6-phosphate dehydrogenase; GDP, Guanosine diphosphate; GST, glutathione S-transferase; GTP, Guanosine-5'-triphosphate; ID, intermediate domain; IP, immunoprecipitation; KD, kinase domain; MAP, mitogen-activated protein; PD, pulldown; PtdIns, phosphatidylinositol; SDS-PAGE, sodium dodecyl sulfate – polyacrylamide gel electrophoresis; VPS, vacuolar protein sorting; WD, tryptophan-aspartate

ABSTRACT

G protein-coupled receptors mediate cellular responses to a wide variety of stimuli, including taste, light and neurotransmitters. In the yeast *Saccharomyces cerevisiae*, activation of the pheromone pathway triggers events leading to mating. The view had long been held that the G protein-mediated signal occurs principally at the plasma membrane. Recently, it has been shown that the G protein α subunit Gpa1 can promote signaling at endosomes and requires two components of the sole phosphatidylinositol-3-kinase in yeast, Vps15 and Vps34. Vps15 contains multiple WD repeats and also binds to Gpa1 preferentially in the GDP-bound state; these observations led us to hypothesize that Vps15 may function as a G protein β subunit at the endosome. Here we show an X-ray crystal structure of the Vps15 WD domain that reveals a seven-bladed propeller resembling that of typical Gβ subunits. We show further that the WD domain is sufficient to bind Gpa1 as well as to Atg14, a potential Gγ protein that exists in a complex with Vps15. The Vps15 kinase domain together with the intermediate domain (linking the kinase and WD domains) also contributes to Gpa1 binding, and is necessary for Vps15 to sustain G protein signaling. These findings reveal that the Vps15 Gβ-like domain serves as a scaffold to assemble Gpa1 and Atg14, whereas the kinase and intermediate domains are required for proper signaling at the endosome.

BACKGROUND AND INTRODUCTION

G protein-coupled receptors are highly conserved in organisms from yeast to humans. Upon stimulation, the receptor activates a G protein heterotrimer, causing the Gα subunit to release GDP, bind GTP, and dissociate from the Gβγ heterodimer. Following dissociation, the Gα and Gβγ subunits are able to activate downstream effector proteins *(1-3)*. Examples include adenylyl cyclase, MAP kinases, phosphatidylinositol (PtdIns) 3-kinase, and phospholipase C-β *(4)*.

In simple eukaryotes such as yeast, G protein-coupled receptors mediate processes essential for proper cell functioning including mating. MAT**a** and MATα cell types secrete small peptide pheromones, called **a**-factor and α-factor, respectively, that promote cell fusion and the formation of an **a**/α diploid. Activation of the pathway by pheromone leads to phosphorylation of various proteins that mediate new gene transcription, altered cell morphology, cell division arrest, and eventually cell fusion. Gβγ (Ste4/Ste18) initiates the pathway that originates from the plasma membrane and results in activation of the MAP kinases Fus3 and Kss1 (2). Gα (Gpa1) initiates a parallel pathway that operates at the endosomal membrane and results in activation of Fus3 in preference to Kss1 *(5)*. The pathway originating from the endosome requires Vps15 and Vps34, the regulatory and catalytic subunits of the only PtdIns 3-kinase known in yeast *(5-12)*. Further, Vps15 directly binds the unactivated (GDP-bound) form of Gpa1, while Vps34 directly engages the activated (GTP-bound form) of Gpa1. Additionally, both Vps15 and Vps34 are necessary for recruitment of Gpa1 to endosomes *(5)*. G protein activation of Vps34 results in elevated production of PtdIns 3-P, and leads to the

endosomal recruitment of phospholipid binding proteins *(5)*.

Vps15 is an extremely large protein (166 kDa) and contains several distinct domains. These include an N-terminal serine/threonine kinase domain *(6, 8, 11, 12)*, a C-terminal WD-repeat containing domain *(5, 13)*, and an internal domain that bridges the kinase- and WD-domains. It has been shown previously that the kinase activity of Vps15 is necessary for full activation of the G protein signal *(5)*. However, the precise role of the kinase domain including any substrates is unknown. The internal domain contains several HEAT repeats that have been shown to be important for protein−protein interactions (hereafter referred to as the intermediate domain or ID) *(13-15)*. The WD domain was of particular interest to us because of the recognized importance of the WD-containing Gβ protein, Ste4, in the pheromone-mediated pathway that originates from the cell plasma membrane.

Here, we examine the roles of the different domains of Vps15 in binding to Gpa1, as well as in transmitting the G protein signal. We demonstrate that the WD-domain of Vps15 has a seven-bladed propeller structure like that of known Gβ proteins. We show further that the Gβ-like domain acts in the manner of a scaffold to bring together proteins that propagate the pheromone response at the endosome. Finally, we show that it is the kinase domain with the intermediate domain that is necessary for Vps15 to transmit the G protein signal leading to activation of Fus3 as well as for other Vps15 signaling functions in the cell.

EXPERIMENTAL PROCEDURES

Protein Expression and Purification

The coding sequence of Vps15 WD repeat domain (residues 1027−1454) was amplified by PCR from *S. cerevisiae* BY4741 genomic DNA and inserted into a modified pFastBac vector through ligation independent cloning *(16)*. Baculovirus coding for production of recombinant His_6-Vps15 WD repeat domain was prepared according to the Bac-to-Bac method (Invitrogen). Two liters of High-Five insect cells cultured in Express Five SFM (Gibco) to a density of 2×10^6 cells/mL were infected with the baculovirus for 48 h at 27 °C.

Cells were harvested by centrifugation at 4400*g* and resuspended in buffer A [20 mM Tris pH 8.0, 300 mM NaCl, 10 mM imidazole, 10% (v/v) glycerol, 0.02% NaN_3] with Complete EDTA-free protease inhibitor cocktail (Roche) and PMSF. The cells were lysed with three passes through an Emulsiflex C5 homogenizer (Avestin) operating at 15000 psi, and the lysate was clarified by centrifugation at 105000*g*. The resulting supernatant was filtered through a 0.45 μm low protein binding filter and applied to a 1 mL HisTrap HP column (GE Healthcare). The column was washed with 30 column volumes (CV) of buffer A followed by 30 CV of 5% buffer B (buffer A containing 1 M imidazole). His_6-Vps15 WD repeat domain was eluted with a step gradient of 30% buffer B. To prevent aggregation during the elution, fractions of 1 mL were collected into tubes containing 2 mL buffer C [20 mM Tris pH 8.0, 300 mM NaCl, 2 mM EDTA, 10% glycerol (v/v), 2 mM DTT, 0.02% (w/v) NaN_3]. The fractions containing the protein were

pooled immediately and applied to a Sephacryl S-300 26/60 column (GE Healthcare) equilibrated with buffer D (buffer C without EDTA). Vps15 WD repeat domain was eluted with buffer D and concentrated to 11 mg/mL in a Centriprep YM10 centrifugal concentrator (Millipore). Aliquots of the protein were quick frozen in liquid nitrogen and stored at −80 °C.

Crystallization and Data Collection

Crystals of the Vps15 WD repeat domain were grown at 18 °C by macroseeding small crystals into microbatch setups. The batch solution was prepared by quickly mixing the protein (6 mg/mL) with an equal volume of precipitant solution composed of 1.4 M ammonium malonate pH 6.5, 100 mM sodium acetate pH 4.6, 4% (v/v) isopropanol. Crystals suitable for X-ray diffraction were obtained within 7−10 days. Prior to data collection, crystals were cryoprotected by stepwise transfer into 20% (v/v) ethylene glycol in synthetic mother liquor (1.2 M ammonium malonate pH 6.5, 100 mM sodium acetate pH 4.6, 2% isopropanol), after which they were suspended in loops (Hampton Research) and quick frozen by immersion into liquid nitrogen. The crystals belong to the space group $P3_121$, with unit cell dimensions of $a = b = 86.5$ Å, $c = 132.8$ Å, and one molecule in the asymmetric unit.

Crystals used in derivative screening were stabilized for several hours in synthetic mother liquor prior to soaking in heavy atom solutions. The gold derivative ultimately used to determine the phases was prepared with a 10 min soak in 5.8 mM $KAu(CN)_2$. A single wavelength anomalous dispersion data set ($\lambda = 11.917$ keV) was collected from a

single crystal at the SER-CAT 22-BM beamline at the Advanced Photon Source (Argonne National Laboratory, Argonne, IL). A native data set was subsequently collected from a single crystal at the SER-CAT 22-ID beamline. All data were processed and scaled with HKL2000 *(17)*. Relevant data collection and processing statistics are listed in Table 2.1.

Phasing, Model Building and Refinement

The positions of the gold atoms in the derivative crystal were found using the program SHELXD *(18)*, and the correct hand for the coordinates was determined with SHELXE. Refinement of the gold atom coordinates and computation of the phases was performed with the CCP4 program MLPHARE, and the phases were subsequently improved with solvent flattening and histogram matching using the method of ref 19. The initial electron density map was easily interpretable, and 319 of the 437 residues in the protein were automatically fitted with the program ARP/wARP *(20)*. Additional residues were built into the map using COOT *(21)*. The structure of the His_6-Vps15 WD repeat domain was completed using native protein data and iterative cycles of model building and refinement with COOT and the CCP4 program REFMAC *(22)*. The final model has a crystallographic R-value of 20.9% (R-free 24.6%) for all data from 50 to 1.8 Å and includes residues 1031−1040, 1042−1386, 1389−1410, and 1424−1454. No electron density was present for the N-terminal histidine tag or Vps15 residues 1027−1030, 1041, 1387, 1388, and 1411−1423. In the Ramachandran plot, 96.2% of the residues are in the most favored region, 3.0% are in the generously allowed region, and 0.8% are in the disallowed region. Relevant phasing and refinement statistics are listed in Table 2.2, and

representative electron density is shown in Supporting Figure 2.1, Supporting Information.

Strains and Plasmids

Standard methods for the growth, maintenance, and transformation of yeast and bacteria and for the manipulation of DNA were used throughout. Yeast *Saccharomyces cerevisiae* strains used in this study are BY4741 (*MAT***a** *leu2*Δ *met15*Δ *his3*Δ *ura3*Δ) and BY4741-derived gene deletion mutants (Invitrogen). The *vps15*Δ strain used is described in ref 5.

Previously described yeast shuttle vectors and expression plasmids are pRS315-ADH-Flag (CEN, amp^R, *LEU2, ADH1* promoter/terminator and either a Flag epitope that can be added 5′ with a *SacI* site or 3′ with an *Xma*I site), pRS316-ADH-Myc (CEN, amp^R, *URA3, ADH1* promoter/terminator and either a Myc epitope that can be added 5′ with a *SacI* site or 3′ with an *Xma*I site) *(23)*, pAD4M-GST, pAD4M-Gpa1-GST, pRS316-ADH-Gpa1−2myc *(24)*, pAD4M-Gpa2-GST *(25)*, pRS423-FUS1-LacZ *(26)*. Truncations of Vps15 were designed based upon the crystal structure of the WD domain of Vps15 (**Figure 2.1**) as well as domain predictions from SMART and three different secondary structure predictions *(27-32)*. For naming purposes, Vps15 is considered to possess three domains: the kinase domain (KD) from residues 1−294, the WD domain (WD) from residues 1027−1454 and the intermediate domain (ID) spanning the region between the kinase domain and the WD domain. Plasmids pRS315-ADH-Flag-$Vps15^{KD}$ (using primers Vps15fn and Vps15ksrn), pRS315-ADH-Flag-$Vps15^{KD,ID}$ (using primers

Vps15fn and Vps15klrn), pRS315-ADH-Flag-Vps15^{ID,WD} (using primers Vps15wdlfn and Vps15rn), pRS315-ADH-Flag-Vps15^{WD} (using primers Vps15wdsfn and Vps15rn), pRS316-ADH-Myc-Vps15^{ID,WD} (using primers Vps15wdlfn and Vps15rn), and pRS316-ADH-Myc-Vps15^{WD} (using primers Vps15wdsfn and Vps15rn) were constructed by PCR amplification of *VPS15* from BY4741 genomic DNA, incorporation of the product into a TOPO vector (Invitrogen), digestion by *SacI*, and ligation into pRS315-ADH-Flag or pRS316-ADH-Myc. Plasmids pRS315-ADH-Vps15^{KD,ID,WD}-Flag (using primers Vps15fc and Vps15rc), pRS315-ADH-Vps15^{ID,WD}-Flag (using primers Vps15wdlfc and Vps15rc), pRS315-ADH-Vps15^{WD}-Flag (Vps15wdsfc and Vps15rc), pRS316-ADH-Vps15^{WD}-Myc (using primers Vps15wdsfc and Vps15rc) were constructed by PCR amplification of *VPS15* from BY4741 genomic DNA, incorporation into a TOPO vector (Invitrogen), digestion by *Xma*I and ligation into pRS315-ADH-Flag or pRS316-ADH-Myc. Plasmids pRS315-ADH-Flag-Atg14 (using primers Atg14fn and Atg14rn) and pRS316-ADH-Myc-Atg14 (using primers Atg14fn and Atg14rn) were generated through PCR amplification of *ATG14* from BY4741 genomic DNA, incorporation of the product into TOPO vector, digestion by *SacI*, and ligation into pRS315-ADH-Flag or pRS316-ADH-Myc. pRS316-ADH-3Myc-Atg14 was constructed by the annealing of two homologous oligonucleotides incorporating the sequence of 2 Myc epitopes as well as overhangs homologous to *Bam*HI and *Sal*I restriction sites (using the primer 2myc and its complement). pRS316-ADH-Myc-Atg14 was then digested with *Bam*HI and *Sal*I and ligated with the annealed oligonucleotides. Myc-Vps15$^{WD\ R1261A}$ (using primer Vps15R1261A and its complement), Myc-Vps15$^{WD\ R1261K}$ (Vps15R1261K and its

complement), Myc-Vps15$^{ID,WD\ R1261A}$ (Vps15R1261A and its complement), Myc-Vps15$^{ID,WD\ R1261K}$ (Vps15R1261K and its complement), Vps15$^{KD,ID,WD\ R1261A}$ Flag (Vps15R1261A and its complement), and Vps15$^{KD,ID,WD\ R1261K}$ Flag (Vps15R1261K and its complement) in pRS316-ADH-Myc and pRS315-ADH-Flag respectively were created using QuikChange (Stratagene). Plasmid pRS306 Vps15$^{KD,ID,WD\ R1261A}$-Flag was created by digestion of the pRS315 construct with *Bam*HI and ligation into the corresponding *Bam*HI site of pRS315 construct. Genomic integration was performed using *Hpa*I. All plasmids described were confirmed by sequencing.

Purification of Flag Epitope-tagged Proteins

Plasmids pRS315-ADH-Flag-Vps15^{KD}, pRS315-ADH-Flag-Vps15^{KD,ID}, pRS315-ADH-Vps15^{KD,ID,WD}-Flag, pRS315-ADH-Flag-Vps15^{ID,WD}, pRS315-ADH-Vps15^{ID,WD}-Flag, pRS315-ADH-Flag-Vps15^{WD}, pRS315-ADH-Vps15^{WD}-Flag, and pRS315-ADH-Flag were transformed into either wildtype or *atg14Δ* cells expressing pRS316-ADH-Myc, pRS316-ADH-Vps15^{WD}-Myc, pRS316-ADH-Gpa1−2Myc, or pRS316-ADH-3Myc-Atg14. A 50 mL culture of cells containing each plasmid was grown in SCD-Ura-Leu until $A_{600\ nm}$ 0.8. Cells were disrupted in buffer E (50 mM Tris-Cl pH 8.0, 200 mM NaCl, 0.1% Triton X-100, 25 mM beta-glycerophosphate, 1 mM EDTA, 2 protease inhibitor cocktail pellets per 50 mL (Roche)) for 15 min at 4 °C using a vortex fitted with a 60-microtube headpiece. Lysates were then combined at 4 °C with gentle rotation for 25 min (this step omitted in several experiments) to ensure solubilization of membrane bound proteins. The lysates were then centrifuged at 16000*g* for 1 min, and then again for

25 min. Protein determination was performed for all samples, and each lane contains an equal total concentration and volume of protein. The supernatant was mixed with 40 μL of Flag affinity resin (Sigma-Aldrich) that had been equilibrated with buffer E. The lysates and beads were mixed with gentle rotation for 2 h at 4 °C. The beads were washed five times with 500 μL of buffer E. Bound proteins were then eluted from the beads with two 20 μL washes of 0.25 mg/mL 3× Flag Peptide (Sigma-Aldrich) and collected by centrifugation at 4900*g* for 1 min. 6× SDS buffer was added to the eluted proteins to a final concentration of 1× and samples were heated at 95 °C for 5 min. Samples were resolved by 10% SDS−PAGE or 7.5% SDS−PAGE and immunoblotting with anti-Myc 9E10 cell culture supernatant at a dilution of 1:100 *(33)*, anti-Flag mouse monoclonal M2 antibodies at a dilution of 1:1000 (Sigma-Aldrich), anti-G6PDH antibodies at a dilution of 1:50000 (Sigma-Aldrich), and the secondary antibodies goat antimouse or goat antirabbit at a dilution of 1:10000 (Biorad). Detection was performed with chemiluminescent ECL substrate (PerkinElmer).

Purification of Glutathione S-transferase (GST) Fusion Proteins

pRS316-ADH-Myc-Vps15$^{WD\ R1261A}$, pRS316-ADH-Myc-Vps15$^{WD\ R1261K}$, pRS316-ADH-Myc-Vps15$^{ID,WD\ R1261A}$, pRS316-ADH-Myc-Vps15$^{ID,WD\ R1261K}$, pRS316-ADH-Myc-Vps15^{ID,WD}, pRS316-ADH-Myc-Vps15^{WD}, and pRS316-ADH-Myc were cotransformed into wildtype strains with either pRS315-ADH-Flag, pAD4M-Gpa1-GST, or pAD4M-Gpa2-GST. Cells were disrupted in buffer F (200 mM Tris pH 7.6, 150 mM NaCl, 1 mM EDTA, 0.1% Triton X-100 and 2 protease inhibitor cocktail pellets per 50 mL) and prepared in a manner similar to that described for purification of Flag epitope

tagged proteins, except that the lysis time was decreased to 10 min. For determination of nucleotide specificity of binding, either 5 mM $MgCl_2$ and 10 μM GDP or 10 mM NaF, 5 mM $MgCl_2$, 10 μM GDP, and 30 μM $AlCl_3$ (GDP-AlF_4^-) was added to buffer F. Supernatants were mixed with 40 μL of glutathione-Sepharose resin (GE Healthcare) equilibrated with buffer F. The glutathione-Sepharose resin was incubated with the lysate and washed in a manner similar to that described above for the immunoprecipitation of Flag-tagged proteins. Bound proteins were then eluted from the beads with two 20 μL washes of 10 mM reduced glutathione, 50 mM Tris pH 8.0 and were collected by centrifugation at 4900*g* for 1 min. 6× SDS buffer was added to the eluted proteins to a final concentration of 1× and samples were heated at 95 °C for 5 min. Samples were resolved by 10% SDS−PAGE and immunoblotting with anti-GST polyclonal antibody at a dilution of 1:1500 (a gift of Joan Steitz), anti-Myc 9E10 monoclonal antibodies at a dilution of 1:100, anti-G6PDH antibodies at a dilution of 1:50000 (Sigma-Aldrich), anti-Ste4 antibodies at a dilution of 1:2000 (a gift of Duane Jenness), and the secondary antibodies goat antimouse or goat antirabbit at a dilution of 1:10000 (Biorad). Detection was performed with chemiluminescent ECL substrate (PerkinElmer).

Cell Extract Preparation and Analysis for MAP kinase Phosphorylation and Carboxypeptidase Y Sorting

Plasmids pRS315-ADH-Flag-Vps15^{KD}, pRS315-ADH-Flag-Vps15^{KD,ID}, pRS315-ADH-Vps15^{KD,ID,WD}-Flag, pRS315-ADH-Flag-Vps15^{ID,WD}, pRS315-ADH-Vps15^{ID,WD}-Flag, pRS315-ADH-Flag-Vps15^{WD}, pRS315-ADH-Vps15^{WD}-Flag, and pRS315-ADH-Flag were transformed into either wildtype or *vps15*Δ cells. Wildtype, *vps15*Δ, and

vps15^{R1261A} strains were also analyzed for MAP kinase phosphorylation and carboxypeptidase Y sorting without any additional plasmid transformation. Cells were grown to $A_{600\ nm}$ 0.8 in 20 mL SCD-Leu and then split and either treated with 3 μM α-MF pheromone or left untreated at 30 °C for 30 min. The reaction was stopped by addition of 5% trichloroacetic acid, and the cells were harvested by centrifugation and frozen at −80 °C. Cell extracts were prepared as previously described *(34)*, and resolved by 10% SDS−PAGE and immunoblotted using p44/p42 MAP kinase antibody at 1:500 (Cell Signaling Technology) or anti-CPY antibody at 1:2000 (a gift of Pat Brennwald), anti-G6PDH antibodies at a dilution of 1:50000 (Sigma-Aldrich), and the secondary antibody goat antirabbit at a dilution of 1:10000 (Biorad). Detection was performed with chemiluminescent ECL substrate (PerkinElmer).

Pheromone Response Assays

Reporter-transcription (β-galactosidase assay utilizing the pRS423-*FUS1-lacZ* plasmid) and growth arrest (halo) assays were performed as described previously *(26, 35)*.

RESULTS

The structure of the Vps15 WD domain is presented in **Figure 2.1**. The protein folds as a seven-bladed propeller as predicted in a prior homology modeling analysis *(5)*. As described previously, the WD repeat units are not equivalent to the blades of the propeller, but are comprised rather of the fourth strand of one blade and the first three strands of the blade that follows *(36)*. The overall architecture of the Vps15 WD domain is similar to that of the transducin G protein β subunit ($G\beta_1$) *(36)*, and superposition of the structures with the CCP4 topological comparison program TOP yields a rms deviation of 2.7 $Å^2$ for the Cα carbons *(37, 38)*. There are several key differences in the overall structures of the two proteins. The N-terminus of Gβ folds as an α-helix that extends away from the propeller. In the case of Vps15, the corresponding region is largely unstructured, and it packs against the bottom surface of the propeller. There are four insertions in the Vps15 propeller (**Figure 2.1A**): an extended loop containing a 3_{10} helix between WD repeats 1 and 2 (residues 1110−1121); an extension of strands 3 and 4 of blade 3 (residues 1156−1172); a large loop with 3_{10} helical twists within the sixth WD repeat (residues 1318−1351), and two additional β-strands within the seventh WD repeat (residues 1385−1426).

Heterotrimeric G protein β subunits form obligate heterodimers with Gγ subunits. The interaction between Gβ and Gγ is largely hydrophobic; the first α-helix of the γ subunit forms a coiled-coil interaction with the Gβ N-terminal α-helix, whereas the second α-helix wraps into a cleft on the bottom surface of the Gβ propeller *(36)* (**Figure**

2.1B). As noted above, the N-terminus of the Vps15 WD repeat domain is folded against the bottom of the propeller (**Figure 2.1C**), and the stretch of N-terminal residues immediately before the propeller partially occlude a potential Gγ binding surface. However, inspection of the hydrophobic regions on the bottom surface of the propeller (upon removal of the N-terminus) of Vps15 indicates there is no equivalent binding cleft for interaction with a Gγ subunit. This finding provides an explanation for our ability to express, purify, and crystallize the Vps15 WD domain in the absence of an associated Gγ. The G protein α subunit typically interacts with Gβγ through two interfaces, termed the "switch interface" and the "N-terminal interface" *(39)*. The interaction at the switch interface involves residues in and around switch I and switch II of Gα as well as conserved hydrophobic residues on the top surface of the Gβ propeller (Tyr-59, Trp-99, Met-101, and Leu-117 in $G\beta_1$). The N-terminal interface is formed by interaction of the Gα N-terminal α-helix with four conserved residues in blade 1 of the Gβ propeller (Leu-55, Lys-78, Ile-80, and Lys-89 in $G\beta_1$). The Vps15 propeller provides neither of these binding surfaces for interaction with a Gα subunit. The region that corresponds to the switch interface is comprised of polar amino acids (Thr-67, Thr-113, Thr-116, and Lys-131). Further, superposition of the Vps15 structure on the Gαβγ heterotrimer suggests the Vps15 residues corresponding to the N-terminal interface (Glu-62, Val-87, Lys-89 and Ser-104) would not form a tight interaction with the Gα N-terminal α-helix (not shown). The inability of the Vps15 WD domain to form these interactions, or the absence of a corresponding Gγ subunit, may explain our failure to isolate a stable heterodimeric complex of Gpa1 with the WD domain-containing fragment of Vps15 (by size exclusion chromatography, not shown).

The data presented above reveal the absence of a canonical Gα-binding interface within the Vps15 WD domain. Thus, we considered whether other domains of Vps15 might contribute to Gpa1 interactions. In order to determine the possible binding role for these other domains, we coexpressed Gpa1 with several truncations of Vps15 including (a) the kinase domain alone, (b) the kinase domain with the intermediate domain, (c) full-length Vps15, (d, e) the intermediate domain with the WD domain, and (f, g) the WD domain alone (**Figure 2.2**). Whereas Gpa1 was tagged with the Myc epitope (located internally to preserve function), variants of Vps15 were tagged at the N- and C-terminus with the Flag epitope. We eliminated from consideration any Flag-tag fusions that did not express. We then immunoprecipitated Vps15 and monitored the presence of coprecipitating Gpa1 by immunoblotting. Differences in the apparent abundance of Vps15 truncations could reflect differences in actual abundance or more likely differences in the position of the epitope tag (compare lanes f and g, containing $Vps15^{WD}$-Flag and Flag-$Vps15^{WD}$ respectively) as well as the size of the tagged protein (which could affect the protein transfer and immunoblot detection). As shown in **Figure 2.2**, the WD domain of Vps15 is sufficient to bind Gpa1, while the kinase domain alone failed to interact. However, the kinase domain with the intermediate domain was capable of binding to Gpa1. These data indicate that the intermediate domain, in addition to the Gβ-like WD domain, of Vps15 contributes to the stable interaction with Gpa1.

Vps15 is known to exist in a stable multiprotein complex that includes Atg14 or Vps38 (UVRAG in animals), as well as Vps34 and Vps30 (Beclin-1 in animals) *(40-45)*. Atg14 has sequence similarity to canonical Gγ proteins (5). Thus, we investigated if the

Vps15 Gβ-like domain binds to the Gγ-like protein Atg14. To this end we immunoprecipitated each of the Vps15 truncation mutants and monitored copurification of Atg14 by immunoblotting, as described above for Gpa1. As shown in **Figure 2.3**, the WD domain of Vps15 is indeed sufficient to bind to Atg14. The kinase domain alone is also capable of binding to Atg14 (**Figure 2.3**). Typical G protein α subunits bind to the Gγ subunit indirectly, through the common binding partner Gβ. Likewise, Gpa1 bound to the Vps15 WD domain even in the absence of Atg14 expression (**Figure 2.4**). Taken together, these data indicate that the Vps15 Gβ-like domain exists in a multisubunit complex with the Gα and Gγ-like proteins.

Although the crystal structure of the WD-like domain of Vps15 shows that it is comprised of a seven-bladed propeller structure, similar to that of canonical Gβ proteins, this analysis also revealed a lack of conservation in the predicted Gα-binding interface. The lack of a canonical Gα-binding site within Vps15 indicates that interaction must occur in a distinct manner. Accordingly, we undertook a molecular evolution analysis to identify potential binding residues within Vps15. We first generated a multiple-sequence alignment of Vps15 orthologs from several fungi, arthropods, mammals, and amphibians (Supporting Information). Invariant and highly conserved residues within this alignment were placed in a spatial context by mapping them onto the crystal structure of Vps15 (far right panel of **Figure 2.1A**). This analysis revealed two residues, Arg-1261 and Phe-1262, that are invariant across all orthologs, implying a strong evolutionary pressure to preserve function. In addition, the side chains protrude into the solvent, making them available for protein−protein interactions. Two additional invariant residues were found

on the opposite side of the Vps15 propeller, Glu-60 and Ser-104. However, these two residues form multiple hydrogen bonds to each other and may therefore be important for structural constraints. We observed no other invariant residues on the surface of Vps15. To determine the importance of the conserved Arg-1261, we examined the functional consequences of replacing this residue within Vps15. For these experiments, we purified Gpa1 fused to glutathione *S*-transferase (GST) and monitored copurification of Vps15 or various Vps15 truncations. Gpa1-GST was used in this case to corroborate the results of the Vps15-immunopreciptation experiments shown above. Additionally, the GST purification method is in our experience better suited for analysis of nucleotide-dependent interactions of G protein α and βγ subunits. Accordingly, the WD domain of Vps15 was coexpressed with Gpa1-GST or with a second G protein α subunit Gpa2-GST, used here as a negative control (**Figure 2.5**). Cell lysates were mixed with glutathione-Sepharose resin, washed extensively, eluted with reduced glutathione, and analyzed by immunoblotting using antibodies against GST (to detect purified Gpa1 or Gpa2) and Myc (to detect any copurifying Vps15). Although Ste4 was tagged with Myc, it did not bind well with an anti-Myc antibody, and was instead detected using an anti-Ste4 antibody (data not shown, see **Figure 2.7**). As shown in **Figure 2.5**, the Vps15 WD domain copurified with Gpa1 but did not copurify with Gpa2.

We then investigated the functional role of the conserved Arg (**Figure 2.1**). This residue was of particular interest because of a similarly conserved arginine "finger" present in most G proteins *(46-52)*. In G protein α subunits the arginine finger acts *in cis* to stabilize the transition state, promote GTP hydrolysis, and turn off the transmitted

signal *(46, 53)*. Thus, we substituted Arg-1261 in both a conservative (to Lys) and nonconservative (to Ala) manner, and determined the ability of each mutant to bind to Gpa1 as described above. As shown in **Figure 2.5**, substitution of Arg-1261 to either Lys or Ala resulted in diminished copurification with Gpa1-GST. This result indicates that Arg-1261 is necessary for Vps15 to bind efficiently to Gpa1. These mutants are likely to be properly folded given that other functions are preserved (see below).

We have shown previously that Vps15 is needed for proper pheromone responses, including pheromone-dependent MAP kinase activation, gene transcription, and cell-division arrest. Thus, we investigated the role of Arg-1261 in pheromone signaling. To monitor MAP kinase activity, cell extracts were analyzed by immunoblotting using antibodies against the dually phosphorylated, fully active forms of Fus3 and Kss1 *(54)*. As shown previously, cells lacking *VPS15* exhibit diminished Fus3 phosphorylation after pheromone stimulation; in contrast, cells expressing Vps15^{R1261A} exhibit wildtype levels of MAP kinase phosphorylation (**Figure 2.6A**). To monitor transcriptional activation, we employed a reporter comprised of a pheromone-inducible promoter and β-galactosidase (*FUS1-lacZ*). As shown previously, cells lacking *VPS15* exhibit dampened induction and a >3-fold rightward shift in the EC_{50} for pheromone stimulation, whereas cells expressing Vps15^{R1261A} exhibited wildtype transcription activity (**Figure 2.6C**). Finally, using the growth arrest plate assay (halo assay), we monitored the ability of the cells to undergo cell division arrest in response to pheromone. Once again, Vps15^{R1261A}-expressing cells produced wildtype zones of growth inhibition (**Figure 2.6D**). Therefore, while it contributes to Gpa1 binding, Arg-1261 does not contribute to Vps15-mediated signaling.

In addition to its role in pheromone signaling, Vps15 has well-established functions in promoting autophagy and at least two types of protein trafficking *(6-8, 10, 12, 42, 45, 55, 56)*. Vps15 is needed for newly synthesized vacuolar proteins, such as carboxypeptidase Y (CPY), to move from the endoplasmic reticulum, through the Golgi, to the endosome, and finally to the vacuole compartment. During transport, the newly synthesized CPY becomes modified in the ER to the pro-CPY1 form (67 kDa), then processed in the Golgi to the pro-CPY2 form (69 kDa), and finally it is modified in the vacuole to yield the mature protein product (61 kDa) *(10, 12, 42, 55)*. To determine if Arg-1261 has any role in CPY sorting, we prepared extracts from $Vps15^{R1261A}$ cells, treated with or without pheromone, and monitored the maturation of CPY by immunoblotting. As shown in **Figure 2.6B**, vacuolar sorting of carboxypeptidase Y is unaffected by substitution of Arg-1261 in Vps15.

We have shown above that the WD domain of Vps15 is sufficient to bind Gpa1 in vitro, and does so in a manner that depends on Arg-1261. Nevertheless, Vps15 is capable of promoting the G protein signal in vivo even when Arg-1261 is mutated. On the basis of these findings, we postulated that the kinase and/or intermediate domains of Vps15 might contribute more substantially to the signaling or trafficking functions of the protein. For instance, we showed above that the Vps15 intermediate domain as well as the WD domain contributes to Gpa1 binding. Thus, we investigated the functionality of Arg mutant forms of Vps15 containing the intermediate domain as well as the WD domain. The wildtype and arginine-substituted forms of Vps15 were coexpressed with either Gpa1-GST or Gpa2-GST, purified, and analyzed by immunoblotting using

antibodies against GST and Myc (to detect any copurifying Vps15). In this case, Gpa1 bound equally well to wildtype and mutant forms of Vps15 (**Figure 2.7A**). These findings indicate that the intermediate domain can compensate for the absence of the conserved arginine present in the WD domain, at least with respect to Gpa1 binding. Our hypothesis was that Arg-1261 functions in the manner of an arginine finger, to promote G protein binding and GTP hydrolysis. However, we have shown that this residue is a relatively minor contributor to binding. It remains to be determined if the adjacent conserved Phe-1262 likewise contributes to binding.

Previously, we showed that Vps15 binds preferentially to the unactivated, GDP-bound, form of Gpa1 *(5)*. Thus, we sought to determine if Arg-1261 contributes to the nucleotide-dependent interaction of Vps15 with Gpa1. Wildtype and mutant Vps15 were coexpressed with Gpa1-GST, then lysed in the presence of either GDP or GDP plus AlF_4^-, a transition state mimic that induces the activated conformation of Gα. As observed previously for full-length Vps15, the WD domain with the intermediate domain of Vps15 bound preferentially to GDP-bound (unactivated) Gpa1. The arginine mutants likewise bound preferentially to unactivated Gpa1 (**Figure 2.7B**). These results indicate that neither the kinase domain nor the conserved Arg-1261 is necessary to maintain the nucleotide-specificity of Vps15 binding to Gpa1.

The data presented above reveal that the intermediate and WD domains of Vps15 both contribute to Gpa1 binding, and are sufficient to confer nucleotide-specificity of interaction. We have shown previously that Vps15 is required for G protein signaling at

the endosome *(5)*. However, we have already ruled out a role for the conserved arginine in sustaining the G protein signaling function of Vps15. These findings suggest that domains necessary for binding and for signaling functions may not fully overlap. Thus, we investigated which domains of Vps15 contribute to pheromone signaling, using the same signaling assays described above in **Figure 2.6**. First we determined which domains of Vps15 are necessary to confer MAP kinase activation. As shown in **Figure 2.8A**, the kinase domain with the intermediate domain is sufficient to sustain MAP kinase activation in response to pheromone. Likewise, by the transcription-reporter assay the kinase domain with the intermediate domain is sufficient to confer wildtype transcriptional activation (**Figure 2.8C**) and growth-inhibition responses (**Figure 2.8D**). Finally, the kinase domain with the intermediate domain of Vps15 is sufficient to sustain at least some degree of carboxypeptidase Y maturation (**Figure 2.8B**). Neither the WD domain alone nor the WD domain with the intermediate domain is sufficient to sustain the signaling functions of Vps15 (**Figure 2.8A−D**).

Taken together, the findings presented above indicate that the WD domain of Vps15 has a Gβ-like structure and is sufficient to bind Gpa1, but cannot by itself sustain signaling. Whereas the conserved arginine contributes to Gpa1 binding, it is not required for Gpa1 signaling. By comparison, the intermediate domain also contributes to Gpa1 binding, and together with the kinase domain is both necessary and sufficient for pheromone signaling and vacuolar sorting activities.

DISCUSSION

The yeast pheromone response pathway represents one of the best-characterized models for the study of G protein signaling and regulation. Upon pheromone activation, Gα as well as Gβγ subunits activate downstream effectors. Release of Gβγ at the plasma membrane leads to activation of the MAP kinases Fus3 and Kss1 *(2)*. At the endosomal membrane, activated Gα transmits a signal that requires the PtdIns 3-kinase and results in activation of Fus3 *(5, 6)*. The endosomal PtdIns 3-kinase Vps34 is a direct binding partner for the GTP-activated form of Gpa1, and this interaction leads to elevated production of PtdIns 3-P. Thus, G protein signaling can occur at the endosomal membrane as well as at the plasma membrane.

Given that cell surface receptors and the Gβγ subunits Ste4 and Ste18 are concentrated at the plasma membrane, we considered whether there is an alternative Gβγ pair at the endosomal membrane. Here we have examined the extent to which Vps15 resembles more typical Gβ proteins such as Ste4. We have shown that Vps15 indeed possesses many structural and functional characteristics of canonical Gβ proteins. Both Vps15 and Ste4 are direct binding partners of Gpa1, and both bind preferentially to the unactivated (GDP-bound) form of the protein. Here we have demonstrated that Vps15 contains a seven-bladed propeller structure resembling that of known Gβ proteins. We showed further that the Gβ-like domain is sufficient to bind to Gpa1, as well as to the putative Gγ protein Atg14. As documented previously for typical Gγ subunits, Atg14 is not necessary to bridge the interaction of the Gα (Gpa1) and Gβ-like (Vps15) proteins.

While these findings highlight similarities between Vps15 and canonical Gβ proteins, there are also many important differences. Ste4 is predominantly expressed at the plasma membrane. Vps15 was previously shown by cell fractionation and fluorescence microscopy methods to be located at the endosome, Golgi, and vacuolar membranes *(11, 57)*. Typical Gβγ pairs are anchored to the plasma membrane through prenylation (and in some cases palmitoylation) of Gγ *(58)*, while the Vps15/Atg14 complex is anchored to the endosomal membrane through myristoylation of Vps15 *(12)*.

We have documented additional important differences between Ste4 and Vps15. The Gβ protein Ste4 is necessary to transmit the signal to downstream effectors at the plasma membrane *(2)*. In contrast, the Gβ-like WD domain of Vps15 is neither necessary nor sufficient to transmit the G protein signal at the endosome. Our efforts to dock Gpa1 onto the β propeller domain of Vps15 (using a similar orientation to that of known Gα-Gβ pairs) revealed no conserved interactions, indicating that the Gpa1-Vps15 interface must differ from that of more typical G protein subunits. Indeed, we have shown here that binding also entails the intermediate domain. Moreover, the intermediate domain and kinase domain are necessary and sufficient to restore full pheromone responsiveness to a *vps15* mutant strain. While binding and signaling activities of Vps15 require the intermediate domain, the sequence of this region provides no clues as to its function. Thus, we limited our analysis to the intermediate domain in conjunction with the well-defined kinase and/or WD domains only. These observations lead us to conclude that the Gβ-like WD domain of Vps15 serves primarily as a scaffold that promotes assembly of key signaling pathway components, including Gpa1 and Atg14, whereas the kinase

domain and the intermediate domain transmit the signal. The same domains that mediate Vps34 interaction *(14)* also mediate G protein signaling and vacuolar sorting.

Taken together, our observations highlight the close interplay of Vps15 in G protein signaling and vacuolar sorting, and are consistent with our earlier suggestion that PtdIns 3-P production is required for both processes *(5)*. Thus just as Gpa1 promotes PtdIns 3-P production, this second messenger could in turn be required for proper trafficking of Gpa1 or some other critical signaling protein, whether or not that protein actually binds to PtdIns 3-P. The signaling phenotypes exhibited by *vps15* and *vps34* are not the result of some global defect in membrane trafficking, however; deletion of *VPS30* or *VPS38* also result in a strong vacuolar sorting defect similar to *vps15* and *vps34 (59)*, but neither component is required for Gpa1 signaling *(5)*. Indeed of the dozens of vacuolar trafficking mutants that have been described, only *vps15* and *vps34* attenuate Gpa1 signaling *(59)*.

In summary, we have defined the signaling and binding functions of specific domains within Vps15. Our findings highlight important similarities and differences between canonical Gβ-proteins at the plasma membrane and Gβ-like proteins located within the cell.

ACKNOWLEDGEMENTS

We thank Sveta Gershburg for preparation of the baculovirus and expression of the protein and Zhongmin Jin for assistance with data collection at the Advanced Photon Source. We thank Jonathan Backer and Patrick Brennwald for valuable advice and feedback.

SUPPORTING INFORMATION AVAILABLE

Table 2.4 shows the alignment of Vps15 used to select conserved residues in the WD domain of Vps15. Representative electron density is shown in Supporting Figure 2.1. This material is available free of charge via the Internet at http://pubs.acs.org.

REFERENCES

(1) Sprang, S. R. (1997) G protein mechanisms: insights from structural analysis, *Annu Rev Biochem 66*, 639-678.

(2) Dohlman, H. G., and Thorner, J. W. (2001) Regulation of G protein-initiated signal transduction in yeast: Paradigms and principles, *Annu. Rev. Biochem. 70*, 703-754.

(3) Oldham, W. M., and Hamm, H. E. (2008) Heterotrimeric G protein activation by G-protein-coupled receptors, *Nat Rev Mol Cell Biol 9*, 60-71.

(4) Neves, S. R., Ram, P. T., and Iyengar, R. (2002) G protein pathways, *Science 296*, 1636-1639.

(5) Slessareva, J. E., Routt, S. M., Temple, B., Bankaitis, V. A., and Dohlman, H. G. (2006) Activation of the phosphatidylinositol 3-kinase Vps34 by a G protein alpha subunit at the endosome, *Cell 126*, 191-203.

(6) Stack, J. H., Herman, P. K., Schu, P. V., and Emr, S. D. (1993) A membrane-associated complex containing the Vps15 protein kinase and the Vps34 PI 3-kinase is essential for protein sorting to the yeast lysosome-like vacuole, *Embo J 12*, 2195-2204.

(7) Stack, J. H., and Emr, S. D. (1994) Vps34p required for yeast vacuolar protein sorting is a multiple specificity kinase that exhibits both protein kinase and phosphatidylinositol-specific PI 3-kinase activities, *J Biol Chem 269*, 31552-31562.

(8) Brown, W. J., DeWald, D. B., Emr, S. D., Plutner, H., and Balch, W. E. (1995) Role for phosphatidylinositol 3-kinase in the sorting and transport of newly synthesized lysosomal enzymes in mammalian cells, *J Cell Biol 130*, 781-796.

(9) Yan, Y., and Backer, J. M. (2007) Regulation of class III (Vps34) PI3Ks, *Biochem Soc Trans 35*, 239-241.

(10) Backer, J. M. (2008) The regulation and function of Class III PI3Ks: novel roles for Vps34, *Biochem J 410*, 1-17.

(11) Herman, P. K., Stack, J. H., DeModena, J. A., and Emr, S. D. (1991) A novel protein kinase homolog essential for protein sorting to the yeast lysosome-like vacuole, *Cell 64*, 425-437.

(12) Herman, P. K., Stack, J. H., and Emr, S. D. (1991) A genetic and structural analysis of the yeast Vps15 protein kinase: evidence for a direct role of Vps15p in vacuolar protein delivery, *Embo J 10*, 4049-4060.

(13) Murray, J. T., Panaretou, C., Stenmark, H., Miaczynska, M., and Backer, J. M. (2002) Role of Rab5 in the recruitment of hVps34/p150 to the early endosome, *Traffic 3*, 416-427.

(14) Budovskaya, Y. V., Hama, H., DeWald, D. B., and Herman, P. K. (2002) The C terminus of the Vps34p phosphoinositide 3-kinase is necessary and sufficient for the interaction with the Vps15p protein kinase, *J Biol Chem 277*, 287-294.

(15) Christofordis, S., Miaczynska, M., Ashman, K., Wilm, M., Zhao, L., Yip, S.C., Waterfield, M.D., Backer, J.M., and Zerial, M. (1999) Phosphatidylinositol-3-OH kinase are Rab5 effectors. *Nat. Cell Biol. 1*, 249-252.

(16) Stols, L., Gu, M., Dieckman, L., Raffen, R., Collart, F. R., and Donnelly, M. I. (2002) A new vector for high-throughput, ligation-independent cloning encoding a tobacco etch virus protease cleavage site, *Protein Expr Purif 25*, 8-15.

(17) Otwinowski, Z., and Minor, W. (1997) Processing of x-ray diffaction data collected in oscillation mode, *Methods Enzymol 276*, 307-326.

(18) Sheldrick, G. M. (2008) A short history of SHELX, *Acta Crystallogr A 64*, 112-122.

(19) Cowtan, K. (1994) DM: An automated procedure for phase improvement by density modification, *Joint CCP4 ESF-EACBM Newsl Protein Crystallogr 31*, 34-38.

(20) Morris, R. J., Perrakis, A., and Lamzin, V. S. (2003) ARP/wARP and automatic interpretation of protein electron density maps, *Methods Enzymol 374*, 229-244.

(21) Emsley, P., and Cowtan, K. (2004) Coot: model-building tools for molecular graphics, *Acta Crystallogr D Biol Crystallogr 60*, 2126-2132.

(22) Murshudov, G. N., Vagin, A. A., and Dodson, E. J. (1997) Refinement of macromolecular structures by the maximum-likelihood method, *Acta Crystallogr D Biol Crystallogr 53*, 240-255.

(23) Zeller, C. E., Parnell, S. C., and Dohlman, H. G. (2007) The RACK1 ortholog Asc1 functions as a G-protein beta subunit coupled to glucose responsiveness in yeast, *J Biol Chem 282*, 25168-25176.

(24) Song, J., Hirschman, J., Gunn, K., and Dohlman, H. G. (1996) Regulation of membrane and subunit interactions by N-myristoylation of a G protein a subunit in yeast, *J Biol Chem 271*, 20273-20283.

(25) Chasse, S. A., Flanary, P., Parnell, S. C., Hao, N., Cha, J. Y., Siderovski, D. P., and Dohlman, H. G. (2006) Genome-scale analysis reveals Sst2 as the principal

regulator of mating pheromone signaling in the yeast Saccharomyces cerevisiae, *Eukaryot Cell 5*, 330-346.

(26) Hoffman, G. A., Garrison, T. R., and Dohlman, H. G. (2000) Endoproteolytic Processing of Sst2, a Multidomain Regulator of G Protein Signaling in Yeast, *J Biol Chem 275*, 37533-37541.

(27) Schultz, J., Milpetz, F., Bork, P., and Ponting, C. P. (1998) SMART, a simple modular architecture research tool: identification of signaling domains, *Proc Natl Acad Sci U S A 95*, 5857-5864.

(28) Letunic, I., Copley, R. R., Pils, B., Pinkert, S., Schultz, J., and Bork, P. (2006) SMART 5: domains in the context of genomes and networks, *Nucleic Acids Res 34*, D257-260.

(29) Bryson, K., McGuffin, L. J., Marsden, R. L., Ward, J. J., Sodhi, J. S., and Jones, D. T. (2005) Protein structure prediction servers at University College London, *Nucleic Acids Res 33*, W36-38.

(30) Ouali, M., and King, R. D. (2000) Cascaded multiple classifiers for secondary structure prediction, *Protein Sci 9*, 1162-1176.

(31) Jones, D. T. (1999) Protein secondary structure prediction based on position-specific scoring matrices, *J Mol Biol 292*, 195-202.

(32) Meiler, J. (2003) PROSHIFT: protein chemical shift prediction using artificial neural networks, *J Biomol NMR 26*, 25-37.

(33) Evan, G. I., Lewis, G. K., Ramsay, G., and Bishop, J. M. (1985) Isolation of monoclonal antibodies specific for human c-myc proto- oncogene product, *Mol Cell Biol 5*, 3610-3616.

(34) Cox, J. S., Chapman, R. E., and Walter, P. (1997) The unfolded protein response coordinates the production of endoplasmic reticulum protein and endoplasmic reticulum membrane, *Mol Biol Cell 8*, 1805-1814.

(35) Hoffman, G., Garrison, T. R., and Dohlman, H. G. (2002) Analysis of RGS proteins in Saccharomyces cerevisiae, *Methods Enzymol 344*, 617-631.

(36) Sondek, J., Bohm, A., Lambright, D. G., Hamm, H. E., and Sigler, P. B. (1996) Crystal structure of a G-protein beta gamma dimer at 2.1A resolution, *Nature 379*, 369-374.

(37) Collaborative Computational Project. (1994) The CCP4 suite: programs for protein crystallography, *Acta Crystallogr D Biol Crystallogr 50*, 760-763.

(38) Lu, G. (1996) A WWW service system for automatic comparison of protein structures, *Protein Data Bank Quarterly Newsletter 78*, 10-11.

(39) Lambright, D. G., Sondek, J., Bohm, A., Skiba, N. P., Hamm, H. E., and Sigler, P. B. (1996) The 2.0 A crystal structure of a heterotrimeric G protein [see comments], *Nature 379*, 311-319.

(40) Aloy, P., Bottcher, B., Ceulemans, H., Leutwein, C., Mellwig, C., Fischer, S., Gavin, A. C., Bork, P., Superti-Furga, G., Serrano, L., and Russell, R. B. (2004) Structure-based assembly of protein complexes in yeast, *Science 303*, 2026-2029.

(41) De Camilli, P., Emr, S. D., McPherson, P. S., and Novick, P. (1996) Phosphoinositides as regulators in membrane traffic, *Science 271*, 1533-1539.

(42) Kihara, A., Noda, T., Ishihara, N., and Ohsumi, Y. (2001) Two distinct Vps34 phosphatidylinositol 3-kinase complexes function in autophagy and carboxypeptidase Y sorting in Saccharomyces cerevisiae, *J Cell Biol 152*, 519-530.

(43) Stack, J. H., DeWald, D. B., Takegawa, K., and Emr, S. D. (1995) Vesicle-mediated protein transport: regulatory interactions between the Vps15 protein kinase and the Vps34 PtdIns 3-kinase essential for protein sorting to the vacuole in yeast, *J Cell Biol 129*, 321-334.

(44) Zhong, Y., Wang, Q. J., Li, X., Yan, Y., Backer, J. M., Chait, B. T., Heintz, N., and Yue, Z. (2009) Distinct regulation of autophagic activity by Atg14L and Rubicon associated with Beclin 1-phosphatidylinositol-3-kinase complex, *Nat Cell Biol 11*, 468-476.

(45) Itakura, E., Kishi, C., Inoue, K., and Mizushima, N. (2008) Beclin 1 forms two distinct phosphatidylinositol 3-kinase complexes with mammalian Atg14 and UVRAG, *Mol Biol Cell 19*, 5360-5372.

(46) Sondek, J., Lambright, D. G., Noel, J. P., Hamm, H. E., and Sigler, P. B. (1994) GTPase mechanism of G proteins from the 1.7-A crystal structure of transducin a-GDP-AIF-4, *Nature 372*, 276-279.

(47) Bourne, H. R. (1997) G proteins. The arginine finger strikes again, *Nature 389*, 673-674.

(48) Kotting, C., Kallenbach, A., Suveyzdis, Y., Wittinghofer, A., and Gerwert, K. (2008) The GAP arginine finger movement into the catalytic site of Ras increases the activation entropy, *Proc Natl Acad Sci U S A 105*, 6260-6265.

(49) Ahmadian, M. R., Hoffmann, U., Goody, R. S., and Wittinghofer, A. (1997) Individual rate constants for the interaction of Ras proteins with GTPase-

activating proteins determined by fluorescence spectroscopy, *Biochemistry 36*, 4535-4541.

(50) Ahmadian, M. R., Stege, P., Scheffzek, K., and Wittinghofer, A. (1997) Confirmation of the arginine-finger hypothesis for the GAP-stimulated GTP-hydrolysis reaction of Ras, *Nat Struct Biol 4*, 686-689.

(51) Mittal, R., Ahmadian, M. R., Goody, R. S., and Wittinghofer, A. (1996) Formation of a transition-state analog of the Ras GTPase reaction by Ras-GDP, tetrafluoroaluminate, and GTPase-activating proteins, *Science 273*, 115-117.

(52) Rensland, H., Lautwein, A., Wittinghofer, A., and Goody, R. S. (1991) Is there a rate-limiting step before GTP cleavage by H-ras p21?, *Biochemistry 30*, 11181-11185.

(53) Bourne, H. R. (1997) How receptors talk to trimeric G proteins, *Curr Opin Cell Biol 9*, 134-142.

(54) Sabbagh, W., Jr., Flatauer, L. J., Bardwell, A. J., and Bardwell, L. (2001) Specificity of MAP kinase signaling in yeast differentiation involves transient versus sustained MAPK activation, *Mol Cell 8*, 683-691.

(55) Jung, G., Ueno, H., and Hayashi, R. (1999) Carboxypeptidase Y: structural basis for protein sorting and catalytic triad, *J Biochem 126*, 1-6.

(56) Obara, K., Noda, T., Niimi, K., and Ohsumi, Y. (2008) Transport of phosphatidylinositol 3-phosphate into the vacuole via autophagic membranes in Saccharomyces cerevisiae, *Genes Cells 13*, 537-547.

(57) Huh, W. K., Falvo, J. V., Gerke, L. C., Carroll, A. S., Howson, R. W., Weissman, J. S., and O'Shea, E. K. (2003) Global analysis of protein localization in budding yeast, *Nature 425*, 686-691.

(58) Hirschman, J. E., and Jenness, D. D. (1999) Dual lipid modification of the yeast ggamma subunit Ste18p determines membrane localization of Gbetagamma, *Mol Cell Biol 19*, 7705-7711.

(59) Bonangelino, C. J., Chavez, E. M., and Bonifacino, J. S. (2002) Genomic screen for vacuolar protein sorting genes in Saccharomyces cerevisiae, *Mol Biol Cell 13*, 2486-2501.

Table 2.1 Data collection parameters and processing statistics. Values in parenthesis refer to the highest resolution shell.

	Native	$KAu(CN)_2$
Unit Cell (Å)	$a, b = 85.5, c = 132.8$	$a, b = 86.0, c = 132.8$
Resolution (Å)	50.0–1.80	50.0–2.20
Observed reflections	518207	637020
Unique reflections	50964	29652
$I/\sigma(I)$	36.0 (1.6)	39.2 (12.3)
Completeness (%)	96.5 (71.2)	100 (100)
Redundancy	10.2 (6.8)	21.5 (22.0)
R_{sym} (%)	8.1 (52.7)	9.7 (24.9)

Table 2.2 Phase calculation and refinement statistics. Values in parenthesis refer to the highest resolution shell.

Phasing	
Resolution (Å)	50–2.5
Number of sites (SHELX)	4
FOM after MLPHARE	0.284
Anomalous R_{cullis} [a]	0.76 (0.82)
FOM after DM	0.819
Refinement	
Resolution (Å)	50–1.80
R_{work}/R_{free} (%)	20.9/24.6
Number of atoms	
Protein	3163
Water	200
Average B-factor (Å^2)	
Protein	35.4
Water	41.0
R.m.s. deviations	
Bond lengths (Å)	0.014
Bond angles (°)	1.524

[a] R_{cullis} = lack of closure/anomalous difference

Table 2.3 Primer sequences.

Primer Name	Sequence (5'-3')
Vps15fn	GAG CTC ATG GGG GCA CAA TTA TCA C
Vps15ksrn	GAG CTC TTA AAT GCC ACG ATA TTT ATT CAG
Vps15klrn	GAG CTC TTA ATA GCT GTT GCT GAC GAC TAC C
Vps15wdlfn	GAG CTC TAT CGT GGC ATT TTC TTC CC
Vps15rn	GAG CTC TTA TTG GAA GAT TCC AAT AAG
Vps15wdsfn	GAG CTC GAA GGC GAC GTT GAA AGC
Vps15fc	CCC GGG ATG GGG GCA CAA TTA TCA C
Vps15rc	CCC GGG TTG GAA GAT TCC AAT AAG
Vps15wdlfc	CCC GGG ATG TAT CGT GGC ATT TTC TTC C
Vp15wdsfc	CCC GGG ATG GAA GGC GAC GTT GAA AG
Atg14fn	GAG CTC CAT TGC CCA ATT TGC CAC CAT AG
Atg14rn	GAG CTC CTA GCC TAC CAC GTA CCA TCG
2myc	TC GAC ATG GAA CAA AAA TTA ATT TCT GAA GAA GAT TTA GCT GAA CAA AAG TTA ATT TCT GAA GAA GAC TTA G
Vps15R1261A	GAT ATA TGG GAT ATC GCT TTC AAC GTG CTG ATA AGG
Vps15R1261K	GAT ATA TGG GAT ATC AAA TTC AAC GTG CTG ATA AGG

FIGURE LEGENDS

Figure 2.1. Structure of the Vps15 WD repeat domain and comparison to the beta subunit of transducin ($G\beta_1$). (A) *Left*: ribbon diagram of $G\beta_1$. Blades of the propeller are numbered consecutively, as are the strands of one blade. *Center*: ribbon diagram of Vps15 WD repeat domain, in the same orientation as $G\beta_1$. Breaks within the structure are indicated by dotted lines. The first break occurs at residue 1041; the short stretch of amino acids visible before this break are shown in this part of the figure but deleted in others. Colored regions highlight major differences in the propeller's structure: blue, N-terminus; magenta, insertion between WD repeats 1 and 2; gold, insertion between WD repeats 2 and 3; green, insertion within WD repeat 6; yellow, insertion within WD repeat 7. The N-terminus and corresponding loop regions of $G\beta_1$ are colored similarly. *Right*: space filling model of Vps15 WD repeat domain (same orientation) with residues highly conserved across genera colored salmon, and those which are invariant colored red. Arg-1261 and Phe-1262 reside on the surface in the loop between WD repeats 4 and 5. (B) *Left*: ribbon diagram of $G\beta\gamma$ oriented to highlight the interaction between the beta and gamma (red) subunits. *Center*: surface representation of $G\beta\gamma$ in the same orientation. *Right*: surface representation of $G\beta_1$ alone, with hydrophobic residues colored light grey to show the binding cavity for $G\gamma_1$. (C) *Left*: ribbon diagram of Vps15 WD repeat domain oriented as $G\beta_1$ in panel B. The N-terminal loop is colored gold. *Center*: surface rendering to illustrate partial occlusion of the potential gamma subunit binding surface. *Right*: surface representation following removal of the N-terminal loop, with hydrophobic

residues colored light grey to reveal the absence of a binding cavity for a gamma-like subunit. This figure was contributed by Janeen Vanhooke and Brenda Temple.

Figure 2.2. The WD domain of Vps15 is sufficient but not necessary to bind Gpa1. Detergent-solubilized extracts (Total) from cells expressing the indicated Flag fusion proteins and Gpa1 fused to Myc were incubated with Flag resin, eluted with 3X Flag peptide (Flag IP), resolved by 7.5% or 10% SDS-PAGE, and analyzed by immunoblotting with antibodies against Flag, Myc, and G6PDH (Load control). C-terminally tagged forms of (a) and (b) did not express. IP, immunoprecipitation. WD, WD domain. KD, kinase domain. ID, intermediate domain. *, indicates protein of interest.

Figure 2.3. The WD domain of Vps15 is sufficient but not necessary to bind Atg14. Detergent-solubilized extracts (Total) from cells expressing the indicated Flag fusion proteins and Atg14 fused to a triple Myc epitope were incubated with Flag resin, eluted with 3X Flag peptide (Flag IP), resolved by 10% SDS-PAGE, and analyzed by immunoblotting with antibodies against Flag, Myc, and G6PDH (Load control). IP, immunoprecipitation. WD, WD domain. KD, kinase domain. ID, intermediate domain. *, indicates protein of interest.

Figure 2.4. Atg14 is not necessary to mediate the interaction of Vps15 and Gpa1. Detergent-solubilized extracts from wild-type (WT) and *atg14*Δ mutant cells expressing the indicated Flag fusion proteins and Gpa1 fused to a Myc epitope were incubated with

Flag resin, eluted with 3X Flag peptide, resolved by 10% SDS-PAGE, and analyzed by immunoblotting with antibodies against Flag, Myc, and G6PDH (Load control). IP, immunoprecipitation. WD, WD domain. KD, kinase domain. ID, intermediate domain. *, indicates protein of interest.

Figure 2.5. **Arg-1261 is necessary for the WD domain of Vps15 to bind efficiently to Gpa1.** Detergent-solubilized extracts (Total) from cells expressing the indicated Myc fusion proteins and Gpa1 or Gpa2 fused to GST were incubated with glutathione-Sepharose resin, eluted with glutathione (GST PD, pulldown), resolved by 10% SDS-PAGE, and analyzed by immunoblotting with antibodies against GST, Myc and G6PDH (Load control). PD, pulldown. GST, glutathione-Sepharose. WD, WD domain. RA, Arg-1261 to Ala. RK, Arg-1261 to Lys.

Figure 2.6. The conserved Arg-1261 is not necessary for G protein signaling at the endosome. (A) Wild-type (WT), *vps15*Δ, and *VPS15*^{R1261A} (Vps15^{RA}) strains were treated with 3μM α-mating factor (MF) for 30 minutes and analyzed by immunoblotting using antibodies against p44/p42 and G6PDH (Load control). (B) The same samples as in panel (A) analyzed using antibodies against carboxypeptidase Y (CPY) and G6PDH. (C) The same strains were transformed with a plasmid containing a pheromone-inducible *FUS1-lacZ* reporter; transcriptional activation was measured by monitoring β-galactosidase activity in response to pheromone. (D) The same strains were plated and treated with 45 micrograms of α factor to induce cell division arrest. α-MF, alpha mating factor. RA, Arg-1261 to Ala.

Figure 2.7. Arg-1261 is not necessary for larger truncations of Vps15 to bind to Gpa1. (A) Detergent-solubilized extracts (Total) from cells expressing the indicated Myc fusion proteins and Gpa1 or Gpa2 fused to GST were incubated with glutathione-Sepharose resin, eluted with glutathione (GST PD), resolved by 10% SDS-PAGE, and analyzed by immunoblotting with antibodies against Myc, GST, Ste4 and G6PDH (Load control). (B) Detergent-solubilized extracts from cells expressing the indicated Myc fusion proteins and Gpa1 fused to GST were lysed in the presence of either GDP or GDP-AlF_4^-, incubated with glutathione-Sepharose resin, eluted with glutathione, and analyzed by immunoblotting with antibodies against Myc, GST, Ste4, and G6PDH. PD, pulldown. GST, glutathione-Sepharose. RA, Arg-1261 to Ala. RK, Arg-1261 to Lys.

Figure 2.8. The kinase domain with the intermediate domain of Vps15 is necessary to promote G protein signaling at the endosome. (A) WT and *vps15*Δ cells expressing the indicated Flag fusion proteins or empty vector were treated with 3 μM α-mating factor (MF) for 30 minutes and analyzed by immunoblotting with antibodies against p44/p42 and G6PDH (Load control). (B) The same samples were analyzed using antibodies against carboxypeptidase Y (CPY) and G6PDH. (C) The same strains were transformed with a plasmid containing a pheromone-inducible *FUS1-lacZ* reporter; transcriptional activation was measured by monitoring β-galactosidase activity in response to pheromone. (D) The same strains were plated and treated with 1.5-45 micrograms of α factor to induce cell division arrest. α-MF, alpha mating factor.

Figure 2.1

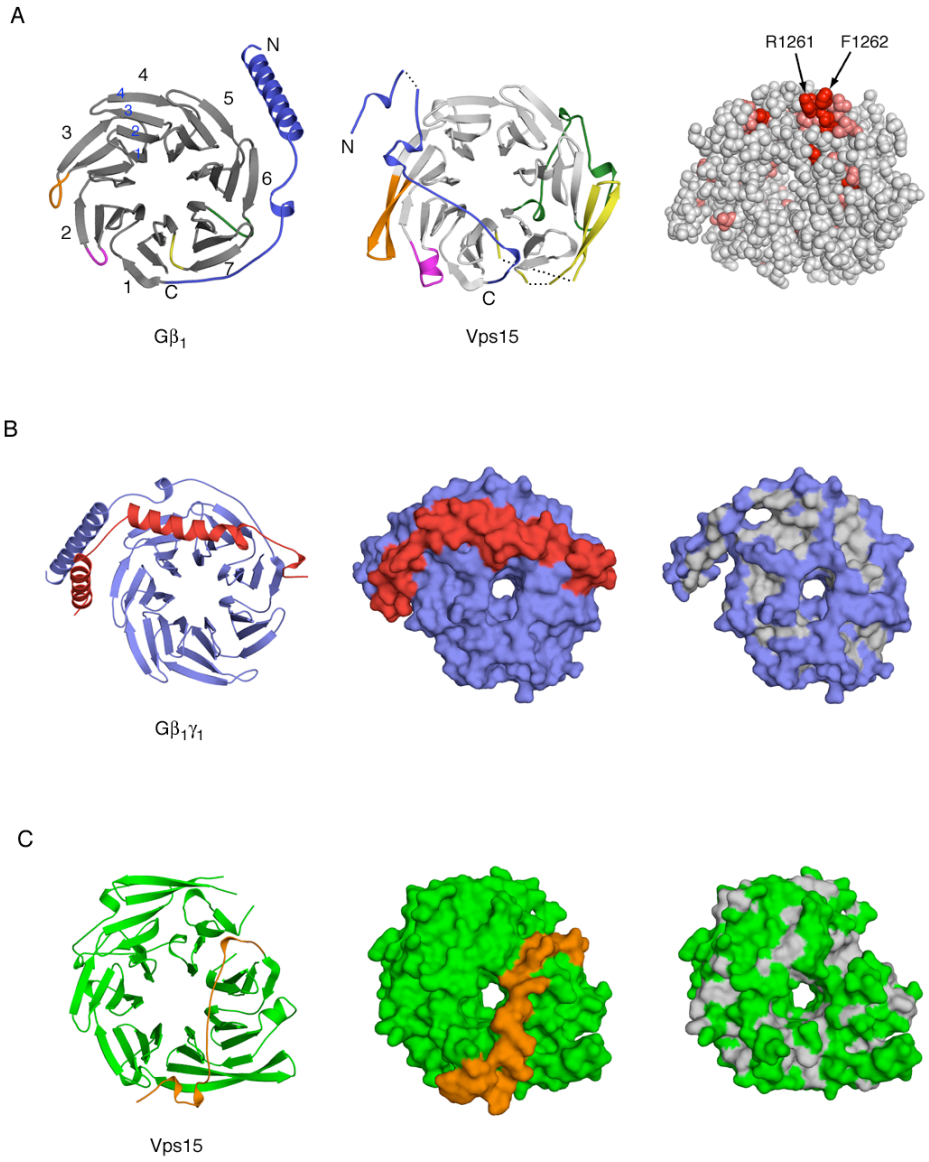

Figure 2.2

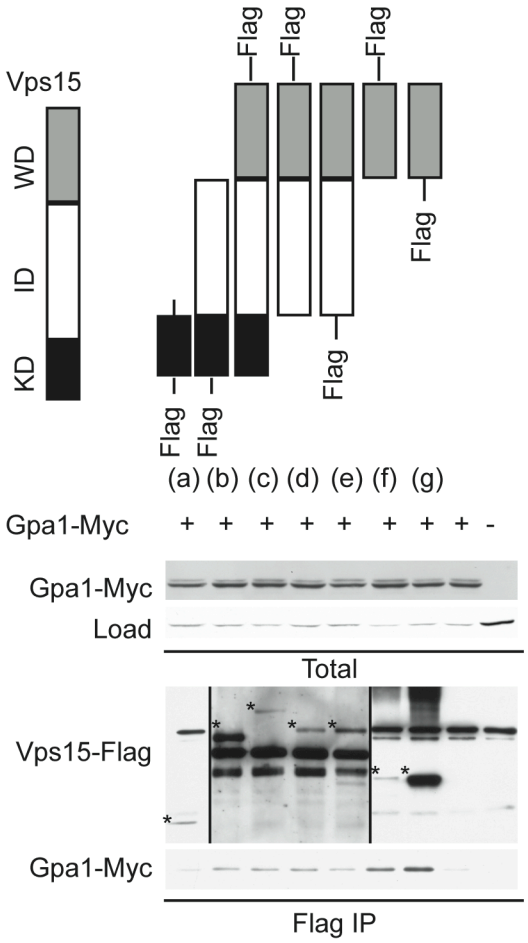
Vps15
WD
ID
KD
Flag
Flag
Flag
Flag
Flag
Flag
(a) (b) (c) (d) (e) (f) (g)
Gpa1-Myc + + + + + + + + -
Gpa1-Myc
Load
Total
Vps15-Flag
Gpa1-Myc
Flag IP

Figure 2.3

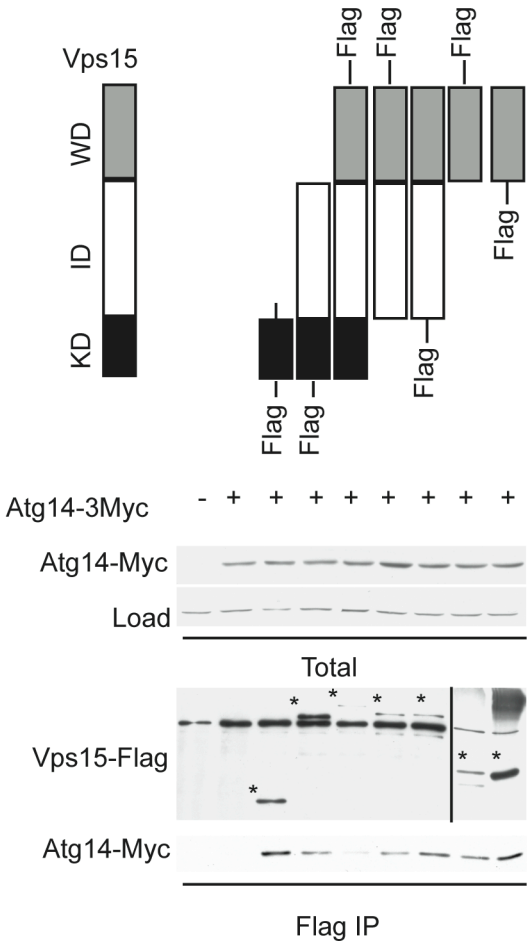
Vps15
WD
ID
KD
Flag
Flag
Flag
Flag
Flag
Flag
Atg14-3Myc
- + + + + + + + +
Atg14-Myc
Load
Total
Vps15-Flag
Atg14-Myc
Flag IP

Figure 2.4

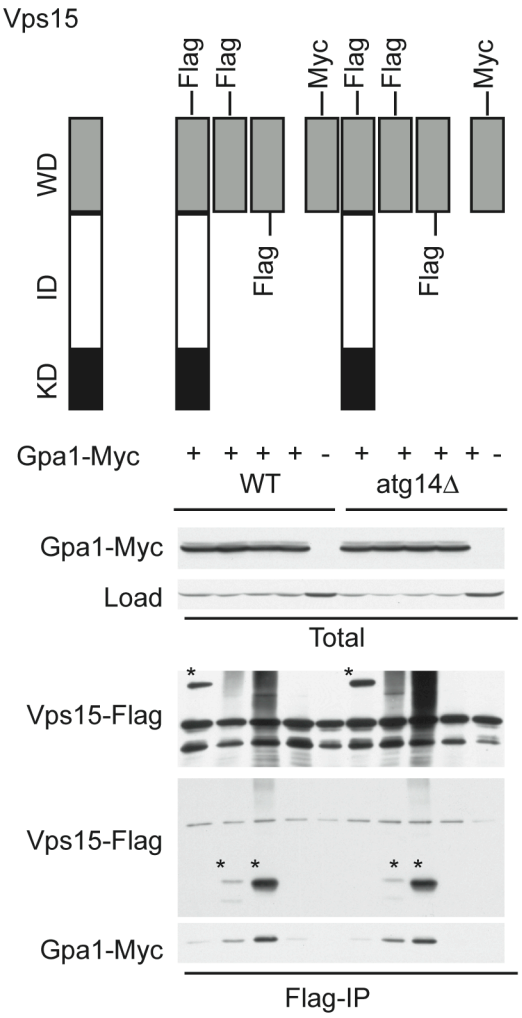
Vps15
Flag
Flag
Myc
Flag
Flag
Myc
WD
ID
KD
Flag
Flag
Gpa1-Myc + + + + - + + + + -
WT
atg14Δ
Gpa1-Myc
Load
Total
Vps15-Flag
Vps15-Flag
Gpa1-Myc
Flag-IP

Figure 2.5

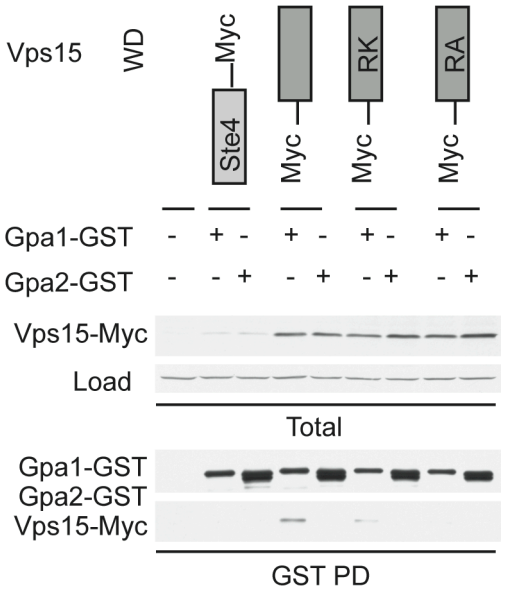
Vps15
WD
Myc
Ste4
Myc
RK
Myc
RA
Myc
Gpa1-GST
Gpa2-GST
Vps15-Myc
Load
Total
Gpa1-GST
Gpa2-GST
Vps15-Myc
GST PD

Figure 2.6

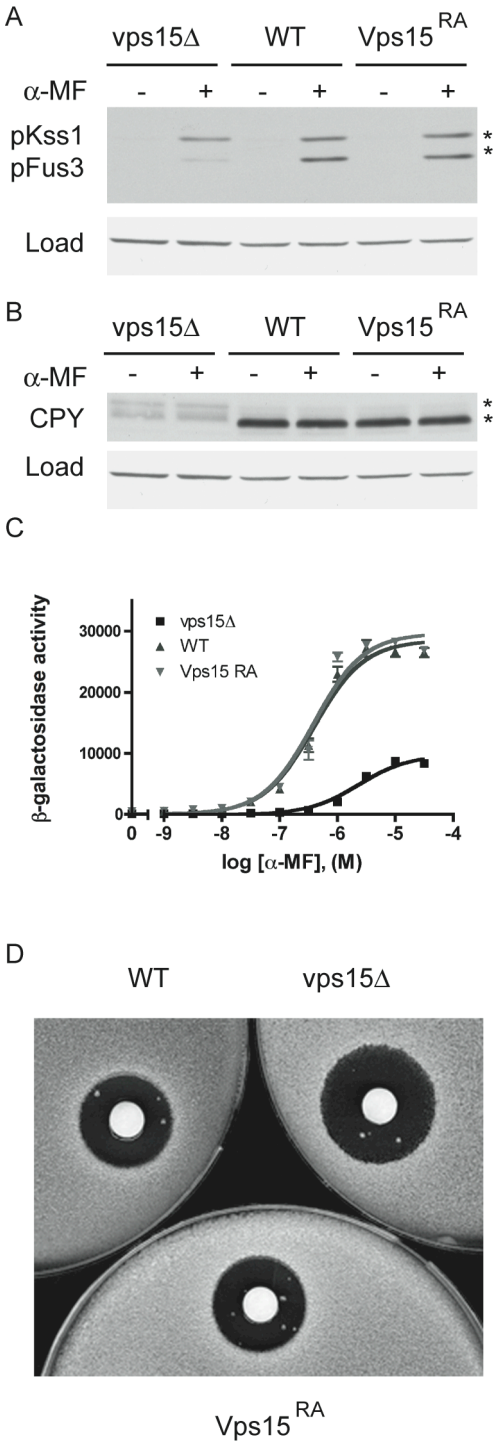
A
vps15Δ
WT
Vps15 RA
α-MF
- + - + - +
pKss1
pFus3
Load
B
vps15Δ
WT
Vps15 RA
α-MF
- + - + - +
CPY
Load
C
β-galactosidase activity
vps15Δ
WT
Vps15 RA
30000
20000
10000
0
0 -9 -8 -7 -6 -5 -4
log [α-MF], (M)
D
WT
vps15Δ
Vps15 RA

Figure 2.7

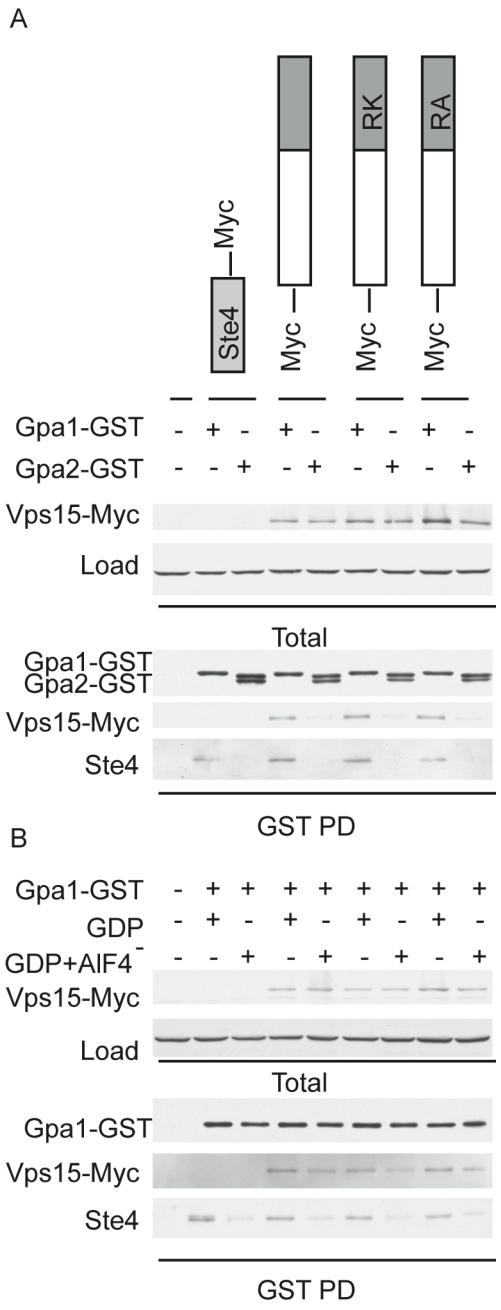
A
Ste4
Myc
Myc
RK
Myc
RA
Myc
Gpa1-GST
Gpa2-GST
Vps15-Myc
Load
Total
Gpa1-GST
Gpa2-GST
Vps15-Myc
Ste4
GST PD
B
Gpa1-GST
GDP
GDP+AlF4-
Vps15-Myc
Load
Total
Gpa1-GST
Vps15-Myc
Ste4
GST PD

Figure 2.8

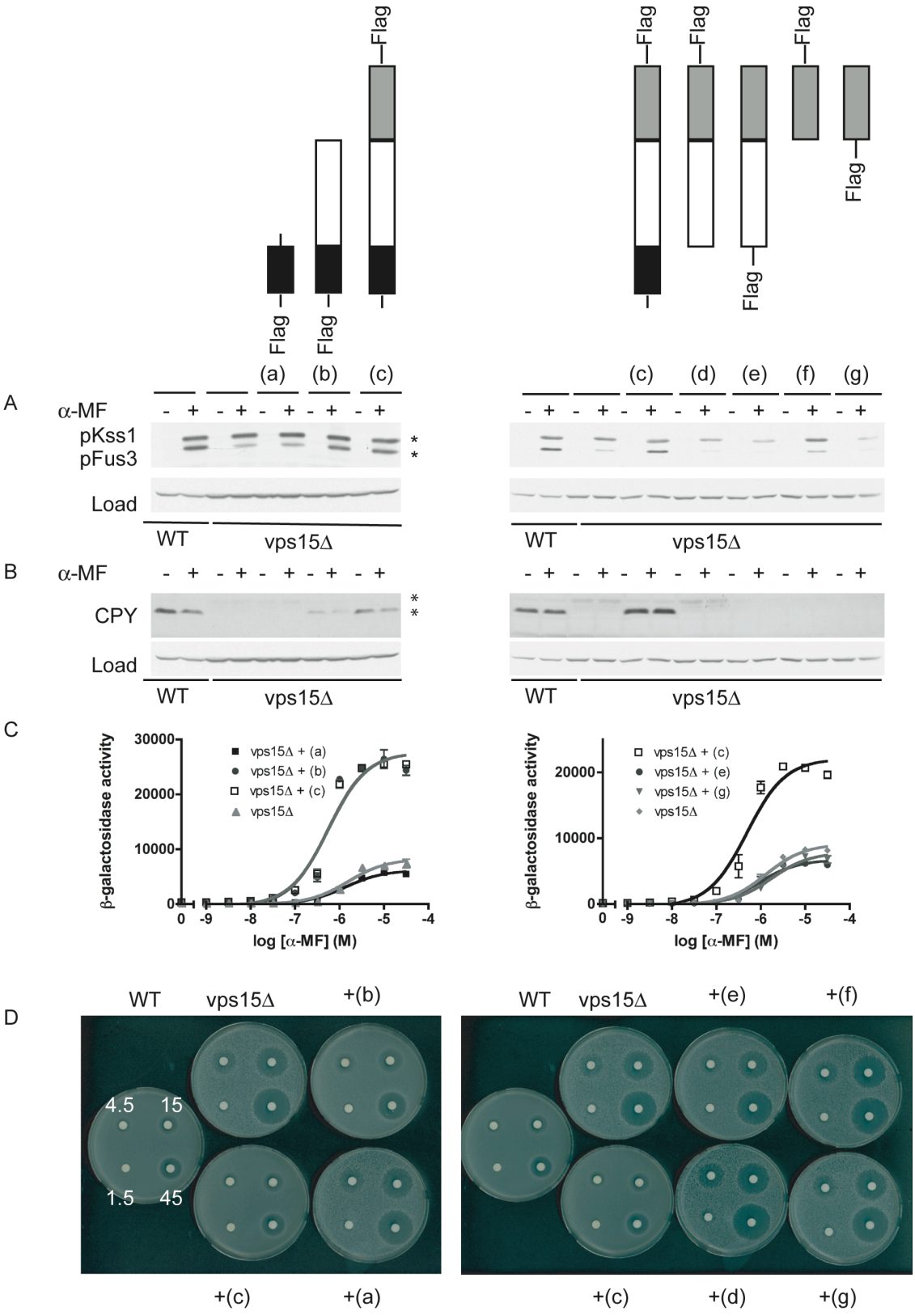
Flag
(a)
(b)
(c)
(d)
(e)
(f)
(g)
A
α-MF
pKss1
pFus3
Load
WT
vps15Δ
B
CPY
C
β-galactosidase activity
vps15Δ + (a)
vps15Δ + (b)
vps15Δ + (c)
vps15Δ
vps15Δ + (e)
vps15Δ + (g)
log [α-MF] (M)
D
4.5
15
1.5
45
+(a)
+(b)
+(c)
+(d)
+(e)
+(f)
+(g)

Chapter 3

The Regulation of Fus3

ABSTRACT

In the yeast *Saccharomyces cerevisiae* pheromones promote a series of events leading to mating. These events include activation of the MAP kinases Fus3 and Kss1, altered gene transcription, and cell cycle arrest in G1. A crystal structure of Fus3 reveals a unique cluster of basic amino acids that could potentially serve as a phospholipid binding site (Lys, Arg, His) or site of ubiquitination (Lys). We have previously demonstrated that the phosphatidylinositol (PtdIns) 3-kinase Vps34 is required for full activation of Fus3 but not Kss1. Here we show that Fus3 activity binds to the Vps34 product PtdIns(3)P. Mutations of basic residues did not alter PtdIns(3) sensitivity or gene transcription activation; however, these Fus3 mutants were less able to undergo ubiquitination, and less able to phosphorylate the cell cycle regulator Far1 or induce cell cycle arrest. These findings reveal a new mode of signal regulation that concomitantly alters MAPK ubiquitination substrate specificity and control of the cell cycle.

BACKGROUND AND INTRODUCTION

G proteins are found in organisms from plants to fungi to humans, and they mediate responses to a wide array of signals. Activation of receptors on the cell surface results in the G protein α subunit releasing GDP and binding GTP. The newly activated Gα then dissociates from the G protein βγ subunit dimer. Either the activated, GTP-bound form of Gα, Gβγ, or both go on to stimulate downstream effector proteins within the cell. Prominent examples include members of the MAPK (mitogen activated protein kinase) and phosphatidylinositol (PtdIns) 3-kinase families. Upon GTP hydrolysis the G protein subunits reassemble and signaling stops (*1, 2*).

In the yeast *Saccharomyces cerevisiae*, G protein signaling pathways mediate the cell-to-cell communication responsible for essential processes, including those leading to mating. Stimulation of G protein-coupled receptors by mating pheromones triggers a series of responses that includes activation of the MAP kinases Fus3 and Kss1, morphological changes, cell cycle arrest, and cell fusion. As in other pathways, the Gα and Gβγ subunits in yeast act in a cooperative manner to transmit the signal. Whereas Gβγ (Ste4/Ste18) is required to initiate MAP kinase activation and functions in the pathway that originates from the plasma membrane (*3*), the GTP-activated form of Gα (Gpa1) amplifies the response in a pathway that originates from the endosome (*4-6*). The pathway mediated by the Gα protein functions through Vps15 and Vps34, the regulatory and catalytic subunits respectively of the only PtdIns 3-kinase in yeast (*7-15*). Whereas GDP-bound Gpa1 binds directly to Vps15, the GTP-bound (activated) form of Gpa1

binds directly to Vps34 and promotes elevated PtdIns(3)P production (*5*).

The production of PtdIns(3)P by Vps34 is critical for the function of many pathways. It is thought that signaling by Vps34 is provoked by the recruitment of proteins that possess PtdIns(3)P binding domains (*13*). PtdIns(3)P binding domains include FYVE domains, zinc-finger binding domains (*16*), and PX domains (*17*). Pathways mediated by PtdIns(3)P include, but are not limited to, assembly of PtdIns(3)P binding proteins to regulate early endosomal docking and fusion (*18, 19*), assembly of the retromer complex required for endosome to Golgi transport (*20*), and the ubiquitin dependent sorting of internalized membrane proteins (*21*). Ubiquitin is added to specific lysine residues within a protein, and generally leads to degradation of a substrate protein. Ubiquitination has been shown to be important in the regulation of many components of the G protein signaling pathway, including Gpa1 and Ste7 (*22-26*).

Whereas pheromone stimulation through Gβγ leads to activation of both Fus3 and Kss1, signaling through Gpa1 is more selective and leads to activation of Fus3 in preference to Kss1. Moreover, deletion of Vps34 or pharmacological inhibition of PtdIns(3)P production results in a selective loss of Fus3 activity (*5*). However the mechanism by which Vps34 or PtdIns(3)P modulates Fus3 activity is unclear. The crystal structure of Fus3 reveals a cluster of basic amino acids that could serve as a site for PtdIns(3)P binding or Fus3 ubiquitination *(25)*. Here we demonstrate that PtdIns(3)P binds Fus3. Mutation of basic patch residues of Fus3 does not affect regulation by

PtdIns(3)P , but it does decrease ubiquitination of Fus3 and alter Fus3 substrate specificity *in vivo*.

EXPERIMENTAL PROCEDURES

Strains and Plasmids

Standard methods for the growth, maintenance, and transformation of yeast and bacteria and for the manipulation of DNA were used throughout. Yeast *Saccharomyces cerevisiae* strains used in this study are BY4741 (*MAT***a** *leu2*Δ *met15*Δ *his3*Δ *ura3*Δ), BY4741-derived gene deletion mutants containing the G418-resistance marker (Invitrogen), and BY4741-derived strains containing a C-terminal GFP tag (Invitrogen) or RFP. All RFP-tagged strains were a gift from Erin O'Shea (Harvard University).

Previously described yeast shuttle vectors and expression plasmids are pRS315-ADH-Flag (contains *ADH1* promoter/terminator and a Flag epitope that can be added 3' with an XmaI site) (*27*), pAD4M, pAD4M GPA1^{Q323L} (*4*), Yep24-Myc-Ubiquitin (*28*) (Also know as pND186 from Nick Davis, Wayne State University), pRS423-FUS1-LacZ (*29*), pGEX-2T, pGEX-2T-FUS3 (*30*), pETARA-miniFar1 (*31*) (from Wendell Lim, University of California), pRS316-FUS3, pRS313-FUS3 (from Nan Hao, University of North Carolina), pRS316-HA-FAR1 (also known as pMP974, from Mike Tyers, University of Toronto), pRS316-HA-FAR1^{T63A} and pRS316-HA-FAR1^{T306A} (from Michal Nagiec, University of North Carolina). Plasmid pRS406-SNF7-RFP was constructed by PCR amplification of SNF7-RFP (using primers 5'-TCC CCG CGG GGA ATG TGG TCA TCA CTT TTT GG-3' and 5'-CCA TCG ATG GGC CTT AGG CGC CGG TGG AG-3') and subcloning into the SacII and ClaI sites of pRS406. Plasmid pRS406-FUS3-GFP constructed by PCR amplification of *FUS3* (using primers 5'-GAA

AGG AAA CTA GTA TGC CAA AGA G-3' and 5'-GAT AAT GAA AGC TTA CTA AAT ATT TCG TTC-3') and subcloning into the SpeI/HindIII sites of pUG35 (contains C terminal enhanced GFP containing optimal codons for *Candida albicans* and 2 substitutions near the chromophore shown to increase fluorescence) (from J. H. Hegemann, Dusseldorf) and then subcloning the *FUS3*-GFP fusion into the XbaI-KpnI sites of pRS406. Genomic integration was directed by AflII digestion. The strain *FAR1*-GFP *fus3Δ* was created by plasmid amplification of the *fus3*::G418 cassette using primers in the promoter and terminator regions of Fus3 (using primers 5'-CGG GAT CCG CAG CGA CTG CAC TAA ACT AGA GG-3' and 5'-CGG AAT TCG TCT AGT AAG ACG GTC TCT TGC TGC-3'). The *FAR1*-GFP strain was then transformed with the purified PCR product and selected for growth on G418. Plasmids pRS316-FUS3$^{H333A/K335A}$ and pRS406-FUS3$^{H333A/K335A}$-GFP were constructed using the QuikChange Site-directed Mutagenesis Kit (Stratagene) and mutagenic primers (5'-GCT TCT TCG AGT TTG ATG CCT ACG CGG AGG CAC TAA CG-3', and its complement). Plasmid pRS315-ADH-FUS3-Flag was created by PCR amplification of *FUS3* (using primers 5'-CCC GGG ATG CCA AAG AGA ATT ATA TAC-3' and 5'-CCC GGG ACT AAA TAT TTC GTT CCA AAT G-3') and subcloning into the Xma1 site of pRS315-ADH-Flag. Plasmids pRS315-ADH-FUS3^{K335R}-Flag and pRS315-ADH-FUS3$^{H333A/K335A}$-Flag were created using the QuikChange Site-directed Mutagenesis Kit and mutagenic primers (using primers 5'-CTT CGA GTT TGA TCA CTA CAG GGA GGC ACT AAC GAC G-3' and 5'-CGT CGT TAG TGC CTC CCT GTA GTG ATC AAA CTC GAA G-3').

Cell Extract Preparation for MAP kinase, Far1, and Ste7 Phosphorylation

Strains were grown to an A_{600nm} ~ 0.8 in the appropriate selective media, and then split and either treated with 3 μM α-factor pheromone or left untreated at 30°C for 30 minutes. The reaction was stopped through the addition of 5% trichloroacetic acid, the cells were harvested by centrifugation and the pellets were frozen at -80°C. Cell extracts were prepared as previously described (*32*), resolved by 10% SDS-PAGE and immunoblotted using p44/p42 MAP kinase antibody at 1:500 (9101 L, Cell Signaling Technology), anti-Fus3 antibodies at 1:500 (sc-6773, Santa Cruz), and anti-G6PDH antibodies at a dilution of 1:50,000 (A-9521, Sigma-Aldrich). Secondary antibodies used were horse radish-conjugated goat anti-rabbit (172-1019, Biorad) or rabbit anti-goat (sc-2768, Santa Cruz) at a dilution of 1:10,000.

To analyze Far1 and Ste7 phosphorylation, samples were resolved by 7 % SDS-PAGE and immunoblotting with rat anti-HA 3F10 antibodies (to detect Far1-HA) (1187423001, Roche Applied Science) at 1:1000 and goat anti-Ste7 antibodies (sc-6770, Santa Cruz) at 1:200. Protein concentration was determined by Dc protein assay (500-0111, Biorad). Antibody detection was by enhanced chemiluminescence detection.

Pheromone Response Assays

Growth arrest (halo) and reporter transcription assays (β-galactosidase) utilizing the plasmid pRS423-FUS1-lacZ were performed as previously described (*29, 33*).

Purification of Flag Epitope-tagged Proteins

Strains expressing the indicated plasmids were grown in a 100 ml culture to A_{600nm} ~ 0.25. The cells were then treated with 100mM copper sulfate for 3 hours at 30°C to induce expression of myc-ubiquitin. Cultures were then split and either treated with 3 μM α-factor or left untreated at 30°C for 1 hour. The reaction was stopped by the addition of sodium azide to a final concentration of 10mM, and the cells were harvested by centrifugation and frozen at -80°C. The procedure for Flag purification has been described in detail previously (*6*). Briefly, cells were disrupted in buffer A (50 mM Tris-Cl pH 8.0, 200 mM NaCl, 0.1% Triton X-100, 25 mM beta-glycerophosphate, 1 mM EDTA) with 2 protease inhibitor cocktail pellets per 50 ml (Roche) for 15 minutes at 4°C using a vortex. Lysates were clarified through centrifugation twice at 16000g, and an equal volume and protein concentration of each lysate was applied to 40 μl of Flag affinity resin (Sigma-Aldrich). After a two hour incubation with gentle rotation at 4°C, the beads were washed five times with 500 μl buffer A and bound proteins eluted with two 20μl washes of 0.25 mg/ml 3X Flag Peptide (Sigma-Aldrich) diluted in buffer A. The samples were resolved by 10% SDS-PAGE and immunoblotting with anti-Myc 9E10 cell culture supernatant at a dilution of 1:100 (*34*), anti-Flag mouse monoclonal M2 antibodies at a dilution of 1:1000 (F3165, Sigma-Aldrich), and anti-G6PDH antibodies and secondary antibodies as described above.

Microscopy Analysis

Yeast cells containing integrated *FUS3*-GFP or *FUS3*$^{H333A/K335A}$-GFP and *SNF7*-RFP were grown to A_{600nm} ~ 0.8 and split. Cells were treated either with 3μM α-factor or

left untreated at 30°C for one hour and harvested by centrifugation. Cells were visualized by differential interference contrast (DIC) and fluorescence microscopy using a Nikon Eclipse TE2000-S with the following laser lines: 488 nm (Blue Argon, for GFP), 568nm (Yellow Krypton, for RFP), and 633nm (Red Helium Neon for DIC), photographed with a Hamamatsu digital camera, and analyzed with MetaMorph Version 5.0 software. Quantitative analysis of translocation was done in cells containing either integrated pRS406-FUS3-GFP or pRS406-FUS3$^{H333A/K335A}$-GFP plasmids and integrated pRS403-SNF7-RFP plasmid (endosomal marker). Images were analyzed using the Just Another Colocalization Plugin (JACoP) (*35*) with ImageJ (NIH). Preprocessing of images included subtraction of a background average level. Colocalization of GFP and RFP fluorescence was evaluated by extracting the Manders Overlap Coefficients using the manual thresholding option of the JACoP Plugin; these values are indicators of the coincidence between the signal in the green and red channels.

Yeast cells containing integrated *FAR1*-GFP in a *fus3Δ* background were transformed with pRS315-ADH-Flag, pRS315-ADH-FUS3-Flag, pRS315-ADH-FUS3^{K335R}-Flag or pRS315-ADH-FUS3-^{H333AK335A}-Flag and grown to $A_{600nm} \sim 0.6$. Cells were split, and either treated with 3μM α-factor or left untreated at 30 °C for two hours and harvested by centrifugation. Cells were imaged as described above and analyzed using ImageJ (NIH).

E. coli expression of GST fusion proteins

GST, GST-Fus3 and GST-Fus3$^{H333A/K335A}$ were purified from *E. coli* BL21 (DE3) cells as described (*5)*. GST-miniFar1-6HIS was purified from Rosetta (DE3) pLysS cells (Novagen, EMD Biosciences) as described (*31*). Glutathione was removed from protein samples on Econo-Pac 10 DG columns (Bio-Rad).

In vitro kinase assay

For phosphorylation time-course analysis, GST-Fus3 and GST-Fus3$^{H333A/K335A}$ proteins (~0.9 mM) were incubated either with myelin basic protein MBP ~14 mM) (Sigma) or GST-miniFar1-6HIS (~1.5 mM) in kinase buffer (25 mM HEPES, 50 mM NaCl, 25 mM $MgCl_2$, 1 mM DTT, pH 7.5) 200 mM ATP, 5 mCi [γ-^{32}P]-ATP/sample at 30 ºC. Samples were taken at the indicated times and the reaction was terminated by the addition of 6X SDS-PAGE sample buffer. Samples were resolved by 15 % (MBP) or 6 % (Far1) SDS-PAGE. ^{32}P incorporation was detected using a PhosphorImager SI (Molecular Dynamics).

Lipid binding assays

Lipid binding assays were performed using PIP Strips from Echelon Biosciences Inc. according to the manufacturer's recommended protocol. Briefly, PIP strips were blocked in 3% fatty acid-free bovine serum albumin in TBST (20 mM Tris, 150 mM NaCl, 0.1% Tween 20, pH 7.5) for 1 hr and incubated with the protein of interest (0.5-1 mg/ml in 3% BSA-TBST) overnight at 4º C. PIP strips were washed 3 times in TBST and

bound protein was detected using anti-GST monoclonal antibodies (G1160, Sigma) at 1:1,000.

RESULTS

Previous mammalian studies have shown that PtdIns 3-kinase promotes activation of the mammalian MAP kinases ERK1 and ERK2 (*36, 37*). Similarly, activation of a yeast MAP kinase Fus3 requires the function of Vps34 and Vps15, the catalytic and regulatory subunits of the only known phosphatidyl-3-kinase present in yeast (*5, 6*). We therefore set out to determine if Fus3 is regulated directly by PtdIns(3)P.

We first considered whether Fus3 binds directly to PtdIns(3)P. To this end we monitored association of purified GST-Fus3 with a panel of lipids spotted onto nitrocellulose membranes. The immobilized protein was detected with anti-GST antibodies. As shown in **Figure 3.1B**, Fus3 binds to several mono-phosphorylated PtdIns lipids including PtdIns(3)P (**Figure 3.1B**, asterix). In contrast, Fus3 does not appear to bind to poly-phosphorylated phosphoinositides, possibly because they contain additional negative charges (requiring additional ion-pairing positively-charged residues within Fus3) or because they are substantially larger than PtdIns(3)P (requiring a larger binding pocket within the protein).

Whereas PtdIns(3)P apparently binds to Fus3, attempts to quantify the affinity of interaction (e.g. by surface plasmon resonance or liposomal binding) were unsuccessful (Mark Lemmon, personal communication) (*38*). As an alternative approach to confirm binding, we investigated whether PtdIns(3)P modulates Fus3 kinase activity. To this end we measured Fus3 catalytic activity *in vitro* in the presence of various concentrations of a

soluble PtdIns(3)P analog. As shown in **Figure 3.1C and D**, PtdIns(3)P has a very modest dose-dependent effect on Fus3 catalytic activity. At PtdIns(3)P concentrations of 20-40 μM Fus3 activity was elevated, while at high concentrations (>150 μM) the activity was diminished. A similar dose-response relationship was evident whether using the test substrate myelin basic protein (MBP, **Figure 3.1C**) or Fus3 itself (auto-phosphorylation, **Figure 3.1D**).

We next investigated the residues in Fus3 responsible for PtdIns(3)P binding. In support of this effort we inspected the crystal structure of Fus3, and found a patch of eight basic amino acids that form a potential binding surface for acidic phospholipids (**Figure 3.1A**) (*31*). Substitution of six of the eight residues abolished kinase activity (data not shown); thus we focused our efforts on the remaining two substitutions. Both of these residues are found in Fus3 but not in the closely related MAPK Kss1. Purified Fus3 and $Fus3^{H333A/K335A}$ were incubated with purified Far1 or MBP (myelin basic protein) and [γ-^{32}P]-ATP, as described above in the methods. Substitutions at positions 333 and 335 ($Fus3^{H333A/K335A}$) yielded near-wildtype catalytic activity towards myelin basic protein (MBP, **Figure 3.1E,** lower band) as well as Fus3 auto-phosphorylation (**Figure 3.1E**, upper band, **Figure 3.1F**, lower band). $Fus3^{H333A/K335A}$ was also fully able to phosphorylate a known cellular substrate Far1 (*31, 39*) (**Figure 3.1F** upper band). Thus $Fus3^{H333A/K335A}$ is fully functional as a protein kinase.

Having determined that the H333A/K335A mutation does not abrogate the kinase function of Fus3, we set out to determine if the mutation affected Fus3's ability to bind

PtdIns(3)P. As can be seen in **Figure 3.1C and D**, the dose-dependent effects of PtdIns(3)P on $Fus3^{H333A/K335A}$ mirrored those obtained with the wild type Fus3 protein. Thus $Fus3^{H333A/K335A}$ is fully functional as a protein kinase, but remains fully sensitive to PtdIns(3)P.

Having determined that $Fus3^{H333A/K335A}$ is able to function normally as a protein kinase *in vitro*, we set out to determine the functionality of the $Fus3^{H333A/K335A}$ mutant *in vivo*. Full activation of Fus3 is dependent on pheromone treatment, as well as the presence of Vps15 and Vps34 and production of PtdIns(3)P (*5, 6*). Given that Fus3 appears to bind to PtdIns(3)P, we investigated whether Fus3 localized with endosomes where PtdIns(3)P is made, and if Fus3 localization is affected by the presence or absence of PtdIns(3)P. Fus3 is already known to localize to the nucleus, cytoplasm, and rarely, small puncta within the cell (*40, 41*). We treated cells with pheromone, or left them untreated, for one hour. We then examined the distribution of Fus3-GFP as compared to the endosomal marker Snf7-RFP (*40*). As can be seen in **Figure 3.2**, Fus3 is concentrated in the nucleus and more rarely in puncta, but these puncta do not colocalize significantly with the endosomal compartment either before or after treatment with pheromone (quantified in Table 3.1). Likewise, we observed no difference in Fus3 and $Fus3^{H333A/K335A}$ localization either in the presence or absence of PtdIns(3)P production (data not shown).

We then measured activation of Fus3 following stimulation of cells. In these experiments, we probed TCA precipitated cell lysates with antibodies specific for

phosphorylated and activated forms of the MAPKs Fus3 and Kss1. As can be seen in **Figure 3.3A**, Fus3$^{H333A/K335A}$ is fully phosphorylated following a 30 minute treatment of pheromone, indicating that mutation does not affect activation of Fus3 *in vivo*. We next sought to ascertain if the mutant is able to sustain transcriptional activation following pheromone stimulation. In these experiments, cells containing the pheromone-inducible reporter *FUS1*-lacZ were treated with varying doses of pheromone, and total transcriptional activation was measured colorimetrically. As can be seen in **Figure 3.3B**, Fus3$^{H333A/K335A}$ confers wildtype levels of activation in a reporter transcription assay. Finally, we sought to determine if the mutant played any role in the growth arrest response, which we monitored using a halo assay. As seen in **Figure 3.3C**, Fus3$^{H333A/K335A}$ shows smaller and more turbid halos as compared with wildtype Fus3. These smaller, more turbid halos are an indication that mutating the basic patch of Fus3 results in a diminished growth arrest response. Therefore, while the Fus3^{H333AK335A} mutation has no effect on one branch of the pheromone signaling pathway, one that is mediated by Fus3 and Kss1 and leads to new gene transcription, it has a clear effect on a second branch of the pathway that leads to growth arrest and requires Fus3 but not Kss1.

The Fus3^{H333AK335A} growth arrest phenotype appears to mirror the phenotype for mutants of the protein Far1. Far1 plays a critical role in many responses of the cell to pheromone, including oriented growth towards a mating partner (*42*) and cell cycle arrest (*43, 44*). Fus3 has been shown to be required for phosphorylation of Far1 at Thr-306, and this phosphorylation event as well as the putative phosphorylation site Thr-63 are necessary for cell cycle arrest (*39, 45*). Moreover, mutation of Thr-306 to Ala leads to a

substantial reduction in the electrophoretic mobility shift that accompanies Far1 phosphorylation (*39*) and slightly smaller and more turbid halos, while mutation of another phosphorylation site Thr-63, with no ensuing reduction in electrophoretic mobility shift, results in smaller and very turbid halos (**Figure 3.4** and (*39*)). These small, turbid halos are similar to those we observed with our Fus3 mutants (compare **Figure 3.4 and 3.3C** and (*39*)). Thus we considered whether the $Fus3^{H333A/K335A}$ mutation impairs phosphorylation of Far1 and/or Far1-mediated growth arrest *in vivo*.

Far1 phosphorylation in cells can be easily monitored by immunoblotting, since the phospho-protein exhibits dramatically diminished electrophoretic mobility (*45*). As shown in **Figure 3.5A and B** (upper panels), Far1 phosphorylation was indeed severely diminished in cells expressing the $Fus3^{H333A/K335A}$ mutant, as compared with the wild-type form of the kinase. Phosphorylation of another known substrate, Ste7, was completely unaffected (**Figure 3.5A and B**, middle panels). Thus when Fus3 is mutated in a manner that disrupts the basic patch, but preserves catalytic activity, Far1 is poorly phosphorylated and the cells fail to undergo proper cell cycle arrest. This loss of activity *in vivo* is particularly surprising given that Fus3 is fully able to phosphorylate Far1 in vitro (**Figure 3.1F**).

Given that Fus3 binds to Far1, we considered whether the $Fus3^{H333A/K335A}$ mutant disrupted the localization of Far1 (*2, 42, 46*). Far1-GFP *fus3Δ c*ells were transformed with either wildtype Fus3 or $Fus3^{H333A/K335A}$. The cells were treated with pheromone and monitored for Far1 localization. As can be seen in the top panels of **Figure 3.6,** while

some cells deficient in Fus3 are still capable of forming the characteristic shmoo in response to pheromone, there is little localization of Far1 to the shmoo tip. The bottom set of panels show cells expressing the $Fus3^{H333A/K335A}$ mutant. Here, we observe wildtype shmoo formation as well as wildtype localization of Far1 (compare to cells expressing wildtype Fus3 directly above). Therefore, although the $Fus3^{H333A/K335A}$ mutant shows a reduction in growth arrest in response to pheromone, this phenotype is not the result of a deficiency in Far1 translocation.

Taken together, the available data indicate that the basic patch mutant results in diminished growth arrest, but normal kinase activity, binding to PtdIns(3)P, Fus3 activation, Far1 localization and transcription-reporter activity. We therefore wondered if the lysine we identified in the basic patch of Fus3 could potentially be a site of regulation by ubiquitination. Many components of the pheromone pathway are known to be ubiquitinated (*22, 26*), and this modification occurs on Lys residues. To test if Lys-335 is ubiquitinated, we made a more conservative mutation within the basic patch of Fus3, in which just the lysine was replaced with arginine. We coexpressed wildtype Flag-tagged Fus3 or $Fus3^{K335R}$ together with an inducible form of myc-tagged ubiquitin. Myc-tagged ubiquitin was used because it is easier to detect and slows the degradation of substrates (*28*). We then purified Fus3, and monitored the co-purification of myc-ubiquitin by immunoblotting. As can be seen in **Figure 3.7**, Fus3 is ubiquitinated in a manner that does not depend on pheromone stimulation. Additionally, mutation of lysine 335 of Fus3 results in a decrease in the ubiquitination of Fus3, although some Fus3 is still modified, as is commonly seen when the primary ubiquitination site is altered. Thus, Lys-335

appears to be one site of ubiquitination in Fus3, although an additional site of ubiquitination probably exists. These findings should be regarded as preliminary.

Having determined that a mutation in the basic patch of Fus3 apparently reduces ubiquitination of Fus3, we set out to determine the ability of $Fus3^{K335R}$ to respond to pheromone and to regulate Far1 localization. As can be seen in **Figures 3.3 and 3.6**, $Fus3^{K335R}$ exhibits diminished growth arrest, but normal Fus3 activation, Far1 localization and transcription-reporter activity. Thus the activities of $Fus3^{K335R}$ mirror those observed for $Fus3^{H333A/K335A}$. Taken together these findings reveal a vital role for the basic patch of Fus3 in one pathway activated by pheromone and mediated by Fus3, as well as in the ubiquitination of Fus3. While mutations of the basic patch do not affect the ability of Fus3 to be activated by pheromone or to stimulate new gene transcription, they do dampen its ability to mediate growth arrest in response to pheromone, potentially through its inability to phosphorylate Far1 at residue 306 *in vivo*.

DISCUSSION

Here we investigate two potential new regulators of Fus3 activity: PtdIns(3)P and ubiquitin. Of these, regulation by ubiquitin can be uncoupled by substitutions in the basic patch of Fus3. Quantitative analysis reveals that $Fus3^{H333A/K335A}$ is fully competent to phosphorylate multiple substrates including Far1 and Fus3 *in vitro*. However, the $Fus3^{H333A/K335A}$ mutant exhibits a diminished ability to sustain cell cycle arrest and phosphorylate Far1 *in vivo*. Additionally, mutation of Lys335 results in a decrease in ubiquitination of Fus3. The loss of mobility shift combined with a decrease in growth arrest mirrors the changes already reported for mutations that disrupt phosphorylation of Far1. Gartner *et al.* have previously reported that mutation of Thr306 to Ala in Far1 results in a decrease in responsiveness to pheromone as well as a loss of mobility shift of Far1, while mutations of other putative phosphorylation sites in Far1, including Thr63, have no effect on mobility. They proposed that Thr306 is a major phosphorylation site of Far1 by Fus3, and that phosphorylation at this locus is required for activation of Far1 (*39*). We propose that mutation of the basic patch of Fus3 may result in an abolition of the ability of Fus3 to phosphorylate Far1 *in vivo* but not *in vitro*.

We have also tested the hypothesis that PtdIns(3)P regulates Fus3 catalytic activity. This model stems from our previous observations that the PtdIns(3)-kinase in yeast is required for efficient propagation of the G protein signaling pathway activated by pheromone. Gpa1 colocalizes with Vps15 and Vps34 at the endosome, binds to Vps15 and Vps34 directly and in a guanine nucleotide-dependent manner, promotes an increase

in cellular PtdIns(3)P, and triggers endosomal translocation of PtdIns(3)P-binding proteins. Moreover, the interaction of Gpa1 with Vps34 triggers most of the events typically seen after treatment with mating pheromones, including activation of Fus3. Deletion or pharmacological inhibition of Vps34 abrogates all of these Gpa1 signaling phenotypes including Fus3 activation. Thus genetic, cell biological, biochemical, and pharmacological evidence support the model that Gpa1 activates Vps34 and that Vps34 activates Fus3. In comparison, Kss1 is much less responsive to changes in Gpa1 or Vps34 activity (*5, 6*).

Taken together, these findings indicate a potential role for mono-phosphorylated phosphoinositides in Fus3 activation. However, the functional effects of PtdIns(3)P are modest at best. Nevertheless this result leaves open the possibility that other proteins bind to PtdIns(3)P and thereby contribute to the regulation of Fus3. For example, Fus3 activation requires the MAPK scaffolding protein Ste5, while Kss1 activation does not. Moreover, Ste5 was shown to bind to PtdIns(4)P and PtdIns(4,5)P_2 *in vitro* (*47*). The possibility remains that Fus3 activity is modulated by Ste5 binding to PtdIns(3)P, PtdIns(4)P or PtdIns(4,5)P_2.

Regardless of the precise mechanism, it is evident that PtdIns(3)P acts intracellularly to alter MAP kinase activation. Thus PtdIns(3)P meets the criteria of a second messenger as originally defined by Earl Sutherland for cAMP in the late 1950s. In contrast to many other second messengers however, PtdIns(3)P does not diffuse throughout the cytoplasm but remains associated with the endosomal membrane where it

is made (*48*). Thus PtdIns(3)P serves as a highly specific marker of subcellular localization, as well as of G protein activity. PtdIns 4-P and PtdIns 4,5-P_2 are produced in different subcellular locations, and these differences could contribute further to signaling specificity and activity. In any event, these discoveries suggest an important and expanded role for phosphoinositides in the pheromone-response pathway. Current investigations are aimed towards purifying and reconstituting known substrates together with the Ste5 protein complex (includes Ste5, Ste11, Ste50, Ste7, and Fus3) and various phosphoinositide lipids.

In summary, we have demonstrated regulation of the MAP kinase Fus3 through ubiquitination. Under normal, pheromone-stimulated conditions, Fus3 promotes Far1 phosphorylation, and morphogenesis leading to cell division arrest. When ubiquitination is diminished, Far1 phosphorylation and cell cycle arrest are compromised. Other Fus3-mediated responses are unaffected. The separation of two arms of a G protein signaling pathway by the mutation of a single residue in Fus3 represents a powerful tool to distinguish the many roles that Fus3 plays in the pathway. Given the broad conservation of G protein, MAP kinase, and PtdIns 3-kinase signaling in eukaryotes, the mechanisms elucidated here for Fus3 are likely to be conserved in other signaling programs and in other cellular systems.

REFERENCES

(1) Goldsmith, Z. G., and Dhanasekaran, D. N. (2007) G protein regulation of MAPK networks. *Oncogene 26*, 3122-42.

(2) Dohlman, H. G., and Thorner, J. W. (2001) Regulation of G protein-initiated signal transduction in yeast: Paradigms and principles. *Annu. Rev. Biochem. 70*, 703-54.

(3) Whiteway, M., Hougan, L., Dignard, D., Thomas, D. Y., Bell, L., Saari, G. C., Grant, F. J., O'Hara, P., and MacKay, V. L. (1989) The STE4 and STE18 genes of yeast encode potential β and γ subunits of the mating factor receptor-coupled G protein. *Cell 56*, 467-77.

(4) Guo, M., Aston, C., Burchett, S. A., Dyke, C., Fields, S., Rajarao, S. J., Uetz, P., Wang, Y., Young, K., and Dohlman, H. G. (2003) The yeast G protein α subunit Gpa1 transmits a signal through an RNA binding effector protein Scp160. *Mol Cell 12*, 517-24.

(5) Slessareva, J. E., Routt, S. M., Temple, B., Bankaitis, V. A., and Dohlman, H. G. (2006) Activation of the phosphatidylinositol 3-kinase Vps34 by a G protein alpha subunit at the endosome. *Cell 126*, 191-203.

(6) Heenan, E. J., Vanhooke, J.L., Temple, B.R., Betts, L., Sondek, J.E., and Dohlman, H.G. (2009) Structure and function of Vps15 in the endosomal G protein signaling pathway. *Biochemistry 48*, 6390-6401.

(7) Auger, K. R., Carpenter, C. L., Cantley, L. C., and Varticovski, L. (1989) Phosphatidylinositol 3-kinase and its novel product, phosphatidylinositol 3-phosphate, are present in *Saccharomyces cerevisiae*. *J Biol Chem 264*, 20181-4.

(8) Schu, P. V., Takegawa, K., Fry, M. J., Stack, J. H., Waterfield, M. D., and Emr, S. D. (1993) Phosphatidylinositol 3-kinase encoded by yeast VPS34 gene essential for protein sorting. *Science 260*, 88-91.

(9) Wenk, M. R., Lucast, L., Di Paolo, G., Romanelli, A. J., Suchy, S. F., Nussbaum, R. L., Cline, G. W., Shulman, G. I., McMurray, W., and De Camilli, P. (2003) Phosphoinositide profiling in complex lipid mixtures using electrospray ionization mass spectrometry. *Nat Biotechnol 21*, 813-7.

(10) Stack, J. H., Herman, P. K., Schu, P. V., and Emr, S. D. (1993) A membrane-associated complex containing the Vps15 protein kinase and the Vps34 PI 3-kinase is essential for protein sorting to the yeast lysosome-like vacuole. *Embo J 12*, 2195-204.

(11) Brown, W. J., DeWald, D.B., Emr, S.D., Plutner, H., and Balch, W.E. (1995) Role of phosphatidylinositol 3-kinase in the sorting and transport of newly synthesized lysosomal enzymes in mammalian cells. *Journal of Cell Biology 130*, 781-796.

(12) Yan, Y., and Backer, J.M. (2007) Regulation of class III (Vps34) PI3Ks. *Biochemical Society Transactions 35*, 239-241.

(13) Backer, J. M. (2008) The regulation and function of Class II PI3Ks: novel roles for Vps34. *Biochemical Journal 410*, 1-17.

(14) Herman, P. K., Stack, J.H., DeModena, J.A., and Emr, S.D. (1991) A novel protein kinase homolog essential for protein sorting to the yeast lysosome-like vacuole. *Cell 64*, 425-437.

(15) Herman, P. K., Stack, J.H., and Emr, S.D. (1991) A genetic and structural analysis of the yeast Vps15 protein kinase: evidence for a direct role of Vps15p in vacuolar protein delivery. *Embo J 10*, 4049-4060.

(16) Stenmark, H., Aasland, R., Toh, B. H., and D'Arrigo, A. (1996) Endosomal localization of the autoantigen EEA1 is mediated by a zinc-binding FYVE finger. *J Biol Chem 271*, 24048-54.

(17) Ponting, C. P. (1996) Novel domains in NADPH oxidase subunits, sorting nexins, and PtdIns 3- kinases: binding partners of SH3 domains? *Protein Sci 5*, 2353-7.

(18) Simonsen, A., Lippe, R., Christoforidis, S., Gaullier, J. M., Brech, A., Callaghan, J., Toh, B. H., Murphy, C., Zerial, M., and Stenmark, H. (1998) EEA1 links PI(3)K function to Rab5 regulation of endosome fusion. *Nature 394*, 494-8.

(19) Simonsen, A., Gaullier, J.M., D'Arrigo, A., and Stenmark, H. (1999) The Rab5 effector EEA1 interacts directly with syntaxin-6. *J Biol Chem 274*, 28857-28860.

(20) Seaman, M. N. J., Caffrey, J.M., and Emr S.D. (1998) A membrane coat complex essential for endosome-to-Golgi retrograde transport in yeast. *J Cell Biol 142*, 665-681.

(21) Piper, R. C., and Katzmann, D.J. (2007) Biogenesis and function of multivesicular bodies. *Annu Rev Cell Dev Biol 23*, 519-547.

(22) Wang, Y., Marotti, L. A., Jr., Lee, M. J., and Dohlman, H. G. (2005) Differential regulation of G protein alpha subunit trafficking by mono- and polyubiquitination. *J Biol Chem 280*, 284-91.

(23) Wang, Y., and Dohlman, H. G. (2002) Pheromone-dependent ubiquitination of the mitogen-activated protein kinase kinase Ste7. *J Biol Chem 277*, 15766-72.

(24) Wang, Y., and Dohlman, H. G. (2006) Regulation of G protein and mitogen-activated protein kinase signaling by ubiquitination: insights from model organisms. *Circ Res 99*, 1305-14.

(25) Marotti, L. A., Jr., Newitt, R., Wang, Y., Aebersold, R., and Dohlman, H. G. (2002) Direct identification of a G protein ubiquitination site by mass spectrometry. *Biochemistry 41*, 5067-74.

(26) Torres, M. P., Lee, M.J, Ding, F., Purbeck, C., Kuhlman, B., Dokholyan, N.V., and Dohlman, H.G. (2009) G Protein Mono-ubiquitination by the Rsp5 Ubiquitin Ligase. *Journal of Biological Chemistry 284*, 8940-8950.

(27) Zeller, C. E., Parnell, S.C., and Dohlman, H.G. (2007) The RACK1 ortholog Asc1 functions as a G-protein beta subunit coupled to glucose responsiveness in yeast. *Journal of Biological Chemistry 282*, 25168-25176.

(28) Roth, A. F., Sullivan, D. M., and Davis, N. G. (1998) A large PEST-like sequence directs the ubiquitination, endocytosis, and vacuolar degradation of the yeast a-factor receptor. *J Cell Biol 142*, 949-61.

(29) Hoffman, G. A., Garrison, T. R., and Dohlman, H. G. (2000) Endoproteolytic Processing of Sst2, a Multidomain Regulator of G Protein Signaling in Yeast. *J Biol Chem 275*, 37533-37541.

(30) Parnell, S. C., Marotti, L. A., Jr., Kiang, L., Torres, M. P., Borchers, C. H., and Dohlman, H. G. (2005) Phosphorylation of the RGS protein Sst2 by the MAP kinase Fus3 and use of Sst2 as a model to analyze determinants of substrate sequence specificity. *Biochemistry 44*, 8159-66.

(31) Remenyi, A., Good, M. C., Bhattacharyya, R. P., and Lim, W. A. (2005) The role of docking interactions in mediating signaling input, output, and discrimination in the yeast MAPK network. *Mol Cell 20*, 951-62.

(32) Cox, J. S., Chapman, R. E., and Walter, P. (1997) The unfolded protein response coordinates the production of endoplasmic reticulum protein and endoplasmic reticulum membrane. *Mol Biol Cell 8*, 1805-14.

(33) Hoffman, G., Garrison, T. R., and Dohlman, H. G. (2002) Analysis of RGS proteins in *Saccharomyces cerevisiae*. *Methods Enzymol 344*, 617-631.

(34) Evan, G. I., Lewis, G. K., Ramsay, G., and Bishop, J. M. (1985) Isolation of monoclonal antibodies specific for human c-myc proto- oncogene product. *Mol Cell Biol 5*, 3610-6.

(35) Bolte, S., and Cordelieres, F. P. (2006) A guided tour into subcellular colocalization analysis in light microscopy. *J Microsc 224*, 213-32.

(36) Duckworth, B. C., and Cantley, L. C. (1997) Conditional inhibition of the mitogen-activated protein kinase cascade by wortmannin. Dependence on signal strength. *J Biol Chem 272*, 27665-70.

(37) Wennstrom, S., and Downward, J. (1999) Role of phosphoinositide 3-kinase in activation of ras and mitogen-activated protein kinase by epidermal growth factor. *Mol Cell Biol 19*, 4279-88.

(38) Zhu, H., Bilgin, M., Bangham, R., Hall, D., Casamayor, A., Bertone, P., Lan, N., Jansen, R., Bidlingmaier, S., Houfek, T., Mitchell, T., Miller, P., Dean, R. A., Gerstein, M., and Snyder, M. (2001) Global analysis of protein activities using proteome chips. *Science 293*, 2101-5.

(39) Gartner, A., Jovanovic, A., Jeoung, D. I., Bourlat, S., Cross, F. R., and Ammerer, G. (1998) Pheromone-dependent G1 cell cycle arrest requires Far1 phosphorylation, but may not involve inhibition of Cdc28-Cln2 kinase, in vivo. *Mol Cell Biol 18*, 3681-91.

(40) Huh, W. K., Falvo, J. V., Gerke, L. C., Carroll, A. S., Howson, R. W., Weissman, J. S., and O'Shea, E. K. (2003) Global analysis of protein localization in budding yeast. *Nature 425*, 686-91.

(41) Choi, K. Y., Kranz, J. E., Mahanty, S. K., Park, K. S., and Elion, E. A. (1999) Characterization of fus3 localization: active fus3 localizes in complexes of varying size and specific activity. *Mol Biol Cell 10*, 1553-68.

(42) Butty, A. C., Pryciak, P. M., Huang, L. S., Herskowitz, I., and Peter, M. (1998) The role of Far1p in linking the heterotrimeric G protein to polarity establishment proteins during yeast mating. *Science 282*, 1511-6.

(43) Chang, F., and Herskowitz, I. (1990) Identification of a gene necessary for cell cycle arrest by a negative growth factor of yeast: FAR1 is an inhibitor of a G1 cyclin, CLN2. *Cell 63*, 999-1011.

(44) Peter, M., and Herskowitz, I. (1994) Direct inhibition of the yeast cyclin-dependent kinase Cdc28-Cln by Far1. *Science 265*, 1228-31.

(45) Breitkreutz, A., Boucher, L., and Tyers, M. (2001) MAPK specificity in the yeast pheromone response independent of transcriptional activation. *Curr Biol 11*, 1266-71.

(46) Nern, A., and Arkowitz, R. A. (1999) A Cdc24p-Far1p-Gbetagamma protein complex required for yeast orientation during mating. *J Cell Biol 144*, 1187-202.

(47) Garrenton, L. S., Young, S. L., and Thorner, J. (2006) Function of the MAPK scaffold protein, Ste5, requires a cryptic PH domain. *Genes Dev 20*, 1946-58.

(48) Gillooly, D. J., Morrow, I. C., Lindsay, M., Gould, R., Bryant, N. J., Gaullier, J. M., Parton, R. G., and Stenmark, H. (2000) Localization of phosphatidylinositol 3-phosphate in yeast and mammalian cells. *Embo J 19*, 4577-88.

Table 3.1 Colocalization of Fus3 and Snf7 in the presence and absence of pheromone.

	- pheromone	+ pheromone
Fus3	Range: 1.6-2.7% Average: 2.1%	Range: 1.9-9.3% Average: 4.5%
$Fus3^{H333A/K335A}$	Range: 1.0-3.1% Average: 2.1%	Range: 1.7-3.5% Average: 2.7%

FIGURE LEGENDS

Figure 3.1. PtdIns(3)P binds to Fus3. (A) Crystal structure of Fus3 (Protein Databank entry 2B9F) showing the ATP substrate (spacefilled representation in red, green, and blue), Fus3 phosphorylation sites (spacefilled residues in orange) as well as a cluster of basic amino acids ("basic patch", spacefilled residues in blue) (*31*) identified by visual inspection and presented using PyMOL (DeLano Scientific**). (**B) Lipid binding properties of Fus3. PIP strips (Echelon) spotted with the indicated lipids were mixed with purified GST or GST-Fus3. Bound protein was detected with anti-GST antibodies. In vitro phosphorylation of MBP (C), Fus3 and Fus3$^{H333A/K335A}$ (auto-phosphorylation) (D) in the presence of different concentrations of PtdIns(3)P. ^{32}P incorporation was quantified following 6% or 15% SDS-PAGE using a PhosphorImager SI and ImageQuant Software. Data shown are averages of at least two independent experiments. *In vitro* phosphorylation of MBP (P-MBP) (E), mini-Far1 (P-Far1) (F), and Fus3 (autophosphorylation, P-Fus3) (E, F) by Fus3 and Fus3$^{H333A/K335A}$ over time. This figure was contributed by Janna Slessareva.

Figure 3.2. Basic patch mutants of Fus3 show normal localization in the presence and absence of pheromone. Cells containing integrated Fus3-GFP or Fus3$^{H333A/K335A}$-GFP and Snf7-RFP were transformed with an empty vector and left untreated or treated with 3μM α-factor for one hour. Cells were monitored by microscopy for colocalization of Fus3 and Snf7, an endosomal marker.

Figure 3.3. The basic patch of Fus3 is necessary for one branch of the G protein signaling pathway mediated by Fus3. (A) Wild-type (WT), *fus3*Δ, and *far1*Δ strains were transformed with the indicated plasmids and treated with 3μM α-mating factor for 30 minutes and analyzed by immunoblotting using antibodies against p44/p42, Fus3 and G6PDH (Load control). (B) The *fus3Δ* strains were transformed with a plasmid containing a pheromone-inducible *FUS1-lacZ* reporter; transcriptional activation was measured by monitoring β-galactosidase activity in response to pheromone. (C) The *fus3Δ* strains were plated and treated with 45 micrograms of α factor to induce cell division arrest. $Fus3^{KR}$ refers to the basic patch single point mutant $Fus3^{K335R}$. $Fus3^{HAKA}$ refers to the basic patch double point mutant $Fus3^{H333A/K335A}$.

Figure 3.4. Far1 phosphorylation mutants show reduced cell cycle arrest in response to pheromone. A *far1*Δ strain was transformed with the indicated plasmids and were plated and treated with 45 micrograms of α factor to induce cell division arrest.

Figure 3.5. An intact basic batch of Fus3 promotes phosphorylation of Far1 in vivo. Far1 mobility was analyzed by immunoblotting in *fus3*Δ (A) and *fus3*Δ*kss1*Δ (B) strains transformed with a plasmid containing either no insert (vector), Fus3 or $Fus3^{H333A/K335A}$. Cells were treated with 3 μM α factor for the indicated times and resolved by 7 % SDS-PAGE and immunoblotting. Pheromone-dependent phosphorylation of Far1 (P-Far1) and Ste7 (P-Ste7) results in an electrophoretic mobility shift detected using antibodies against Far1 (HA epitope) or Ste7. Note that the slowest-migrating form of Far1 is the fully phosphorylated species. Note also that a 60 min pheromone treatment results in elevated

Far1 expression. G6PDH, loading control. Band intensity was quantified by densitometry and analyzed using ImageJ. This figure was contributed by Janna Slessareva.

Figure 3.6. Basic patch mutants of Fus3 show normal localization of Far1 in response to pheromone. Far1-GFP *fus3Δ c*ells were transformed with either wildtype Fus3, $Fus3^{K335R}$ or $Fus3^{H333A/K335A}$ and left untreated or treated with 3 μM α-factor for two hours. Cells were monitored by microscopy for shmoo formation and translocation of Far1 to the shmoo tip.

Figure 3.7. Fus3 ubiquitination is reduced by mutation of the basic patch. Detergent-solubilized extracts from *fus3*Δ cells expressing the indicated Flag fusion proteins and ubiquitin fused to a Myc epitope were incubated with Flag resin, eluted with 3X Flag peptide, resolved by 10% SDS-PAGE, and analyzed by immunoblotting with antibodies against Flag, Myc, and G6PDH (Load control). *, indicates protein of interest.

Figure 3.1

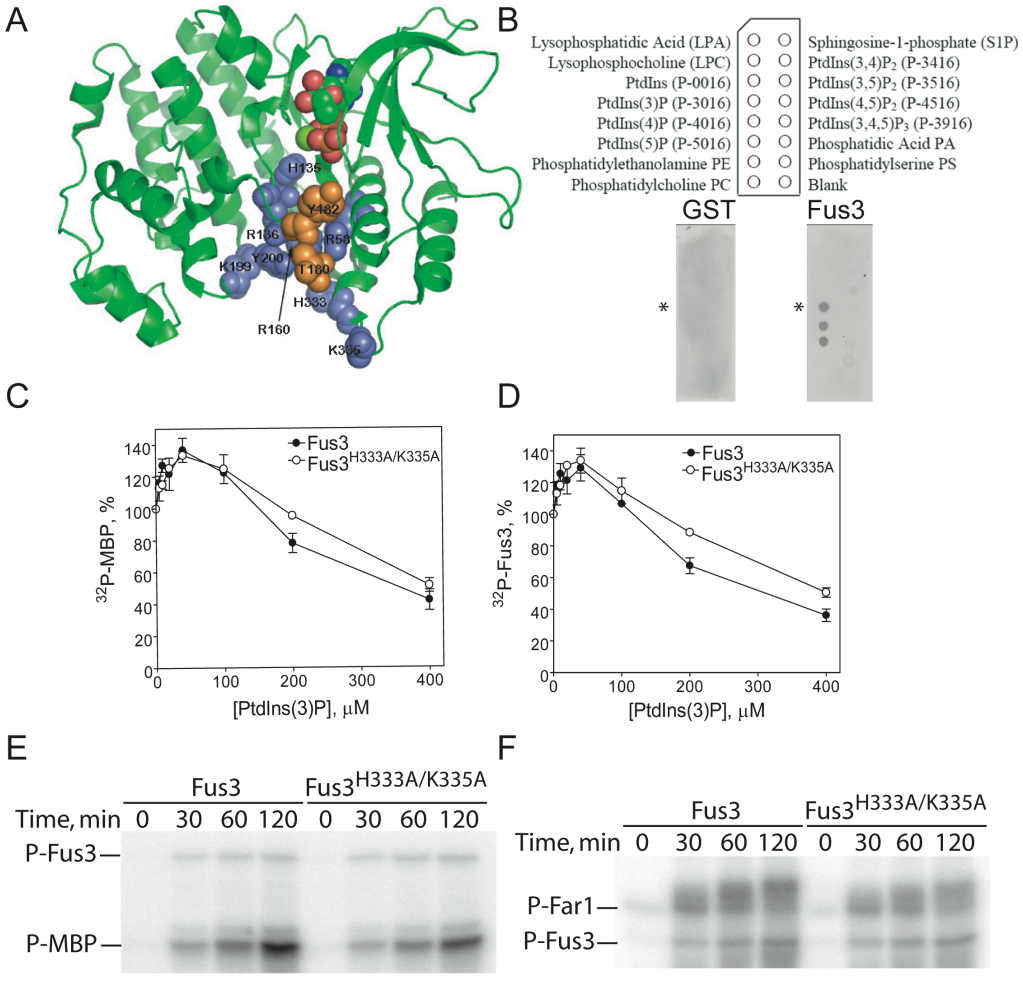
A
H136
Y182
R186
R58
Y200
K199
T160
H333
R160
K335
B
Lysophosphatidic Acid (LPA)
Lysophosphocholine (LPC)
PtdIns (P-0016)
PtdIns(3)P (P-3016)
PtdIns(4)P (P-4016)
PtdIns(5)P (P-5016)
Phosphatidylethanolamine PE
Phosphatidylcholine PC
Sphingosine-1-phosphate (S1P)
PtdIns(3,4)P2 (P-3416)
PtdIns(3,5)P2 (P-3516)
PtdIns(4,5)P2 (P-4516)
PtdIns(3,4,5)P3 (P-3916)
Phosphatidic Acid PA
Phosphatidylserine PS
Blank
GST
Fus3
C
Fus3
Fus3H333A/K335A
32P-MBP, %
[PtdIns(3)P], μM
D
Fus3
Fus3H333A/K335A
32P-Fus3, %
[PtdIns(3)P], μM
E
Fus3
Fus3H333A/K335A
Time, min 0 30 60 120 0 30 60 120
P-Fus3
P-MBP
F
Fus3
Fus3H333A/K335A
Time, min 0 30 60 120 0 30 60 120
P-Far1
P-Fus3

Figure 3.2

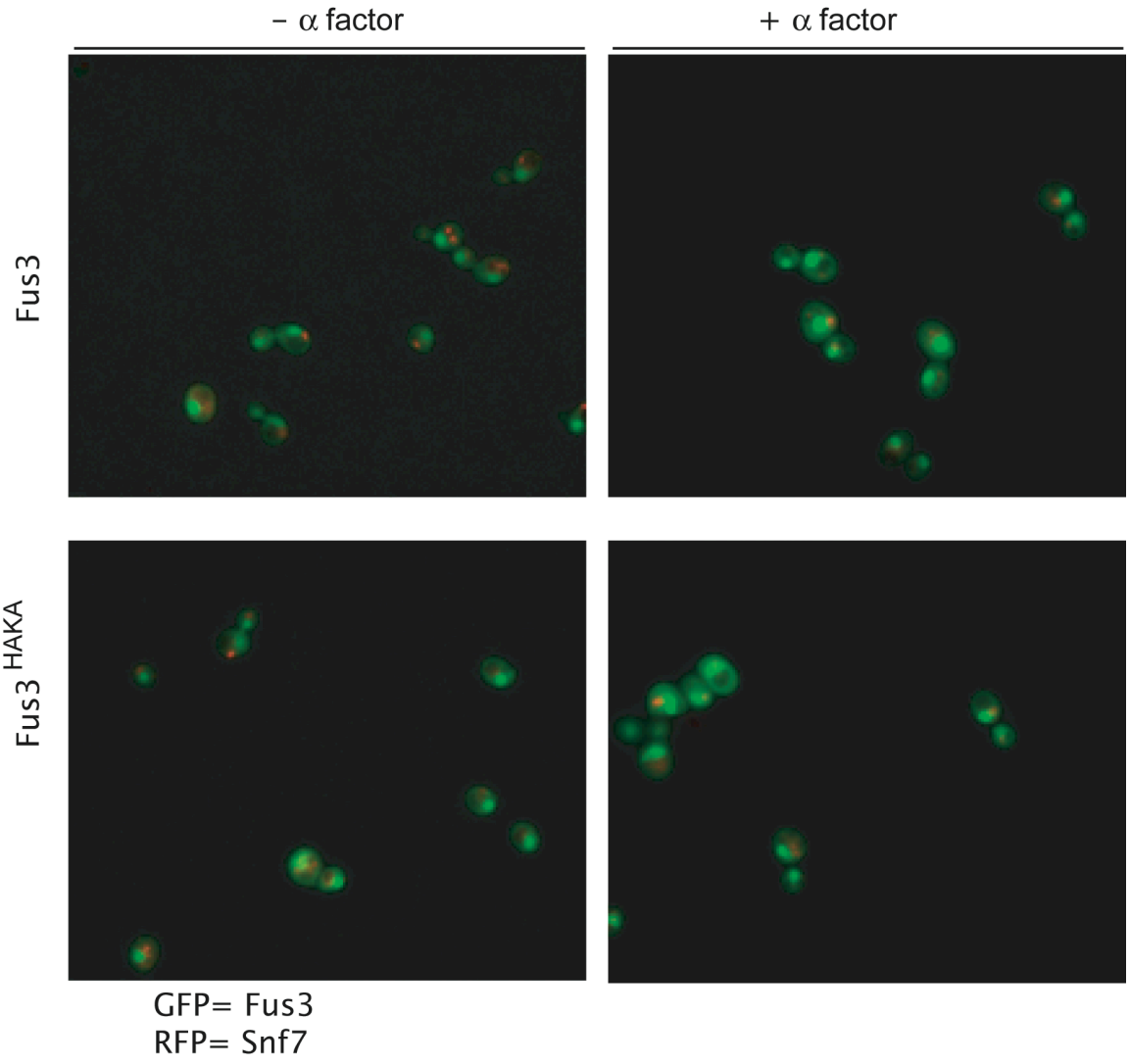

Figure 3.3

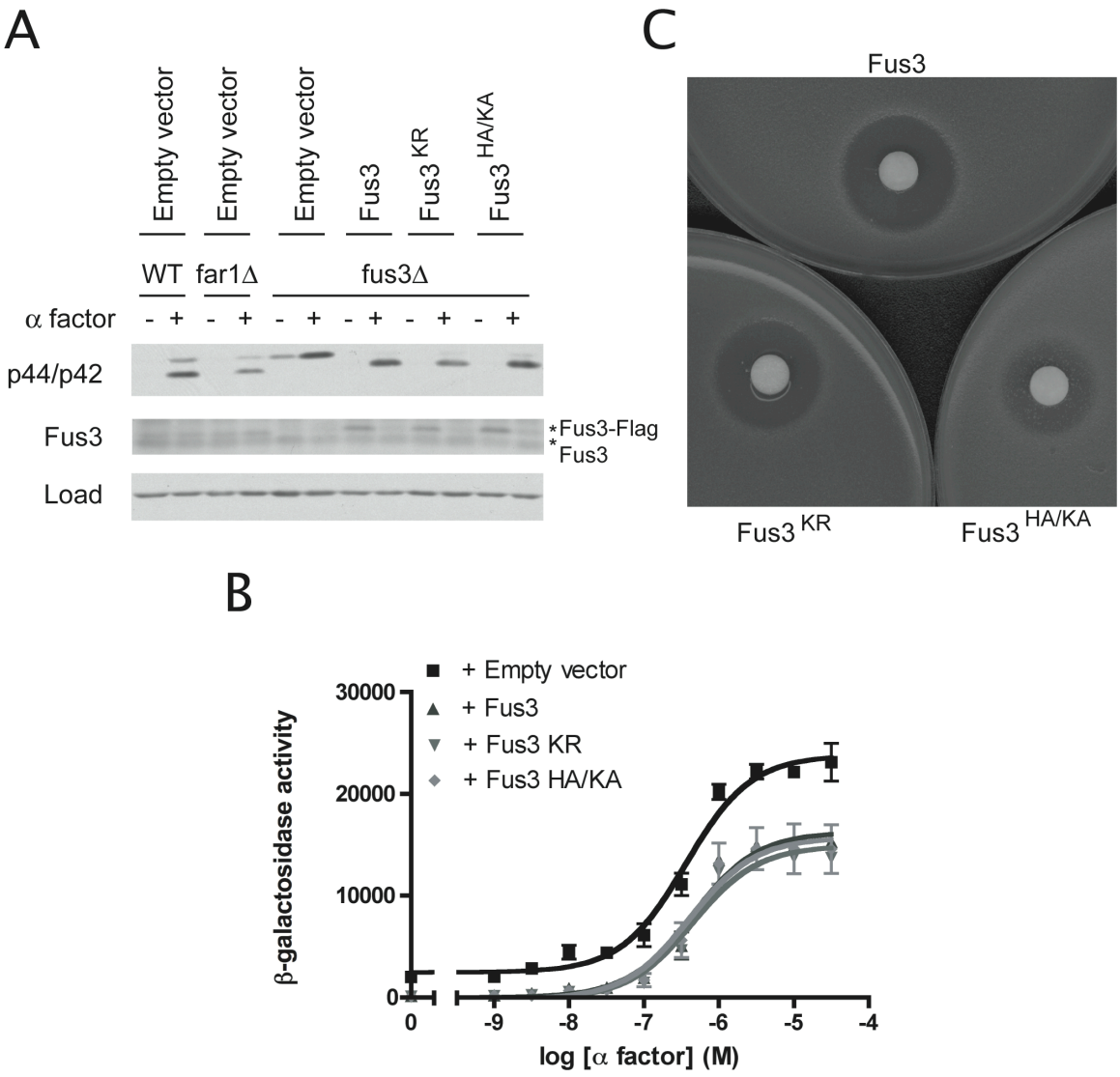
A
Empty vector
Empty vector
Empty vector
Fus3
Fus3 KR
Fus3 HA/KA
WT
far1Δ
fus3Δ
α factor
- + - + - + - + - + - +
p44/p42
Fus3
*Fus3-Flag
*Fus3
Load
C
Fus3
Fus3 KR
Fus3 HA/KA
B
+ Empty vector
+ Fus3
+ Fus3 KR
+ Fus3 HA/KA
β-galactosidase activity
30000
20000
10000
0
0
-9
-8
-7
-6
-5
-4
log [α factor] (M)

Figure 3.4

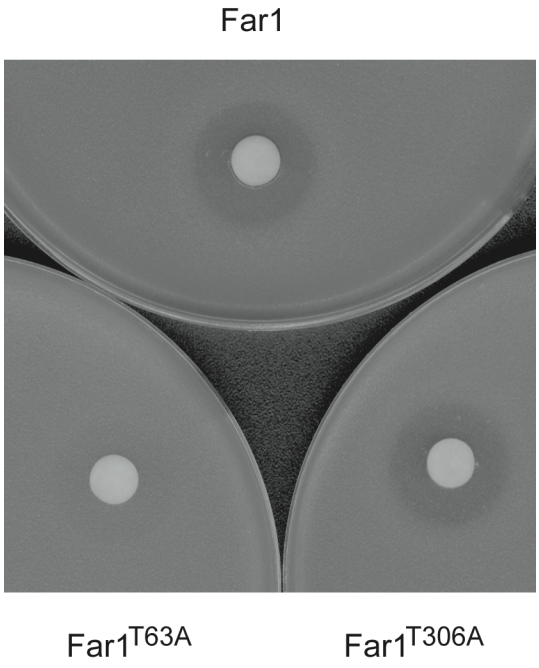

Figure 3.5

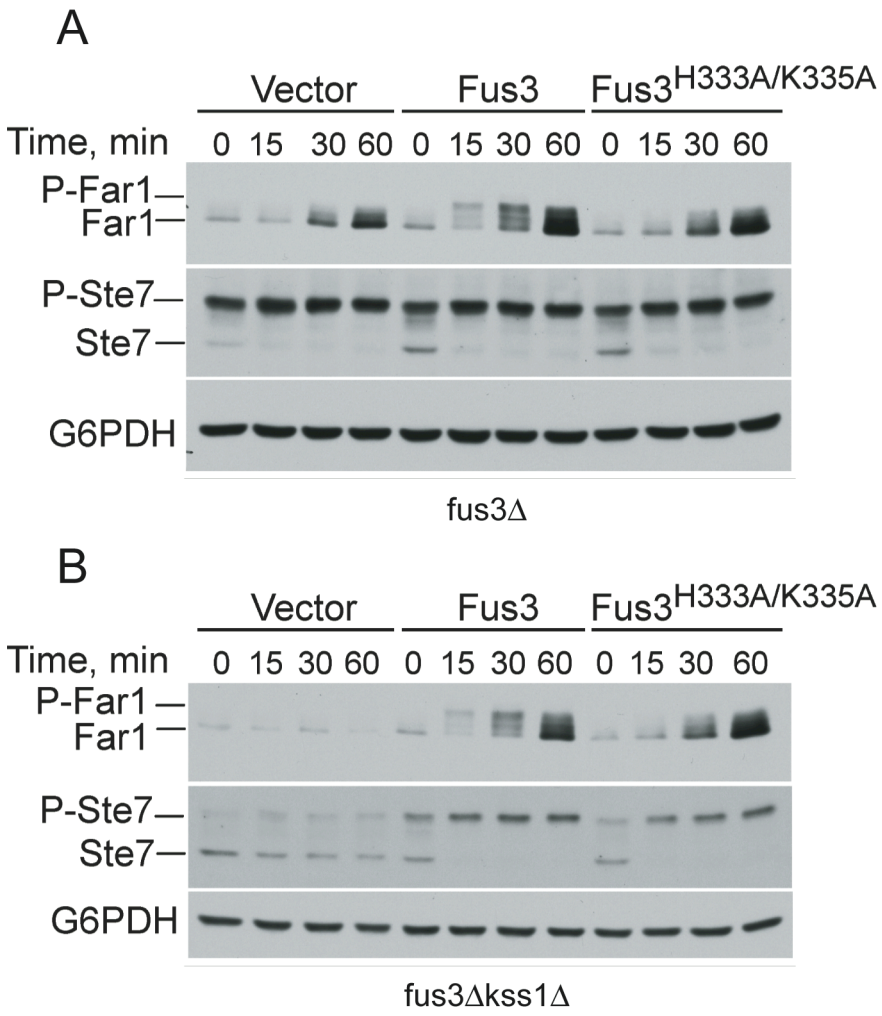
A
Vector
Fus3
Fus3H333A/K335A
Time, min
0 15 30 60 0 15 30 60 0 15 30 60
P-Far1
Far1
P-Ste7
Ste7
G6PDH
fus3Δ
B
Vector
Fus3
Fus3H333A/K335A
Time, min
0 15 30 60 0 15 30 60 0 15 30 60
P-Far1
Far1
P-Ste7
Ste7
G6PDH
fus3Δkss1Δ

Figure 3.6

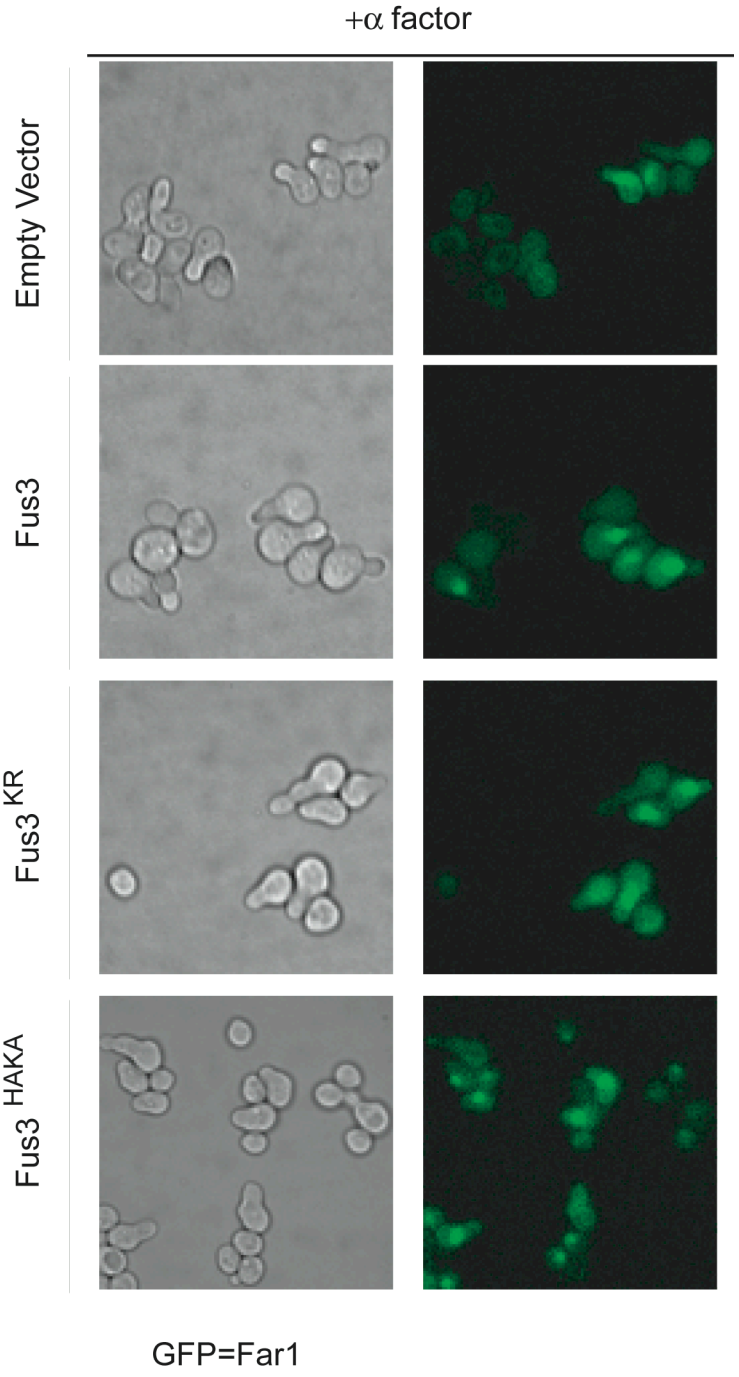

Figure 3.7

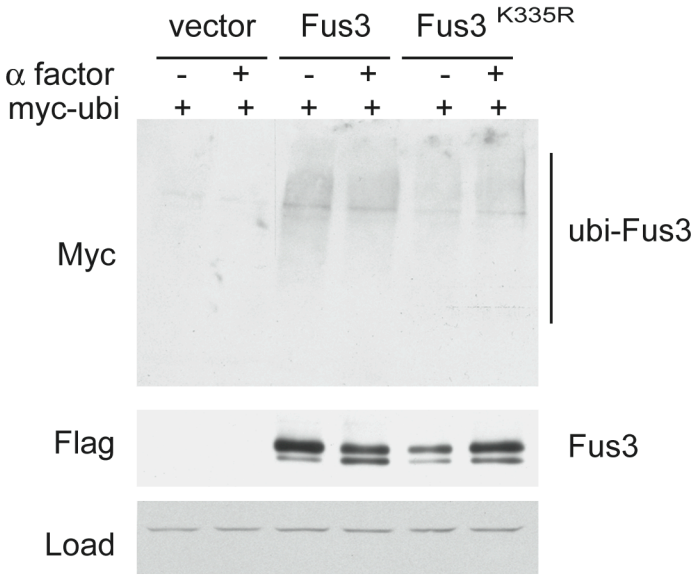
vector
Fus3
Fus3 K335R
α factor
- + - + - +
myc-ubi
+ + + + + +
Myc
ubi-Fus3
Flag
Fus3
Load

Chapter 4

The Kinase Domain of Vps15

INTRODUCTION

G protein signaling is highly conserved in organisms from yeast to humans. We have shown that, in addition to the pathway induced by pheromone that originates from the plasma membrane, there is a parallel and complementary pathway that originates from the endosome (*1-3*). This endosomal pathway requires Vps34 and Vps15, the catalytic and regulatory subunits respectively of the only known phosphotidylinositol-3-kinase (PI3K) present in yeast (*2, 4, 5*). The pathway preferentially activates the MAP kinase Fus3, and produces most, but not all, of the same signaling outputs as does the pathway that originates at the plasma membrane (*2*).

Vps15 is a large protein with three primary domains: an N-terminal kinase domain, a C-terminal 7 WD-40 repeat domain, and an intermediate domain that bridges these two domains and contains multiple heat repeats that are important for protein-protein interactions (*2, 6-8*). Vps15 is a known Ser/Thr protein kinase, and is believed to autophosphorylate, although no other substrates of its kinase activity are known (*6, 9, 10*). It has been noted that mutations of the kinase activity of Vps15 also result in a disruption of its association with binding partners, including Vps34, which itself is a protein kinase (*7*). Moreover, the kinase activity of Vps15 is required for full activation of the endosomal G protein signaling pathway (*2*). We have shown that it is the kinase domain with the intermediate domain that is both necessary and sufficient to bind to $Gpa1^{G\alpha}$ and well as to propagate the G protein signal in response to pheromone, while the

WD domain of Vps15 serves as a scaffold to assemble the various binding partners of Vps15 (*4*).

To further elucidate the role of the kinase domain of Vps15 in pheromone-mediated G protein coupled signaling in the cell, we sought to determine if it is the activation of Vps15 by phosphorylation or the kinase activity of Vps15 itself that is required for G protein coupled signaling. We also sought to identify potential sites of phosphorylation in Vps15, and determine the effect of mutation of these sites on Vps15's role in various signaling pathways, including G protein signaling.

Before we could make further inroads into determining the role of the kinase domain of Vps1 on G protein signaling, we sought to confirm the reports of its purported kinase activity. Doubts were raised about Vps15's function as a protein kinase based on two primary pieces of evidence. The first is that mutations in the kinase domain of Vps15 that result in a loss of its "autophosphorylation", also result in a loss of interaction with binding partners, including Vps34 (*7*). It is therefore theoretically possible that mutations of the "kinase activity" of Vps15 actually just disrupt an interaction between Vps15 and the protein that phosphorylates it. Second, in early experiments done to show Vps15 is autophophorylated, Vps15 may have not been purified to homogeneity (indeed, Vps34 was probably purified with it since Vps15 and Vps34 form a tight association), and so it is possible that the phosphorylation of Vps15 in these experiments was actually due to a contaminating kinase and not to the kinase activity of Vps15 itself.

Here we confirm that Vps15 is indeed phosphorylated, and that mutation of the kinase activity of Vps15 abolishes phosphorylation of Vps15. We also show that phosphorylation of Vps15 is abolished in the absence of Vps34. Finally, we demonstrate that the absence of Vps34 also results in an extreme reduction of Vps15's total protein level in the cell.

EXPERIMENTAL PROCEDURES

Strains and Plasmids

Standard methods for the growth, maintenance, and transformation of yeast and bacteria and for the manipulation of DNA were used throughout. Yeast *Saccharomyces cerevisiae* strains used in this study are BY4741 (*MAT***a** *leu2*Δ *met15*Δ *his3*Δ *ura3*Δ), and BY4741-derived gene deletion mutants containing the G418-resistance marker (Invitrogen). Previously described plasmids and yeast shuttle vectors are: pRS315-ADH-Flag (contains *ADH1* promoter/terminator and a Flag epitope that can be added 3' with an XmaI site) (*11*), pRS316-VPS34^{N736K} (*2*), and pRS315-ADH-VPS15-Flag (*4*). Plasmid pRS315-ADH-VPS15^{E200R}-Flag was created by using the previously described mutagenic primers (*2*) and performing QuikChange Site-directed mutagenesis on the pRS315-ADH-VPS15-Flag plasmid.

Metabolic Labeling Experiments

The metabolic labeling procedure is based on a previously described method (*12*). Briefly, 50 mls of transformed cells were grown to an $A_{600\ nm}$ of ~0.8 in selective media. The cells were centrifuged at 1200g for 5 minutes and washed once with 25 mls of ddH_2O. Cells were then resuspended in 35 mls of phosphate-free selective media and transferred to a fresh 250 ml flask. 1mCi of ^{32}P was added to each flask, and the cells were grown with shaking for 1 hour at 30°C. The cells were then spun down and the media discarded. The cells were washed once with 25 mls ddH_2O and the wash was discarded. Cells were then washed once with 0.5 ml ddH_2O and transferred to an o-ring

screwcap tube. Any remaining ddH_2O wash was removed and pellets were frozen at -80°C. Pulldown experiments were then performed as described below.

Purification of Flag Epitope-tagged Proteins

For strains that had not previously undergone metabolic labeling, strains expressing the indicated plasmids were grown in a 50 ml culture to $A_{600nm} \sim 0.8$. Growth was stopped by the addition of sodium azide to a final concentration of 10mM, and the cells were harvested by centrifugation and frozen at -80°C. The procedure for Flag purification has previously been described in detail (*4*). Briefly, cells were disrupted by glass bead lysis in buffer A (50 mM Tris-Cl pH 8.0, 200 mM NaCl, 0.1% Triton X-100, 25 mM beta-glycerophosphate, 1 mM EDTA) with 2 protease inhibitor cocktail pellets per 50 ml (Roche) for 15 minutes at 4°C using a vortex (for metabolic labeling experiments, 400mM NaCl was used in buffer A). Lysates were clarified through centrifugation twice at 16000g, and an equal volume and protein concentration of each lysate was applied to 40 µl of Flag affinity resin (Sigma-Aldrich). After a two hour incubation with gentle rotation at 4°C, the beads were washed five times with 500 µl buffer A and bound proteins eluted with two 20µl washes of 0.25 mg/ml 3X Flag Peptide (Sigma-Aldrich) diluted in buffer A. The samples were resolved by 10% SDS-PAGE and immunoblotting with anti-Flag mouse monoclonal M2 antibodies at a dilution of 1:1000 (F3165, Sigma-Aldrich). The secondary antibodies used was horse radish-conjugated goat anti-mouse (170-1011, Biorad) at a dilution of 1:10,000.

RESULTS

The first step in investigating the kinase activity of Vps15 was confirming that it is in fact phosphorylated, as has been reported. As can be seen in **Figure 4.1**, Vps15 is phosphorylated *in vivo* as measured by the incorporation of radioactive phosphate. This phosphorylation event is abrogated when the kinase activity of Vps15 is abolished by the mutation E200R.

As detailed above, mutation of the kinase activity of Vps15 has also been shown to result in a disruption of the interaction of Vps15 and many binding partners, including Vps34, which has also been shown to be a protein kinase *(7)*. We therefore wondered if Vps15 would still be able to undergo a phosphorylation event in the absence of Vps34. As can be seen in **Figure 4.2**, the phosphorylation of Vps15 *in vivo* as measured by metabolic labeling is abolished in *vps34*Δ cells.

While it is apparent that Vps34 is necessary for Vps15 to become phosphorylated, it is not clear if Vps34 actually phosphorylates Vps15, or if it is necessary for the stabilization for Vps15. To determine if Vps34 is necessary for the stable expression of Vps15, we immunoprecipitated Flag-tagged Vps15 from *vps15*Δ and *vps34*Δ cells and looked at abundance of purified protein. As can be seen in **Figure 4.3**, in the absence of Vps34, overall protein levels of Vps15 are dampened, indicating that the presence of Vps34 is necessary for Vps15 to be expressed.

We were then interested to see if Vps34 binding to Vps15 is sufficient for stable expression of Vps15. In order to do test the role of Vps34 binding in Vps15 stability, we used a point mutation of Vps34, $Vps34^{N736K}$, that is deficient in both protein kinase and PI3K activities, but has been shown by two-hybrid to be capable of binding to Vps15 (*7*). As can be seen in the preliminary data presented in **Figure 4.4**, $Vps34^{N736K}$ appears to result in reduced expression of Vps15, indicating that some aspect of the protein kinase and PI3K activities may be necessary for the expression of Vps15. Further experiments are necessary to confirm these data.

DISCUSSION AND SUMMARY

The kinase domain of Vps15 is integral to many aspects of Vps15's role in the cell, from binding to Vps34, to transmitting the G protein coupled signal, to vacuolar protein sorting (as monitored by the sorting of Carboxypeptidase Y) (*5*). While Vps15 has long been presumed to be a protein kinase, many aspects of its reported kinase activity have remained unclear. As mentioned previously, point mutations of the kinase domain of Vps15 result in an interruption of Vps15's interaction with binding partners (*7*), and, as described above, the autophosphorylation activity of Vps15 has never been proven conclusively. Before we could further investigate the role of the kinase domain in G protein signaling, it was therefore necessary to show that Vps15 is actually a kinase.

Here, we have shown that Vps15 is phosphorylated, and that a point mutation of Vps15 abolishes phosphorylation of Vps15. We have also shown that Vps15 is no longer phosphorylated when Vps34 is not present. Additionally, preliminary data appears to show that a form of Vps34, $Vps34^{N736K}$, that has no kinase activity or PI3K activity, but is capable of binding to Vps15, also results in a drop in total Vps15. These data clearly show that Vps34 is necessary for the expression of Vps15, but the exact role of Vps34 in the phosphorylation of Vps15 is unclear. It is possible that fully active Vps34 is necessary for the stable expression of Vps15, and that Vps34 is necessary for Vps15 autophosphorylation or phosphorylation by another protein. It is also possible that Vps34 is the kinase that phosphorylates Vps15.

FUTURE DIRECTIONS

While much progress has been made, at least two major questions remain unanswered. First, is Vps15 a protein kinase? If so, what is the role of Vps15 autophosphorylation? Second, how does ubiquitination alter Fus3 kinase activity?

In order to more fully investigate the kinase domain of Vps15 as well as the role of Vps34 in Vps15 phosphorylation, we have been working in coordination with Jonathan Backer, M.D. at the Albert Einstein College of Medicine, an expert in the field of PI3Ks. The Backer lab has found unique point mutations in the kinase domain of mammalian Vps15 that result in the typical phenotype seen with catalytically inactive (kinase dead) forms of Vps15, namely a loss of both kinase activity and binding to Vps34. However, when these kinase dead forms of Vps15 are incubated with ATP analogs adpated by the Backer lab, they remain kinase dead but regain their ability to bind Vps34. A great deal of research has been done on the ability of ATP analogs to act as inhibitors of kinase activity (*13-15*), however Dr. Backer speculates that in the mammalian Vps15 mutants, the ATP analogs may actually be inducing a conformational change that allows Vps15 to bind to Vps34. The use of ATP analogs is proving to be useful in pharmacology, as well as a powerful tool to gain insight into the mechanisms of action of kinase pathways (*13-15*). However, this tool is not without its hurdles to be overcome. In particular, in order to use some ATP analog inhibitors one must reengineer the binding pocket of the kinase in a manner that allows the inhibitor to bind successfully, as well as determine the most effective ATP analog for the kinase of interest (*13-15*).

We are working with Dr. Backer to make a similar set of Vps15 mutants in yeast that are integrated with a Flag-tag under the control of the endogenous Vps15 promoter. If these mutants act in a manner similar to the mammalian mutants, they will be uniquely positioned to allow us to determine the role of Vps34 in Vps15 phosphorylation. As these Vps15 mutants will still be capable of binding to Vps34, and potentially other binding partners, we will be able to investigate solely the kinase activity of Vps15. This system will allow us to determine if it is the kinase activity of Vps15 that is required for autophosphorylation, or if Vps15 is still phosphorylated in the absence of its kinase activity, which would be an indication that it is Vps34, or another protein kinase, that is responsible for the phosphorylation of Vps15.

If Vps15 is found to be phosphorylated even with mutations in its putative kinase domain that allow it to interact with Vps34, we will attempt to identify the kinase responsible for the phosphorylation of Vps15 and determine residues in Vps15 that undergo phosphorylation. In order to identify the kinase responsible for the phosphorylation of Vps15, we will examine the phosphorylation state of Vps15 in strains deleted with each of the 120 known non-essential kinases present in yeast, and investigate which kinase deletion strain results in a lack of phosphorylation of Vps15. To determine the sites of phosphorylation in Vps15 as well as the role of pheromone treatment in the phosphorylation of Vps15, we will perform large scale batch purification of tagged-full length Vps15 from *Saccharomyces cerevisiae* cells that have been left untreated or treated with pheromone. Purified Vps15 will then undergo liquid chromatography-mass spectrometry to identify phosphorylated residues. Having identified phosphorylated

residues in Vps15, we will mutate these residues and determine the effect of a lack of Vps15 phosphorylation on both G protein signaling and the PI3K activity of Vps34 in cells.

More research also remains to be performed on the basic patch present in Fus3 and its role in G protein signaling. Experiments will be undertaken to further confirm that mutations in the basic patch of Fus3 result in a decrease in the ubiquitination of Fus3 by utilizing a 0K form of myc-ubiquitin, so only mono-ubiquitinated Fus3 will be purified. A single Fus3 band will make differences in ubiquitination more apparent and easier to quantify. Future experiments may be undertaken to determine if mutations of the basic patch of Fus3 result in a decreased association between Fus3 and its binding partners, with special attention paid to the association between Fus3 and Far1. Mutations at the basic patch could abrogate an association between Far1 and Fus3, and this disruption may be an explanation for the reduction in Far1 phosphorylation in Fus3 basic patch mutants, as well as for the growth arrest defects seen in Fus3 basic patch mutants.

The experiments described above represent a natural extension of the work performed in this thesis. They will result in an increased understanding of G protein signaling at the endosome, and the mechanisms that are used to regulate this pathway. A greater understanding of the endosomal pathway will give us insight into the role of the G protein pathway at the endosome, and the way in which it acts to complement the pathway that originates from the plasma membrane.

REFERENCES

(1) Dohlman, H. G., and Thorner, J. W. (2001) Regulation of G protein-initiated signal transduction in yeast: Paradigms and principles. *Annu. Rev. Biochem. 70*, 703-54.

(2) Slessareva, J. E., Routt, S. M., Temple, B., Bankaitis, V. A., and Dohlman, H. G. (2006) Activation of the phosphatidylinositol 3-kinase Vps34 by a G protein alpha subunit at the endosome. *Cell 126*, 191-203.

(3) Slessareva, J. E., and Dohlman, H. G. (2006) G protein signaling in yeast: new components, new connections, new compartments. *Science 314*, 1412-3.

(4) Heenan, E. J., Vanhooke, J.L., Temple, B.R., Betts, L., Sondek, J.E., and Dohlman, H.G. (2009) Structure and function of Vps15 in the endosomal G protein signaling pathway. *Biochemistry 48*, 6390-6401.

(5) Backer, J. M. (2008) The regulation and function of Class III PI3Ks: novel roles for Vps34. *Biochemical Journal 410*, 1-17.

(6) Herman, P. K., Stack, J. H., DeModena, J. A., and Emr, S. D. (1991) A novel protein kinase homolog essential for protein sorting to the yeast lysosome-like vacuole. *Cell 64*, 425-37.

(7) Budovskaya, Y. V., Hama, H., DeWald, D. B., and Herman, P. K. (2002) The C terminus of the Vps34p phosphoinositide 3-kinase is necessary and sufficient for the interaction with the Vps15p protein kinase. *J Biol Chem 277*, 287-94.

(8) Murray, J. T., Panaretou, C., Stenmark, H., Miaczynska, M., and Backer, J.M. (2002) Role of Rab5 in the recruitment of hVps34/p150 to the early endosome. *Traffic 3*, 416-427.

(9) Herman, P. K., Stack, J. H., and Emr, S. D. (1991) A genetic and structural analysis of the yeast Vps15 protein kinase: evidence for a direct role of Vps15p in vacuolar protein delivery. *Embo J 10*, 4049-60.

(10) Stack, J. H., and Emr, S. D. (1994) Vps34p required for yeast vacuolar protein sorting is a multiple specificity kinase that exhibits both protein kinase and phosphatidylinositol-specific PI 3-kinase activities. *J Biol Chem 269*, 31552-62.

(11) Zeller, C. E., Parnell, S.C., and Dohlman, H.G. (2007) The RACK1 ortholog Asc1 functions as a G-protein beta subunit coupled to glucose responsiveness in yeast. *Journal of Biological Chemistry 282*, 25168-25176.

(12) Torres, M. P., and Borches, C.H. (2007) Mitotic phosphorylation of the anaphase-promoting complex inhibitor subunit Mnd2 is necessary for efficient progression therough meiosis I. *J Biol Chem 282*, 17351-17362.

(13) Shah, K., Liu, Y., Deirmengian, C., and Shokat, K.M. (1997) Engineering unnatural nucleotide specificity for Rous sarcoma virus tyrosine kinase to uniquely label its direct substrates. *Proc Natl Acad Sci USA 94*, 3565-3570.

(14) Parang, K., and Cole, P.A. (2002) Designing bisubstrate analog inhibitors for protein kinases. *Pharmacology and Theraputics 83*, 145-157.

(15) Turk, B. E. (2008) Understanding and exploiting substract recognition by protein kinases. *Curr Opin Chem Biol 12*, 4-10.

FIGURE LEGENDS

Figure 4.1. Vps15 undergoes a phosphorylation event, and mutation of the kinase domain abrogates phosphorylation of Vps15. Detergent-solubilized extracts from *vps15*Δ cells expressing the indicated Flag fusion proteins that had undergone metabolic labeling were incubated with Flag resin, eluted with 3X Flag peptide, resolved by 7.5% SDS-PAGE, and analyzed using a phosphorimage screen. *, indicates protein of interest.

Figure 4.2. Vps15 is not phosphorylated in the absence of Vps34. Detergent-solubilized extracts from *vps15*Δ cells and *vps34*Δ expressing the indicated Flag fusion proteins that had undergone metabolic labeling were incubated with Flag resin, eluted with 3X Flag peptide, resolved by 7.5% SDS-PAGE, and analyzed using a phosphorimage screen. *, indicates protein of interest.

Figure 4.3. Vps15 has reduced expression in the absence of Vps34. Detergent-solubilized extracts from *vps15*Δ cells and *vps34*Δ expressing the indicated Flag fusion proteins were incubated with Flag resin, eluted with 3X Flag peptide, resolved by 7.5% SDS-PAGE, and analyzed using antibodies specific for Flag. *, indicates protein of interest. NSB, nonspecific Flag band used for loading control.

Figure 4.4. The PI3K and kinase activity of Vps34 are necessary for maximal expression of Vps15. Detergent-solubilized extracts from *vps15*Δ cells and *vps34*Δ cells expressing the indicated Flag fusion proteins were incubated with Flag resin, eluted with 3X Flag peptide, resolved by 7.5% SDS-PAGE, and analyzed using antibodies specific

for Flag. *, indicates protein of interest. NSB, nonspecific Flag band used for loading control.

Figure 4.1

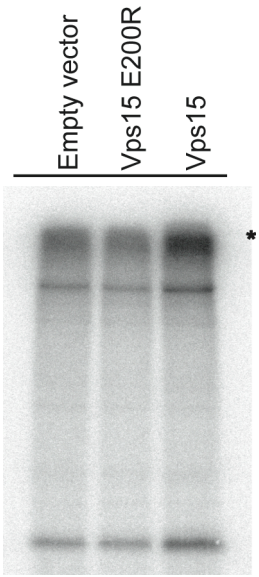

Figure 4.2

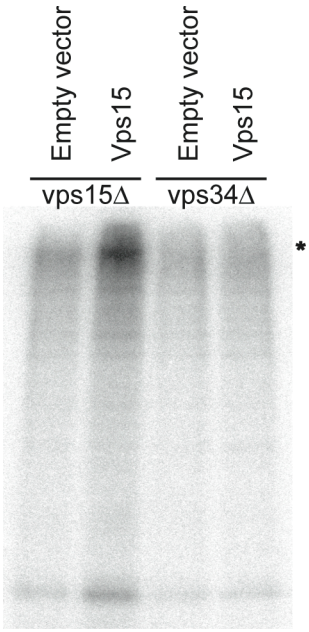

Figure 4.3

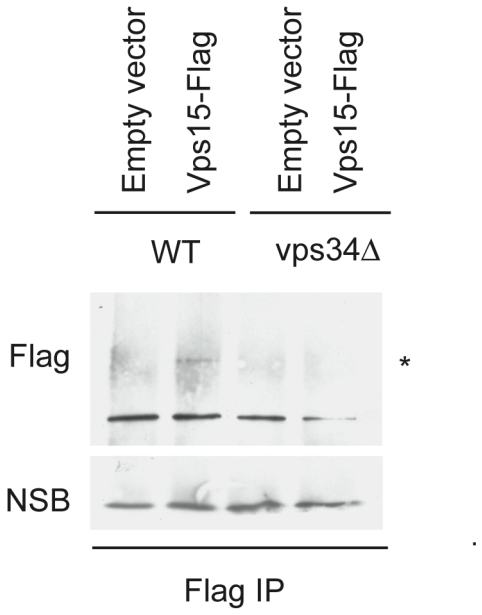
Empty vector
Vps15-Flag
Empty vector
Vps15-Flag
WT
vps34Δ
Flag
*
NSB
Flag IP

Figure 4.4

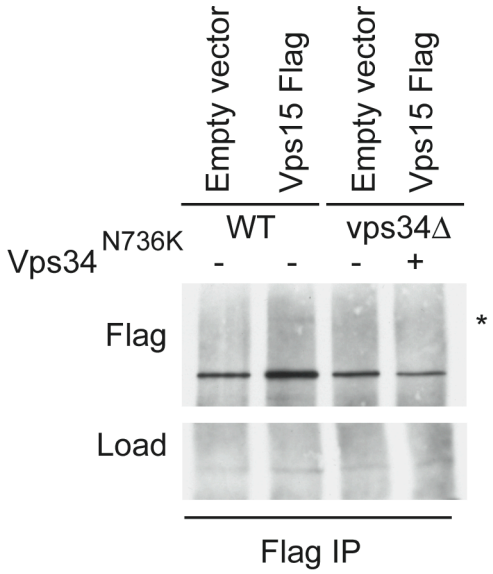
Empty vector
Vps15 Flag
Empty vector
Vps15 Flag
WT
vps34Δ
Vps34 N736K
- - - +
Flag
*
Load
Flag IP